

# THROTTLEABLE THRUSTOR SYSTEM

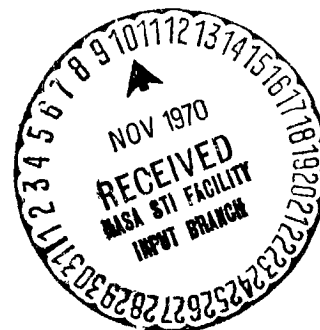
## FINAL REPORT

REPORT NO. 70.4726.3-28

JPL CONTRACT 952344

SUBCONTRACT UNDER  
NASA CONTRACT NAS 7-100

APRIL 1970



**TRW**  
SYSTEMS GROUP

N71-10763 (ACCESSION NUMBER)	(THRU)	53
	(CODE)	28
102 (PAGES)	(CATEGORY)	
02-110903 (NASA CR OR TMX OR AD NUMBER)		

Final Report  
THROTTLEABLE THRUSTOR SYSTEM

JPL Contract No. 952344  
Report No. 70.4726.3-28

28 April 1970

Prepared By: R. J. Kenny  
R. J. Kenny

D. F. Reeves  
D. F. Reeves

Approved By: V. A. Moseley  
V. A. Moseley  
Program Manager

This work was performed for the Jet Propulsion  
Laboratory, California Institute of Technology,  
as sponsored by the National Aeronautics and  
Space Administration under Contract NAS7-100.

TRW SYSTEMS  
One Space Park • Redondo Beach • California

## ABSTRACT

This report summarizes a three-phase effort in which a throttleable monopropellant hydrazine thruster system for planetary lander vehicles was investigated. A trade off study with total system weight as the primary criteria included 300 to 1200 lb<sub>f</sub> thrust catalytic and thermal decomposition chambers, electromechanical and electrohydraulic throttle valve actuation, and various control techniques. Based on these studies, a 600 lb<sub>f</sub> catalytic throttleable thruster system weighing 14.8 pounds was designed, fabricated, and demonstrated. This thruster, together with an electromechanically actuated throttle valve incorporating position feedback control, demonstrated performance/response levels consistent with planetary lander requirements.

This report contains information prepared by TRW Systems Group under JPL subcontract. Its content is not necessarily endorsed by the Jet Propulsion Laboratory, California Institute of Technology, or the National Aeronautics and Space Administration.

## CONTENTS

	<u>Page</u>
1. INTRODUCTION AND SUMMARY . . . . .	i
2. TECHNICAL DISCUSSION . . . . .	4
2.1 Phase I - Preliminary Design . . . . .	4
2.1.1 Conceptual Design . . . . .	4
2.1.2 System Evaluation . . . . .	4
2.1.3 Flow Control System . . . . .	23
2.2 Phase II - TTS Detail Design . . . . .	24
2.2.1 System Optimization . . . . .	24
2.2.2 System Design . . . . .	37
2.2.3 Throttle Valve Design . . . . .	45
2.2.4 Thrust Chamber Design . . . . .	53
2.3 Phase III - Fabrication and Test . . . . .	55
2.3.1 Thrust Chamber Fabrication . . . . .	59
2.3.2 Acceptance Tests . . . . .	61
2.3.3 Operational and Environmental Testing System Checkout and Baseline Sea Level Performance . . . . .	70
3. CONCLUSIONS AND RECOMMENDATIONS . . . . .	89
BIBLIOGRAPHY . . . . .	90
APPENDIX A - Specification - Flow Control Assembly . . . . .	A-1
APPENDIX B - New Technology Reports . . . . .	B-1

## 1. INTRODUCTION AND SUMMARY

The Throttleable Thrustor System (TTS) program was conducted for the purpose of advancing the hydrazine monopropellant engine technology required for planetary soft landing missions. The program was performed in three phases:

- Phase I - Concept Selection
- Phase II - Detailed Design
- Phase III - Fabrication and Test

A representative Mars landing profile involving atmospheric deceleration, parachute descent, and propulsive terminal landing was used to establish thrustor/system requirements.

For the purpose of the study, the propulsion system configuration was identical for all the systems evaluated except for the design of the engine itself. A schematic of the basic system used in the performance studies is presented in Figure 1. The primary measure of system performance was considered to be the total propulsion subsystem mass.

The throttling duty cycle presented in Figure 2 was arbitrarily selected for purposes of estimating average specific impulse and total impulse. Although a thrust range of 300 lb<sub>f</sub> to 1200 lb<sub>f</sub> was studied, the emphasis was on the 600 lb<sub>f</sub> engine and 1200 lb<sub>m</sub> initial lander weight because this technology appeared more relevant to current needs. The normalized percent thrust versus time of Figure 2 results in a total impulse, and therefore vehicle size, which is a direct function of thrust level. This approach was selected over the possibility of considering a constant vehicle size with variable maximum thrust engines. Table 1 presents the specific requirements applied for the study and design.

The selection of the basic engine design was achieved during the Phase I program, where eight conceptual designs were evaluated primarily on the basis of total system weight. During this phase of the program various reactors, nozzles and flow control devices were evaluated. The final engine configuration was chosen based on its relatively low system weight and utilization of "state-of-the-art" technology.

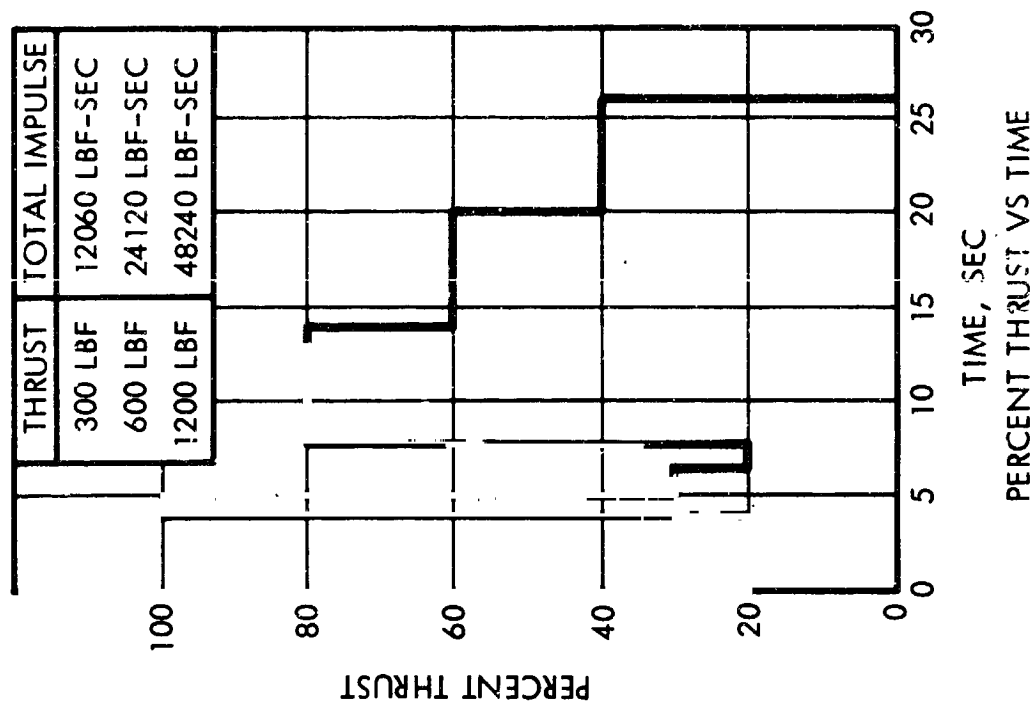


Figure 2. Duty Cycle

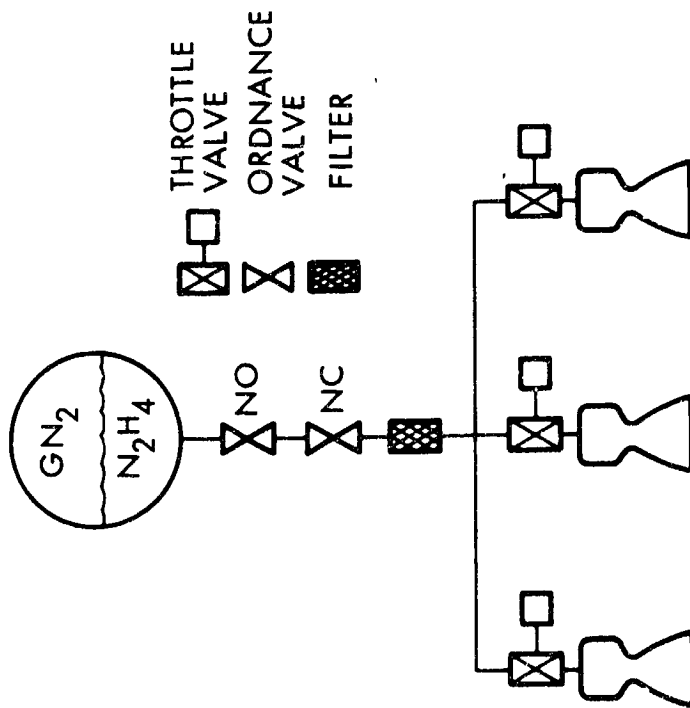


Figure 1. TTS Model1 Schematic

Table 1. Throttleable Thrustor System Design and Performance Requirements

Parameter	TTS Design Goal
Thrust	300, 600, 1200 $lb_f$
Throttle Ratio (At Constant Inlet Pressure)	6:1 Minimum 10:1 Goal
Nozzle Separation Criteria	No Separation At $P_{AMB} = 0.3$ psia
Life	500 sec
Specific Impulse	210 $lb_f$ -sec/ $lb_m$ , Minimum (Ambient Pressure - Vac.)
Heat Sterilization	6 Cycles of 64 Hours/Cycle at 275°F
Step Response (to 90%)	< 75 msec
Overshoot	$\leq 25\%$ of Step
Frequency Response (5 CPS) Amplitude Ratio	$\geq 0.70 @ 60 \pm 10\%$ Thrust
Phase Angle	$\geq -45^\circ$

During Phase II, additional design details were evolved from a more sophisticated analysis of the requirements and operating characteristics of the rocket engine assembly. Materials were selected based on their structural properties and minimum fabrication costs. Throttle valve requirements were established and procurements of one valve each from LTV and Moog were initiated. Manufacturing drawings and procedures were prepared.

The final phase of the program involved the fabrication and test of the 600  $lb_f$  thrust engine assembly. The throttle valves were produced per the requirements of the TRW technical specifications and applicable interface drawings. A primary feature of the valve development program was the simultaneous evaluation of two different flow control concepts.

The remainder of this report is devoted to details of the three program phases and resultant conclusions.

## 2. TECHNICAL DISCUSSION

This section presents the evolution of the TTS through the three phases from conceptual studies to performance demonstration. The basic thruster design and operating characteristics were established and demonstrated. Throttling via non-cavitating position feedback regulated electromechanically driven valves was selected, and two different types of valves were built and tested. The only significant problem encountered in the course of this activity was chamber pressure roughness in the initial configuration. This was satisfactorily corrected with one catalyst bed configuration iteration, and all the objectives of the program were met.

### 2.1 Phase I - Preliminary Design

#### 2.1.1 Conceptual Design

As a first step in identifying the basic engine configuration, a preliminary design phase was initiated to evaluate the potential design approaches and to determine the optimum concept for more extensive development. This study was initially concerned with identifying the possible alternatives for the various components of the rocket engine assembly. Basic parameters and assumptions used for the initial study are outlined in Table 2. Table 3 is a summary of the basic design variations considered. From this general survey it was possible to combine the components into nine basic engine configurations of which eight were later evaluated in greater detail. Table 4 is a summary of the basic system configurations evolved. The throttle valve selection was based primarily on "state-of-the-art" development and expected performance while the engine configuration selection was also influenced by a determination of the expected total weight of the propulsion system. Note that the circled numbers in Table 4 identify the design concepts used in the respective configurations selected for further study.

#### 2.1.2 System Evaluation

Based on the established requirements and ground rules, eight of the candidate systems were evaluated for performance and weight by a consistent

Table 2. Throttleable Thrustor System Performance Studies  
Ground Rules and Assumptions

A. ENGINE SYSTEM - (THREE ENGINES PER SYSTEM)

1.  $F = 300, 600, 1200 \text{ Lbf}$
2.  $P_c = 50 \text{ TO } 500 \text{ PSIA}$
3.  $\epsilon = 5 \text{ TO } 80$
4.  $C^*$  EMPIRICAL CURVE DEPENDENT ON  $\%$  THRUST
5.  $C_F$  THEORETICAL CURVE DEPENDENT ON  $\%$  THRUST AND  $\epsilon$
6.  $\Delta P$  INJECTOR = 100 PSI
7.  $\Delta P$  CATALYST = 50 PSI
8. NOZZLE SEPARATION WHEN  $P_e < 0.12 \text{ PSIA}$
9. MATERIAL L-605 (MINIMUM GAGE = 0.015 IN.)
10. SAFETY FACTOR = 1.5 @ OPERATING TEMPERATURE

B. PROPELLANT SUPPLY SYSTEM - (ONE PRESSURANT AND PROPELLANT TANK COMBINED)

1. PROPELLANT MIL-P-265368 HYDRAZINE
2. PRESSURANT MIL-P-274018 NITROGEN
3.  $\Delta P_{\text{VALVE}} = 0.10 P_{\text{TANK}}$
4.  $\Delta P_{\text{LINES}} = 10 \text{ PSI}$
5. SAFETY FACTOR = 2.2
6. BLOW DOWN PRESSURE RATIO = 50%
7. COMPONENT WEIGHTS = 4, 5, 6 LBM FOR 300, 600, 1200 LBF SYSTEMS RESPECTIVELY
8. TANK MATERIAL 6 AL 4V TITANIUM ( $F_{TU} = 150,000 \text{ PSI}$ )

Table 3. Conceptual Designs

Engine Designs	Injectors		Reactors		Chambers		Nozzles	
	Spray		Catalytic		Cylindrical		DeLaval	
	Sheet		Thermal		Spheroidal		Spike	
	Showerhead				Annular		Expansion Deflection	
Throttle Methods	Control System		Actuators		Valve Design			
	Position Feedback		Electro-Mechanical		Linear Plug			
	$P_c$ Feedback		Electro-Hydraulic		Rotary Plug			
	G and C Sensing		Electro-Pneumatic		Ball or Blade			
			Fluidic		Flapper or Spool			

Table 4. Thrustor System Comparison Chart

DEVELOPMENT REQUIRED: SA = STATE OF ART MD = MODERATE DEVELOPMENT ED = EXTENSIVE DEVELOPMENT  
 CONCEPT FEASIBILITY: QF = QUESTIONABLE FEASIBILITY RF = RELATIVELY FEASIBLE HF = HIGHLY FEASIBLE  
 ESTIMATED PERFORMANCE BANKING: 1-10 10 = HIGH PERFORMANCE 1 = LOW PERFORMANCE  
 SYSTEM CONFIGURATION: ① - ⑨

REACTOR CONCEPT	NOZZLE CONCEPT			FLOW CONTROL CONCEPT					
	DE LAVAL	SPIKE	EXPANSION DEFLECTION	CAVITATING VENTURI			NON-CAVITATING VENTURI		
				FIXED AREA INJECTOR	VARIABLE LOSS INJECTOR	FIXED AREA INJECTOR	VARIABLE LOSS INJECTOR	FLOW CONTROL INJECTOR	FLOW CONTROL INJECTOR VARIABLE AREA NOZZLE
CATALYTIC CYLINDRICAL	SA ①	MD ①	ED ③	SA ②	MD	SA ②	MD	MD	ED ③
	HF ②	HF ⑥	RF ⑧	RF ⑤	RF ⑤	RF ⑤	RF ⑤	RF ⑦	RF ⑧
	5	6	8	5	5	5	5	7	8
ANNULAR	MD	MD ④	ED	ED	ED	ED	ED	ED	ED
	QF ③	HF ⑦	QF ⑥	RF ④	QF ③	RF ④	QF ③	QF ⑥	QF ⑦
	3	7	6	4	3	4	3	6	7
SPHEROIDAL	SA ⑧	MD	ED ⑤	MD ⑧	MD	MD ⑧	MD	ED ⑤	ED
	HF ⑤	QF ⑥	RF ⑨	RF ⑦	QF ⑦	RF ⑦	RF ⑦	RF ⑧	QF ⑨
	5	6	9	7	7	7	7	8	9
THERMAL CYLINDRICAL	SA ⑥	SA ⑥	ED ⑨	MD	MD ⑥	MD	MD	MD	ED ⑨
	HF ⑤	HF ⑥	HF ⑧	QF ⑥	HF ⑥	QF ⑥	RF ⑥	RF ⑧	RF ⑨
	5	6	8	6	6	6	6	8	9
ANNULAR	SA ⑦	MD ⑦	ED	MD	MD	MD	MD	ED	ED
	QF ③	HF ⑦	QF ⑥	QF ⑤	HF ⑤	QF ⑤	RF ⑦	RF ⑦	QF ⑧
	3	7	6	5	5	5	5	7	8

analytical technique. A valid comparison of the various systems was achieved by developing engine configurations using identical propellant feed systems in all concepts. The method of analysis involved two basic computations; first to determine the performance of each engine over the range of operating variables considered, and second to compute the system mass and ideal velocity increment for each case. The system optimization was performed to determine the most desirable configuration with overall systems mass a primary consideration. The ideal velocity increment ( $\Delta V$ ) generally represents the most significant parameter for propulsion system evaluation and is expressed as:

$$\Delta V = \bar{I}_s g \ln \frac{W_i}{W_f}$$

where  $\bar{I}_s$  is average specific impulse and  $\frac{W_i}{W_f}$  is the ratio of the initial (pre-maneuver) mass to final (post maneuver) mass. Equivalent system weight calculations indicated that the velocity increment calculation was not necessary to establish relative merit. Therefore, system weight values were used as a basis for optimization. In addition, it was necessary to identify the optimum chamber pressure, expansion ratio and mass velocity (G) for the selected concept. It is important to note that the lightest engine does not necessarily produce the lightest system since operating pressure requirements and specific impulse are significant influence parameters. Consequently, the total propulsion system concept must be considered if meaningful results are to be achieved.

#### Engine Performance

The engine performance was determined for each of the candidate engine erations. Two reactor designs (catalytic and thermal decomposition) and four nozzle types (DeLaval, fixed and variable throat expansion deflection and plug) were evaluated. The characteristic exhaust velocity ( $C^*$ ) was established for each chamber design based on test experience for the range in thrust surveyed. Figure 3 shows a comparison of  $C^*$  for each design as a function of percent thrust with the fraction of ammonia dissociation (X) indicated. The data presented were measured on engines

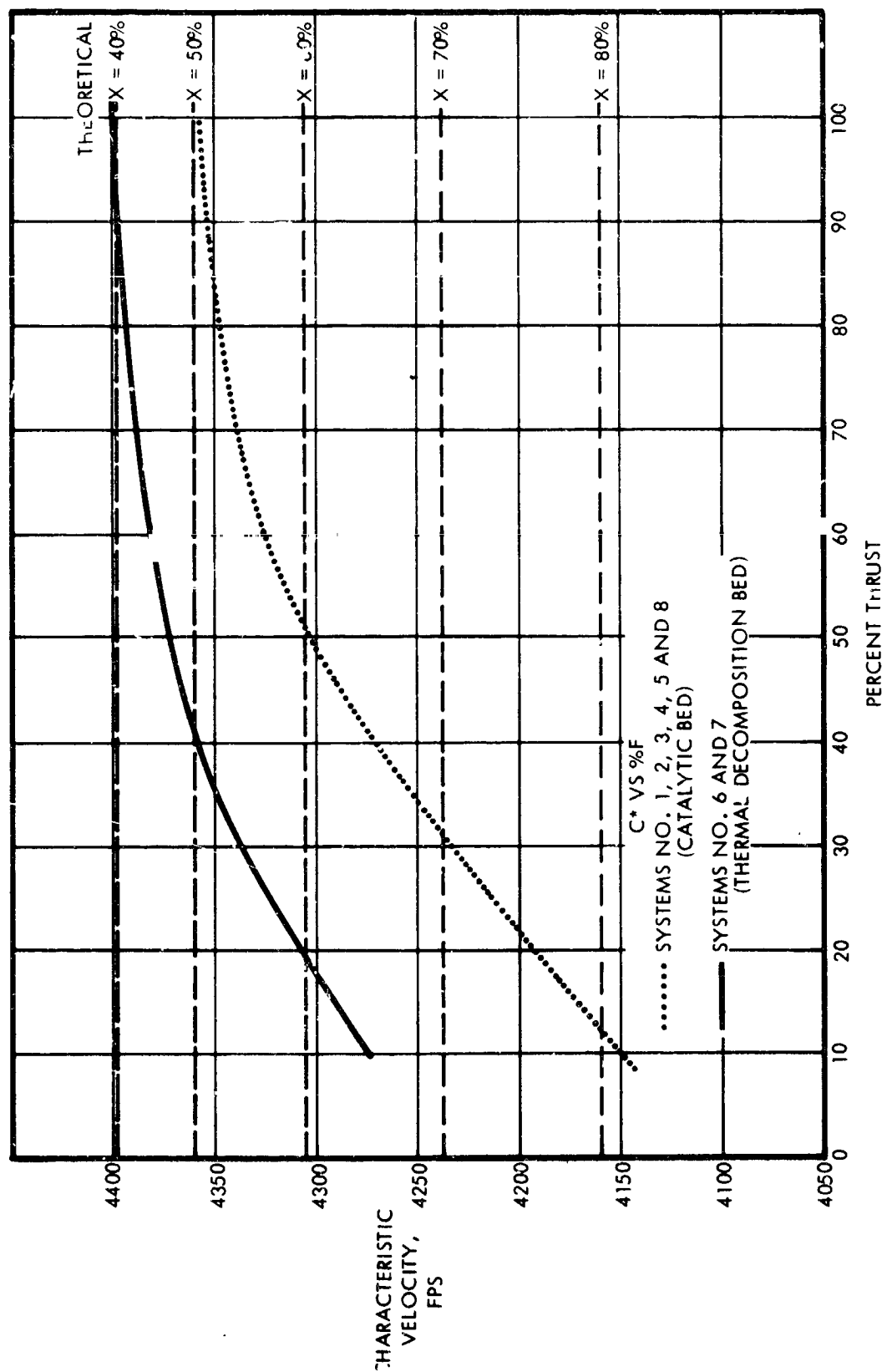


Figure 3. Characteristic Velocity Throttling Performance

which had a chamber pressure of approximately 300 psia at thrust levels of 400 to 600 lb<sub>f</sub>. Note that a slight performance increase can be realized with the thermal decomposition reactor and this advantage increases as the engine is throttled to lower thrust levels. The primary reason for this increase in performance with the thermal decomposition chamber is due to the decrease in ammonia dissociation achieved with the lower surface area heat sink material as compared to catalyst.

Theoretical values of the important decomposition parameters are indicated in Figure 4. Based on the assumed dissociation during throttling the pertinent gas properties are shown in Figure 5. The C\* performance is independent of chamber pressure based on theoretical and experimental results.

The thrust coefficient ( $C_F$ ) is influenced primarily by the particular nozzle type and expansion ratio. Values for the nozzle efficiency and effective specific heat ratios were selected on the basis of experimental concepts.

The Rao nozzle  $C_F$  was used in the DeLaval nozzle engine configurations. However, the one dimensional  $C_F$  was used for expediency in defining nozzle performance of the advanced nozzle concepts because additional sophistication was not warranted at this point in the study. The resultant vacuum thrust coefficient under various throttling conditions is shown as a function of area ratio in Figure 6 for the DeLaval and advanced nozzle concepts.

Engine performance with the conventional nozzle was computed over the entire range in chamber pressure and expansion ratio without consideration of possible separation at the nozzle exit because of the possible variations in ambient pressure, expansion characteristics and separation criteria. Figure 7 shows the range in separation conditions based on the Summerfield criteria, i.e., separation in the nozzle occurs when the exit pressure is equal to or less than 40 percent of ambient pressure. Applying this criteria to the optimum design which employs a DeLaval nozzle and a relatively low chamber pressure and expansion ratio indicates that separation will not occur with a 10:1 throttle ratio and 0.3 psia ambient pressure based on the two dimensional results. The performance of the two

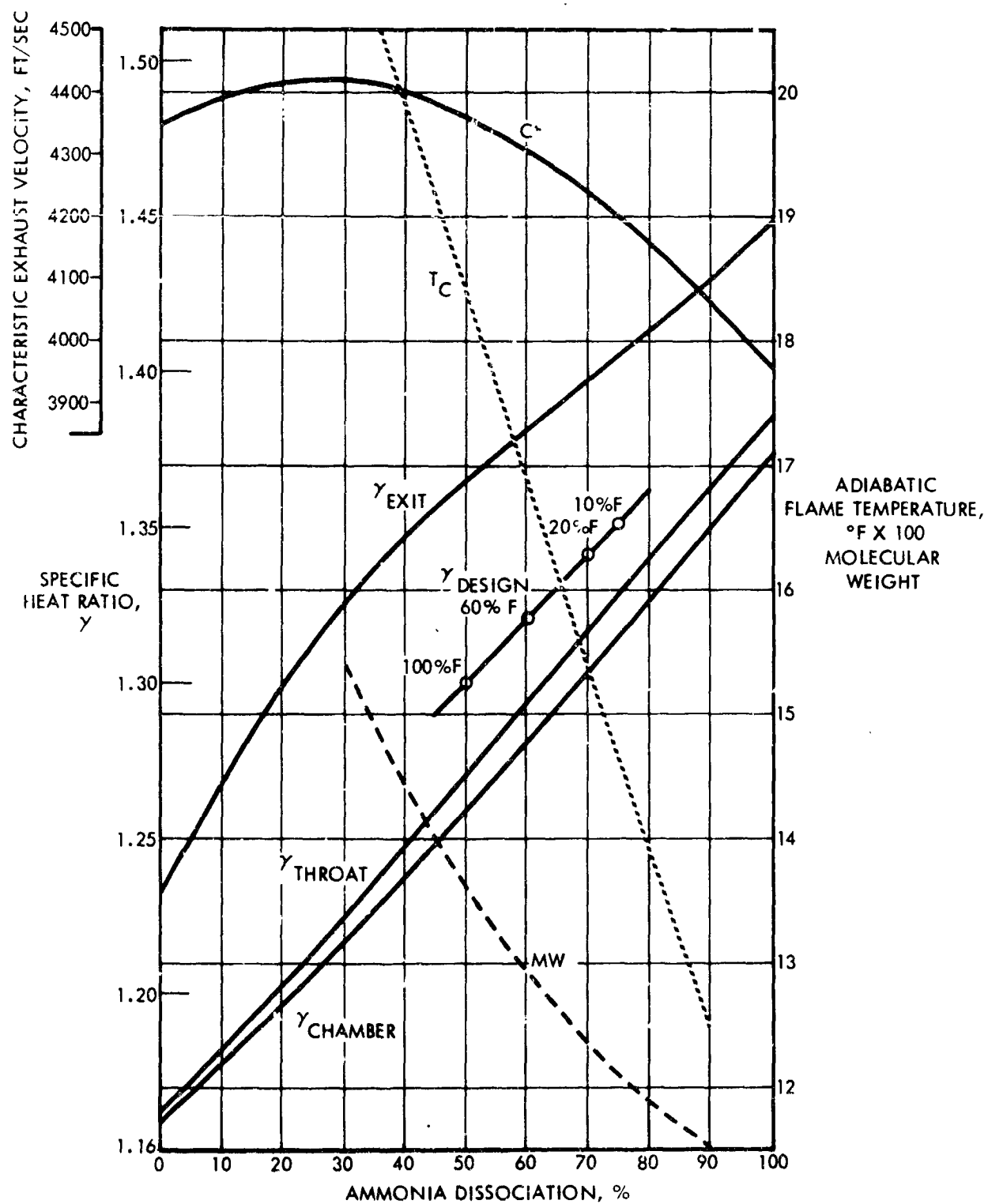


Figure 4. Hydrazine Decomposition Characteristics

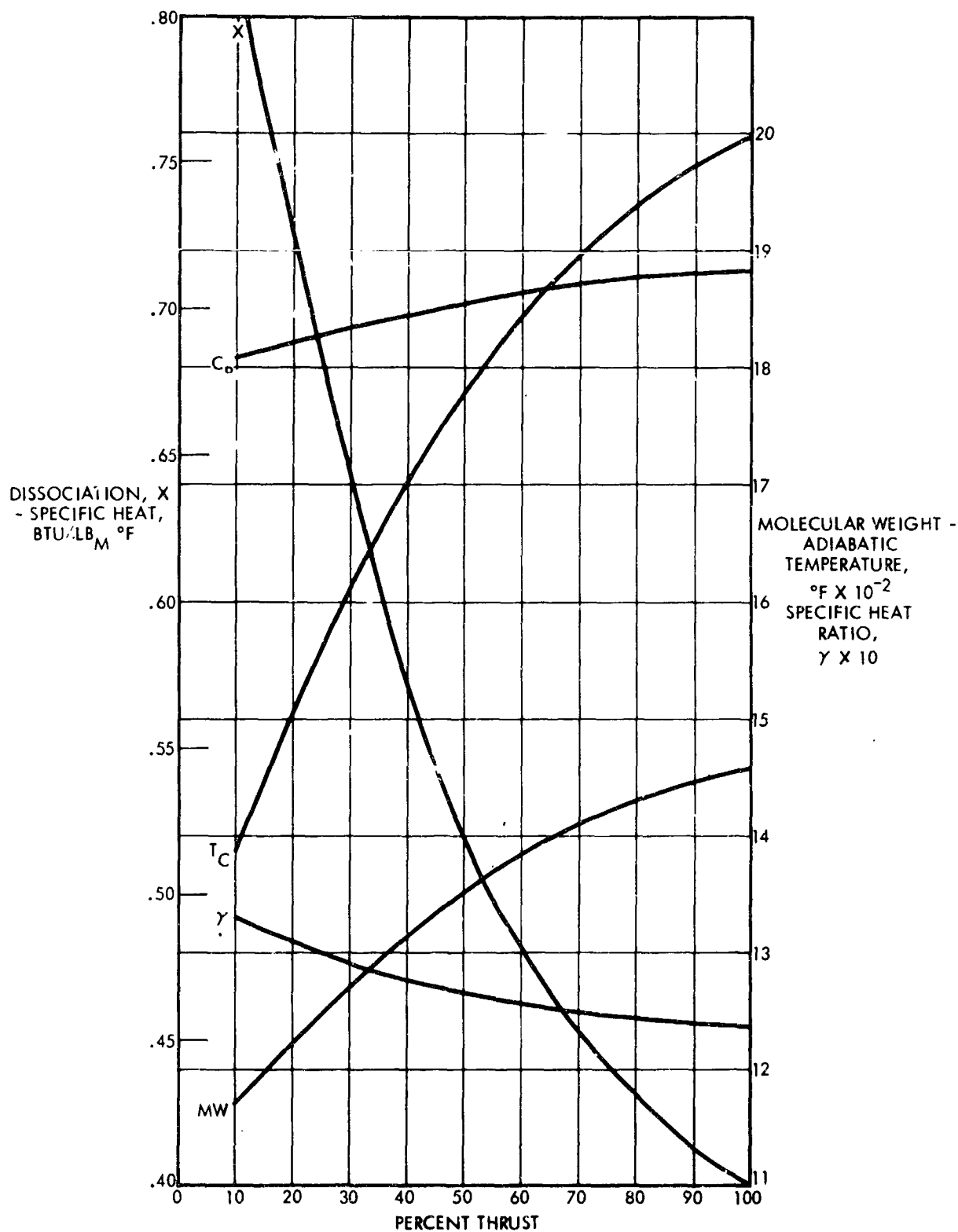


Figure 5. Theoretical Chamber Exit Conditions

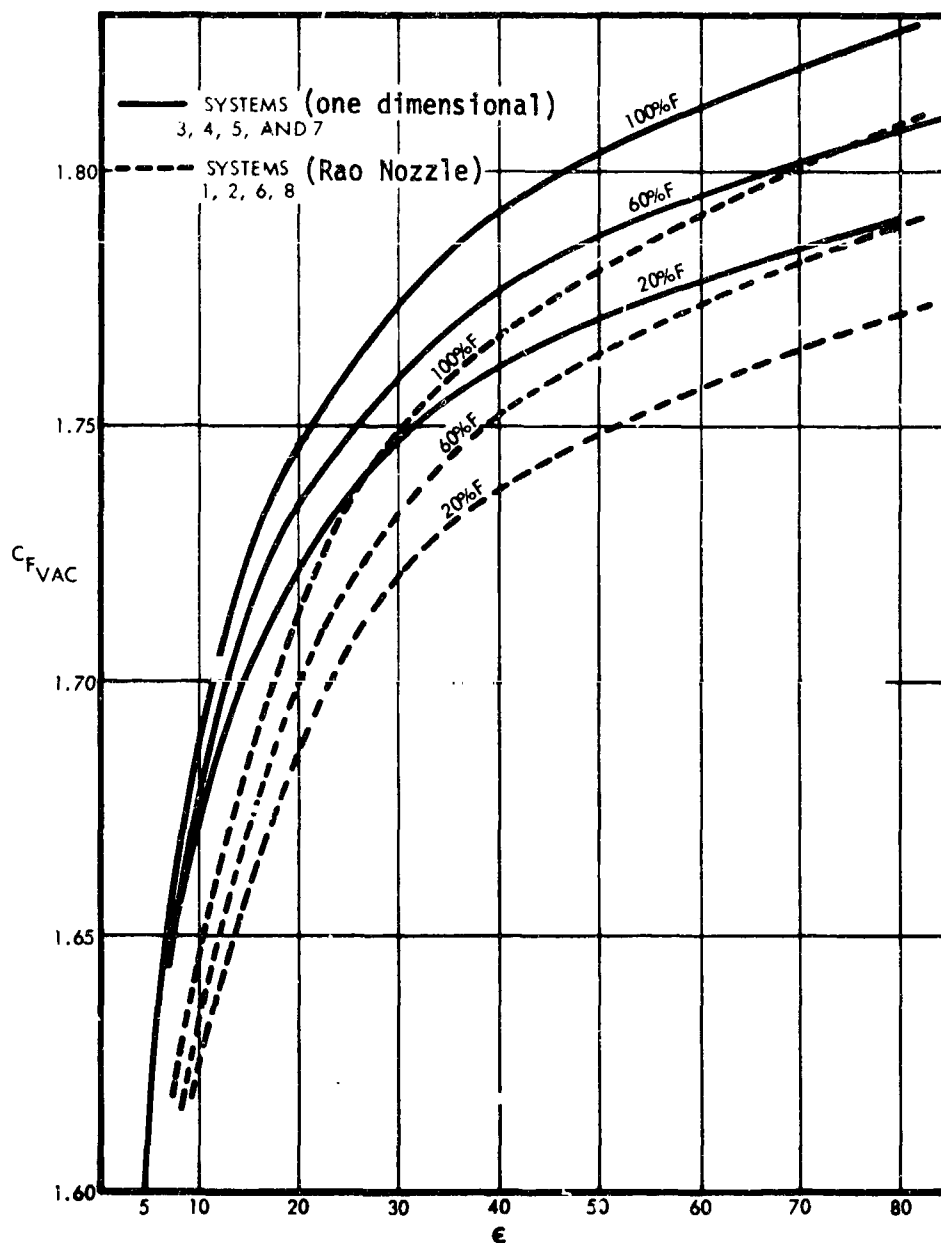


Figure 6. Theoretical Thrust Coefficient

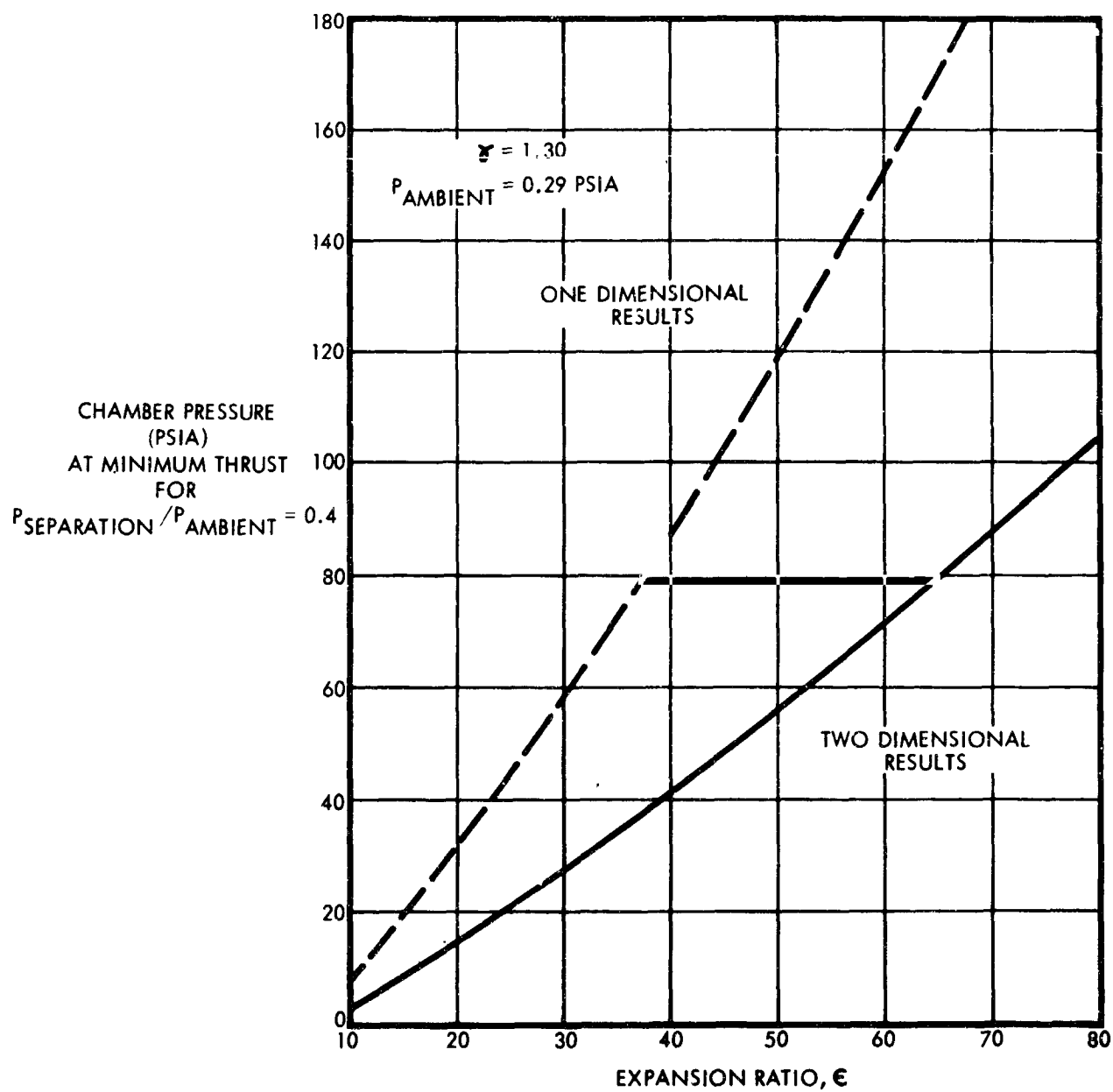


Figure 7. Nozzle Separation Criteria

dimensional nozzles is different from the one dimensional results due to the difference in static pressure at the nozzle wall. For optimum contour nozzles designed by the method of Rao, the pressure varies across the nozzle exit and the wall pressure is appreciably higher than the one dimensional result thus allowing higher expansion ratios.

The specific impulse was computed for each system over the expected throttling range based on the classical relationship:

$$I_s = \frac{C^* C_F}{g}$$

The performance of the various configurations at a maximum chamber pressure of 200 psia and expansion ratio of 20:1 is shown in Figure 8 with a comparison showing the performance loss due to the specified ambient atmospheric pressure (0.3 psia) displayed in Figure 9. The thrust coefficient ( $C_F$ ) advantage of the advanced nozzle concepts is evidenced by the higher performance achieved during throttling operation.

Figure 10 shows the conventional catalytic engine performance as a function of area ratio for a 5:1 throttle ratio with the one dimensional separation points indicated. The optimum area ratio shifts as a function of the throttle point because of the finite  $P_c/P_a$  ratio. For the mission conditions used in this study, approximately 30 percent of the propellant is consumed at thrust levels less than 50 percent.

The effect of chamber pressure on engine performance is shown in Figure 11. For hydrazine engines, the specific impulse is less sensitive to chamber pressure than for bipropellant engines due to the small effect on the generated gas properties and reaction temperature. However, thrust coefficient losses produce a significant performance decrease at chamber pressures less than 200 psia and an ambient pressure of 0.3 psia. If the Mars atmospheric pressure is lower, as is now expected, the optimum chamber pressure decreases. One encouraging aspect, though, is the fact that total system weight is relatively insensitive to chamber pressure and expansion ratio selection.

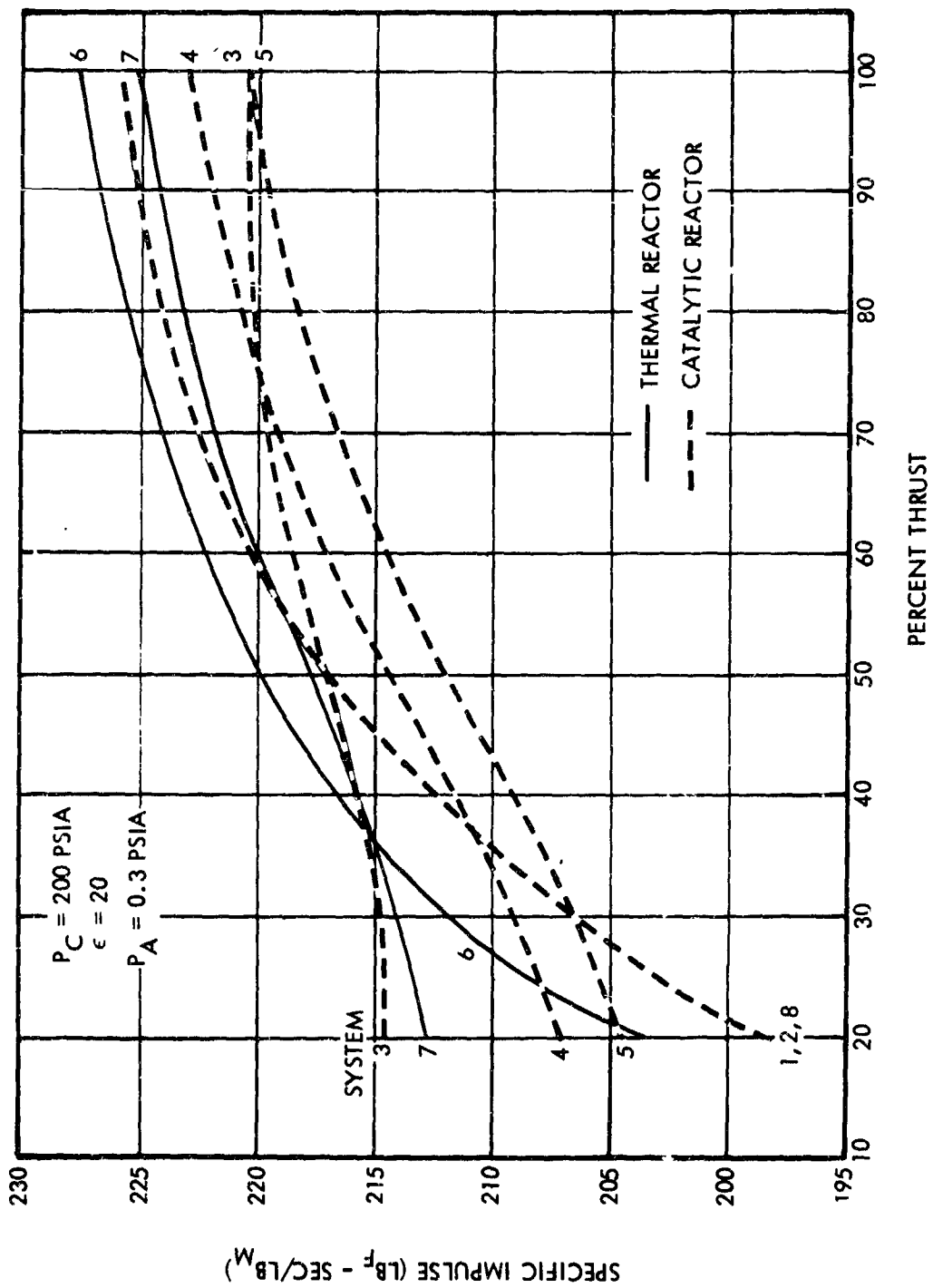


Figure 8. Throttling Performance of Various TTS Configurations

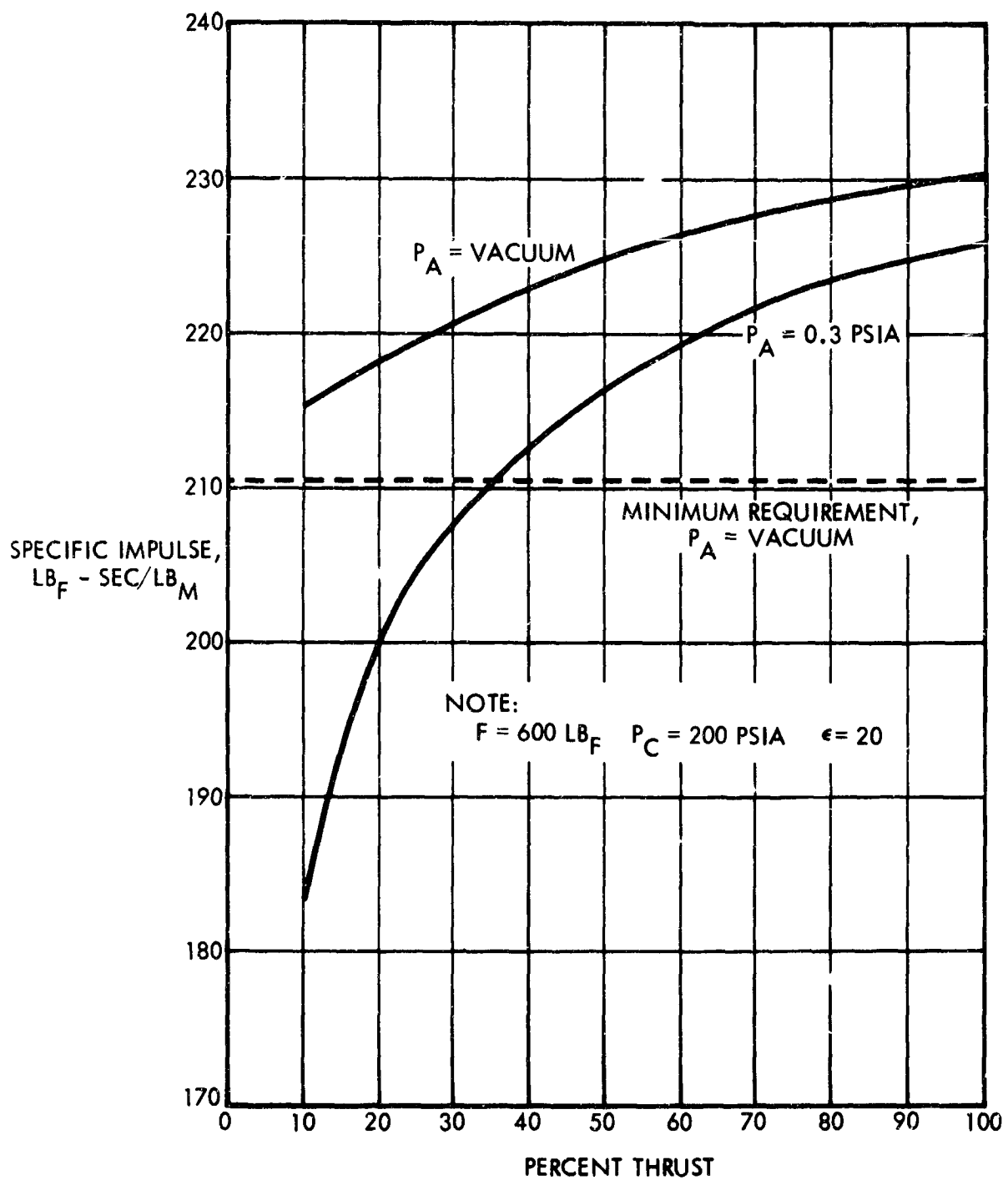


Figure 9. TTS Throttling Performance Comparison

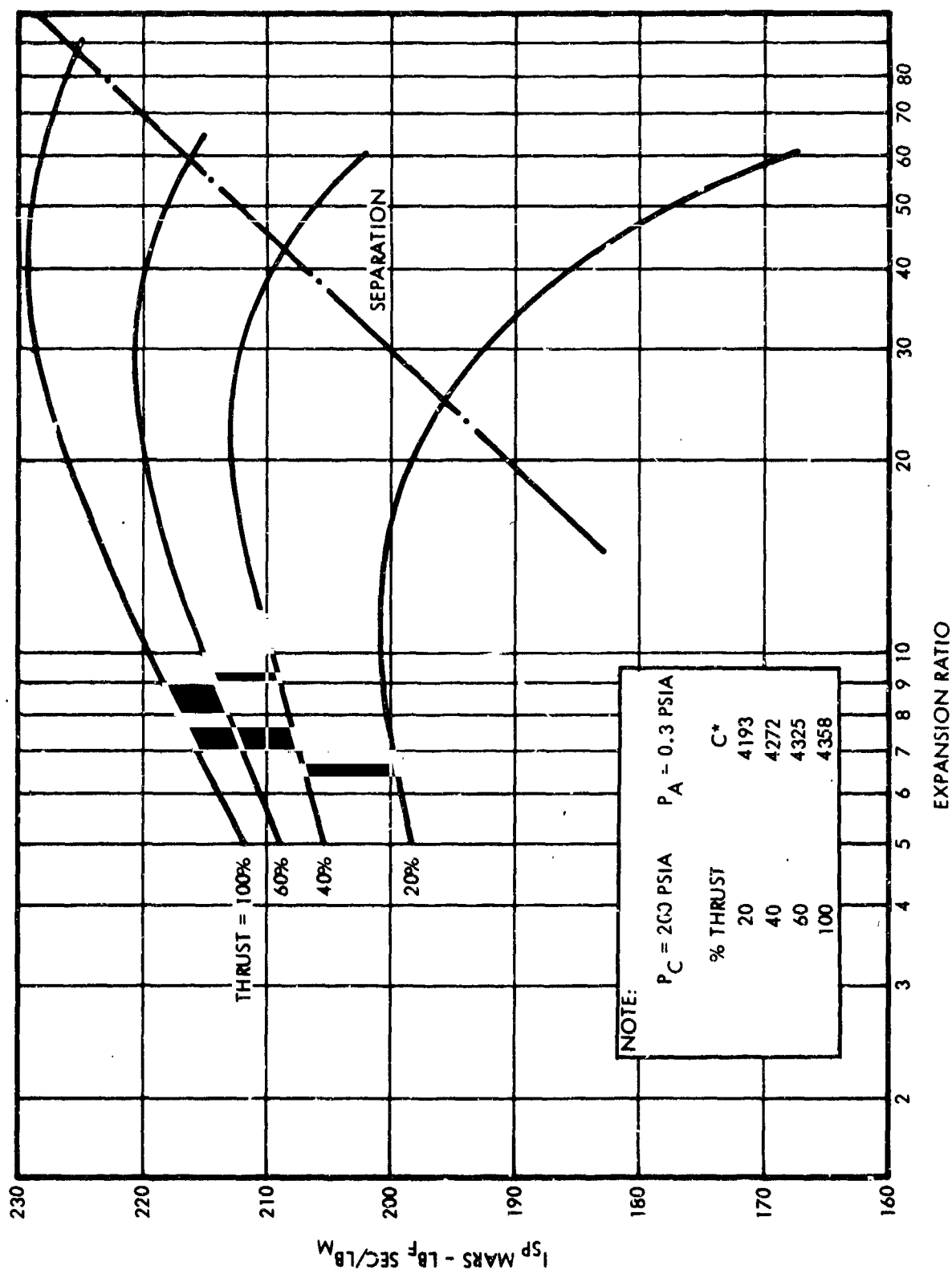


Figure 10. Conventional (System Eight) Catalytic Engine Performance

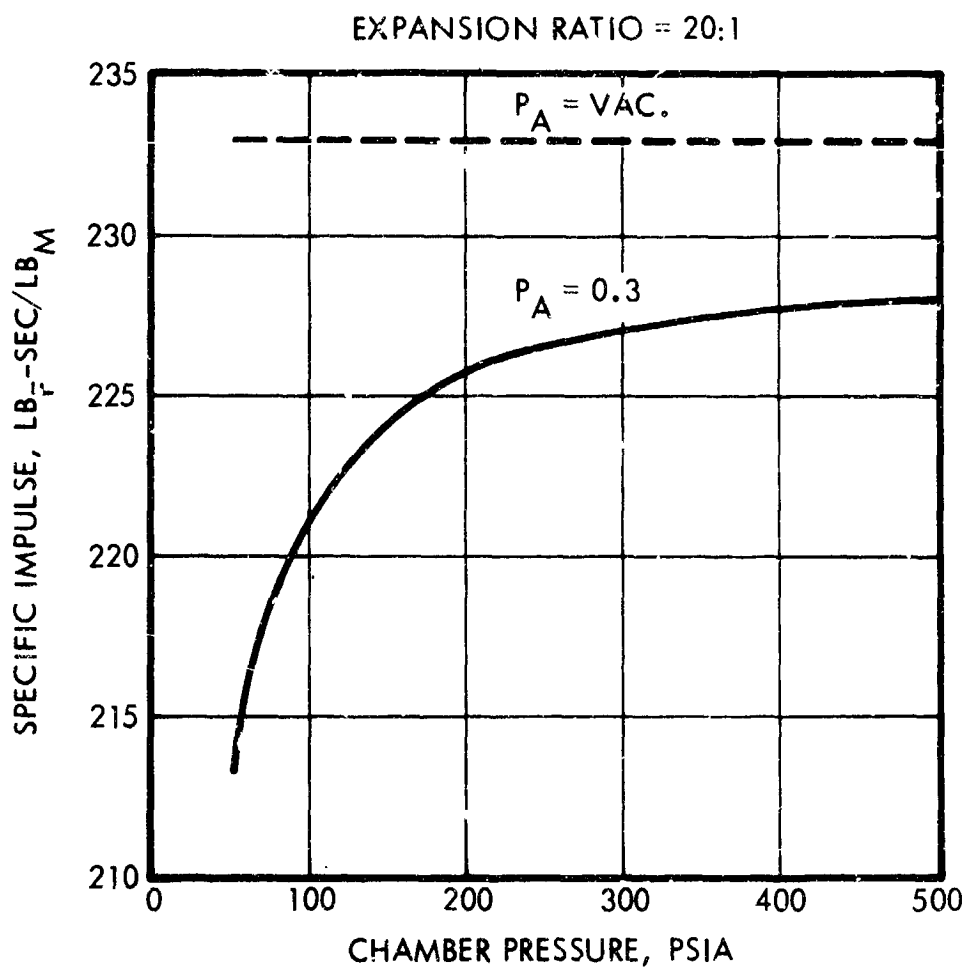


Figure 11. Chamber Pressure Effects on Engine Performance at Full Thrust

### Engine Weight

The engine weight was determined utilizing the detailed weight breakdown computed for each of the preliminary designs as a baseline and employing appropriate scaling criteria. The effects and ranges of the following variables were studied:

Thrust	300, 600, 1200 lbf
Chamber Pressure	50 to 500 psia
Expansion Ratio	5:1 to 80:1

Since the preliminary designs had considered only a thrust level of 600 lbf, the first step was to establish corresponding baseline engine weights for the 300 and 1200 lbf thrust engines. The chamber dimensions were established based on maintaining an arbitrary catalyst bed loading of 0.06 lbf/sec-in<sup>2</sup>.<sup>\*</sup> A minimum wall thickness of .015 inch was maintained for manufacturing reasons. The baseline nozzle thickness contour was based on structural buckling criteria for an expansion ratio of 80:1 and this contour was simply truncated for lower expansion ratios. This technique yielded nozzle weights that were later determined to be somewhat conservative, as shown in Figure 12, but the relative effect on the various engine configurations is identical so that comparisons are valid. The engine weight includes the throttle valve, catalyst (where applicable), screens, retainer and plate, thermal standoff and injector. The plug nozzle engines were sized for a range in expansion ratio, between 20:1 and 40:1. A larger range was not considered practical because the reactor bed imposes size limitations on the annular throat radius. For the expansion deflection engine, a full range in area ratio was investigated since there are no practical limitations on this concept. Based on the results of this study, summarized in Figure 13, the catalytic reactor with a spherical chamber and DeLaval nozzle (System 8) was recommended. This system was selected over the 3-pounds lighter System 5 because the development risk associated with the latter did not justify the small weight gain.

---

<sup>\*</sup>This 0.06 lb/sec-in<sup>2</sup> bed loading is quite conservative and tended to penalize the catalytic thruster configurations. However it had no impact on the outcome of the study.

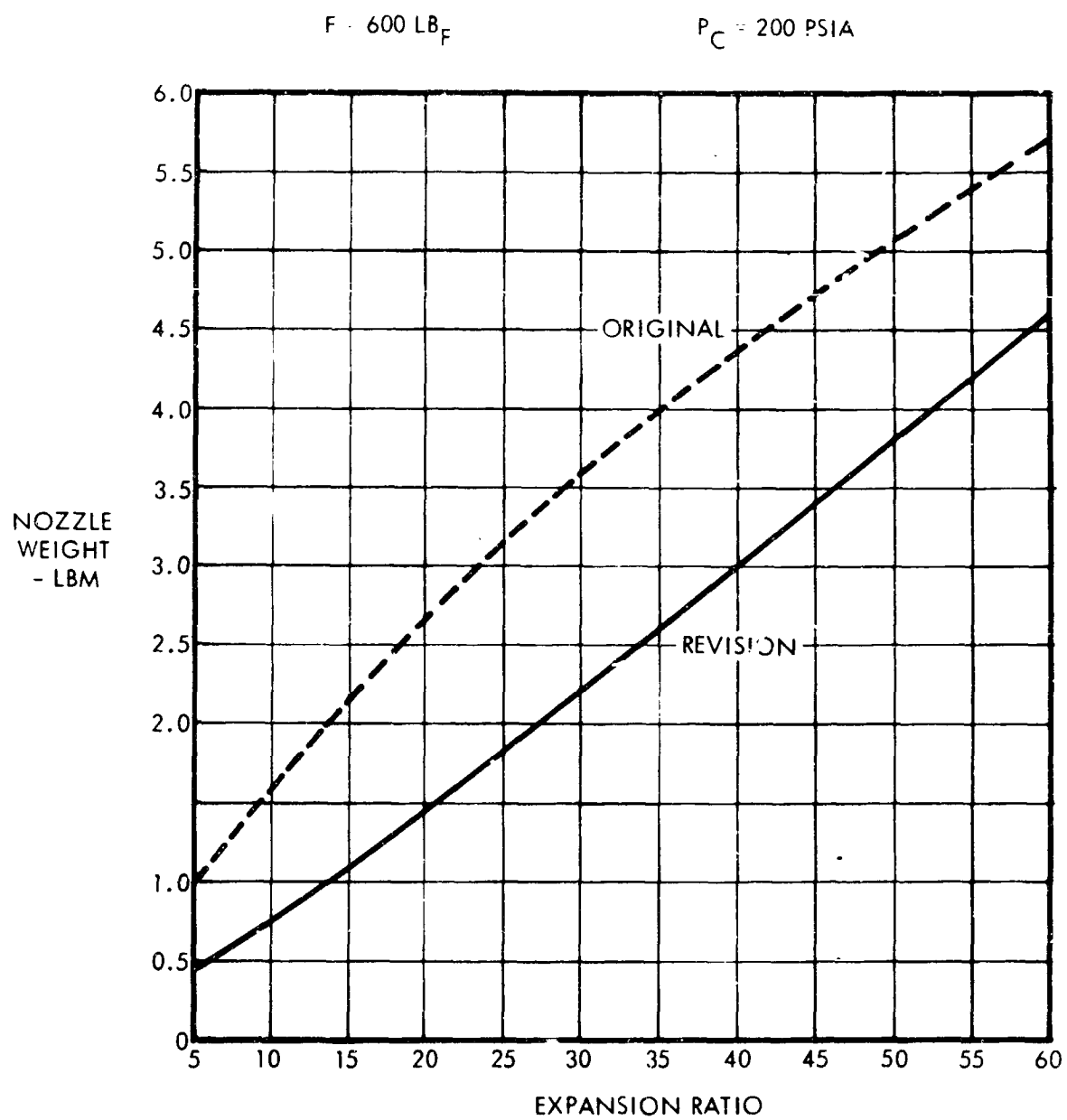


Figure 12. TTS Engine Nozzle Weights

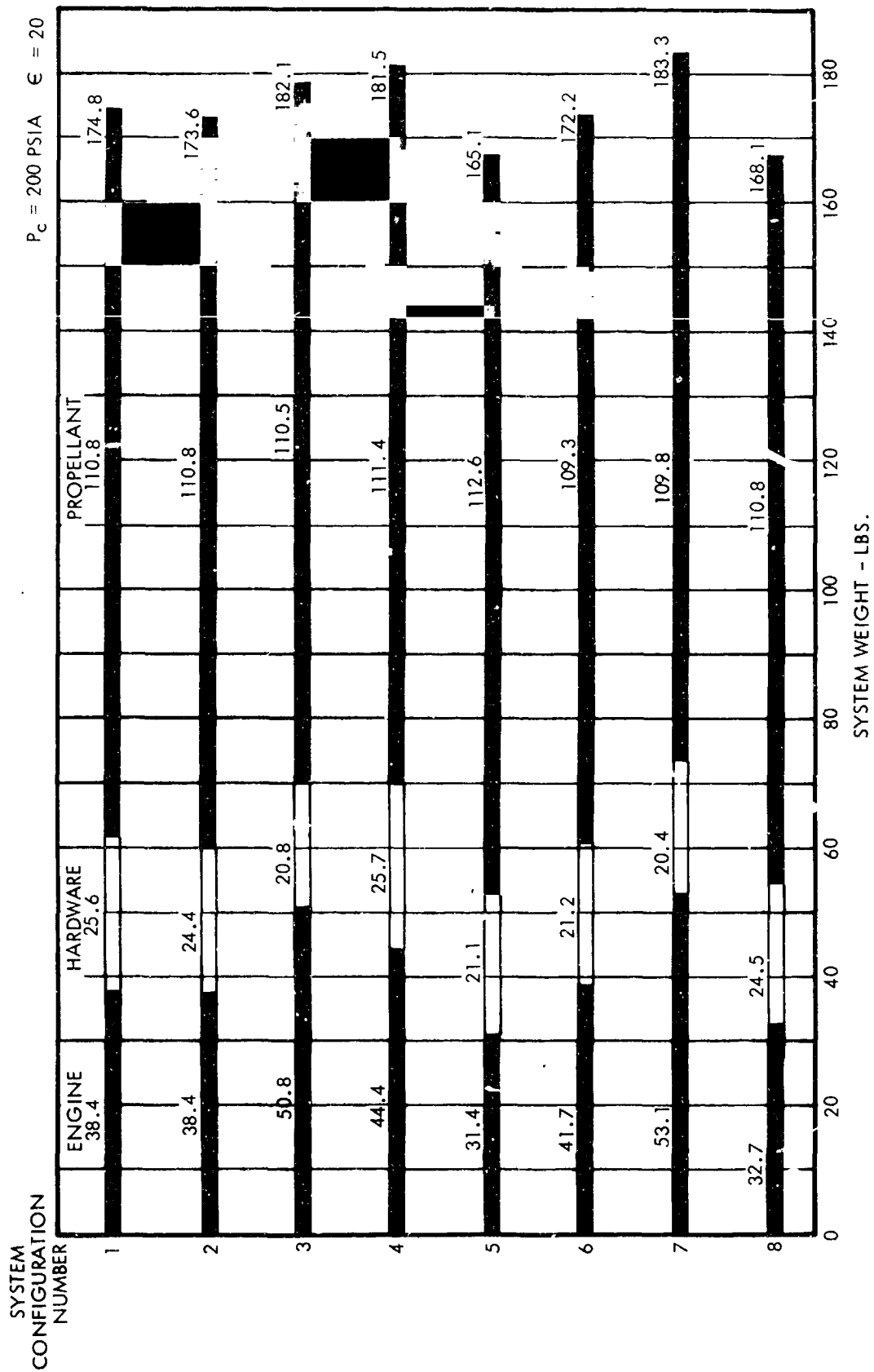


Figure 13. System Weight Comparison - 600 LBF

### 2.1.3 Flow Control System

Selection and mechanization of the monopropellant engine throttling concept was basically governed by the type of reactor used and the desired throttle range. Additional factors which influenced this decision were (1) available tank pressure, (2) injector design requirements, (3) chamber pressure characteristics, (4) engine response, (5) thrust linearity, and (6) integrated throttling/shutoff capabilities.

Thrust control can essentially be implemented at three points in the propulsion system:

- Upstream of the injector
- At the injector
- At the engine throat

Use of any of these methods for a catalytic decomposition engine is relatively straightforward while the thermal decomposition engine generally requires control of parallel flow paths: (1) the pilot stage, and (2) the main reactor. In addition, it is possible to combine actively or passively two of these control modes if there is some advantage to be gained. This section describes the general and specific requirements which were used to select a throttling concept as well as the throttle valves (2) which were selected for further evaluation.

#### System Selection

In order to select a thrust control system, it was necessary to evaluate candidate concepts for each of the three major subassemblies: (1) flow control valve, (2) actuator, and (3) control method.

The flow control concepts evaluated included:

- Non-cavitating throttle valve plus fixed area injector
- Cavitating throttle valve plus fixed area injector
- Variable area injector
- Non-cavitating throttle valve plus constant delta P injector
- Cavitating throttle valve plus constant delta P injector
- Variable throat area nozzle

In order to maintain overall guidance loop stability, it is necessary to provide a thrust versus command signal characteristic (gain) which does not change by more than approximately 2.4:1\* over the total tank pressure range. A summary of the gain ratio characteristics for the various flow control concepts evaluated are presented in Figure 14 and shows that the use of a non-cavitating valve or variable area injector is acceptable for maximum chamber pressure designs below 500 psia. Cavitating valves provide the minimum gain ratio due to their independence of downstream elements (i.e., conductances). In order to minimize this gain ratio (defined as the ratio of maximum to minimum gains at a given throttle setting), a linear relationship is required at the average tank pressure with variations over the pressure range depending upon the type of metering valve selected. The variation in gain ratio as a function of pressure distribution for a 600 lbf maximum thrust engine is shown in Figure 15. This figure was based on a total available tank pressure of 500 psia and shows that as the catalyst bed pressure drop increases, the chamber pressure must be reduced to maintain the flow gain ratio below 2.4:1.

A thrust control system using upstream flow throttling was selected primarily due to its being a proven concept capable of meeting all the design requirements and thus representing a minimum development risk approach. However, a variable area injector system has several potential advantages including weight reduction which warrants further investigation. The primary advantage of the variable area injector is shown in Figure 16 where a comparison of the pressure budget for the eight candidate systems is presented. Systems 3 and 5 use injector throttling.

## 2.2 Phase II - TTS Detail Design

### 2.2.1 System Optimization

At the conclusion of the parametric engine system weight study it was recognized that a more detailed examination of the recommended configuration

---

\*This is based on Viking control requirements as defined at the time of this study.

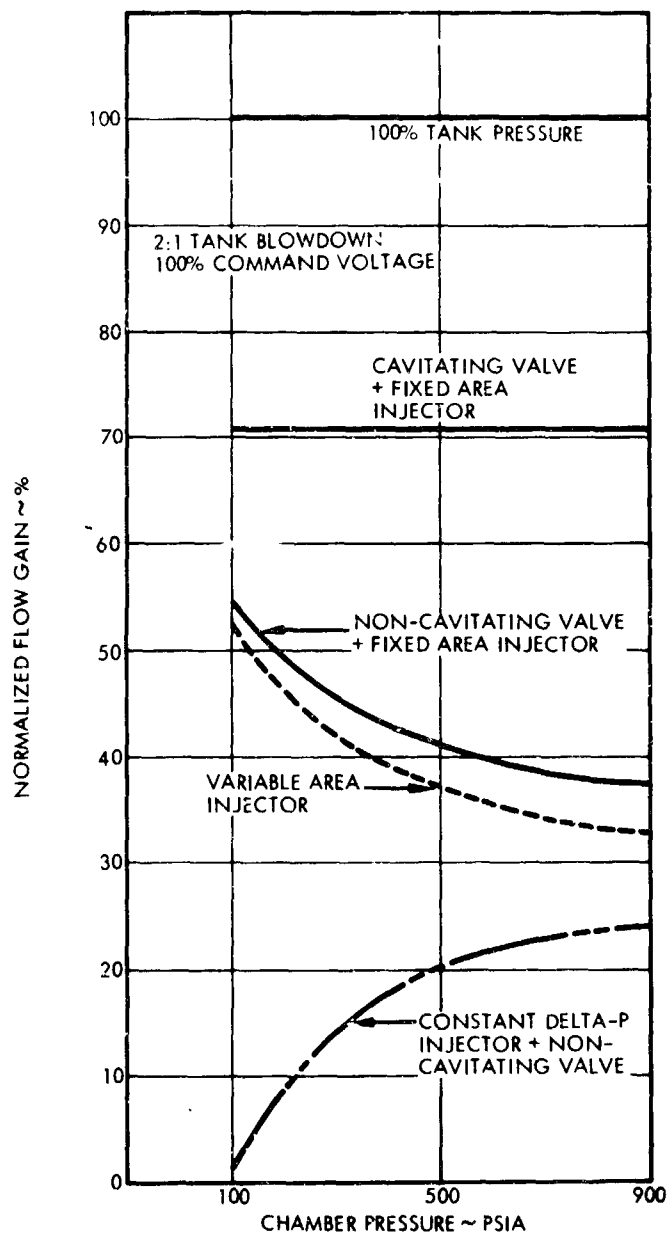


Figure 14. Normalized Flow Gain

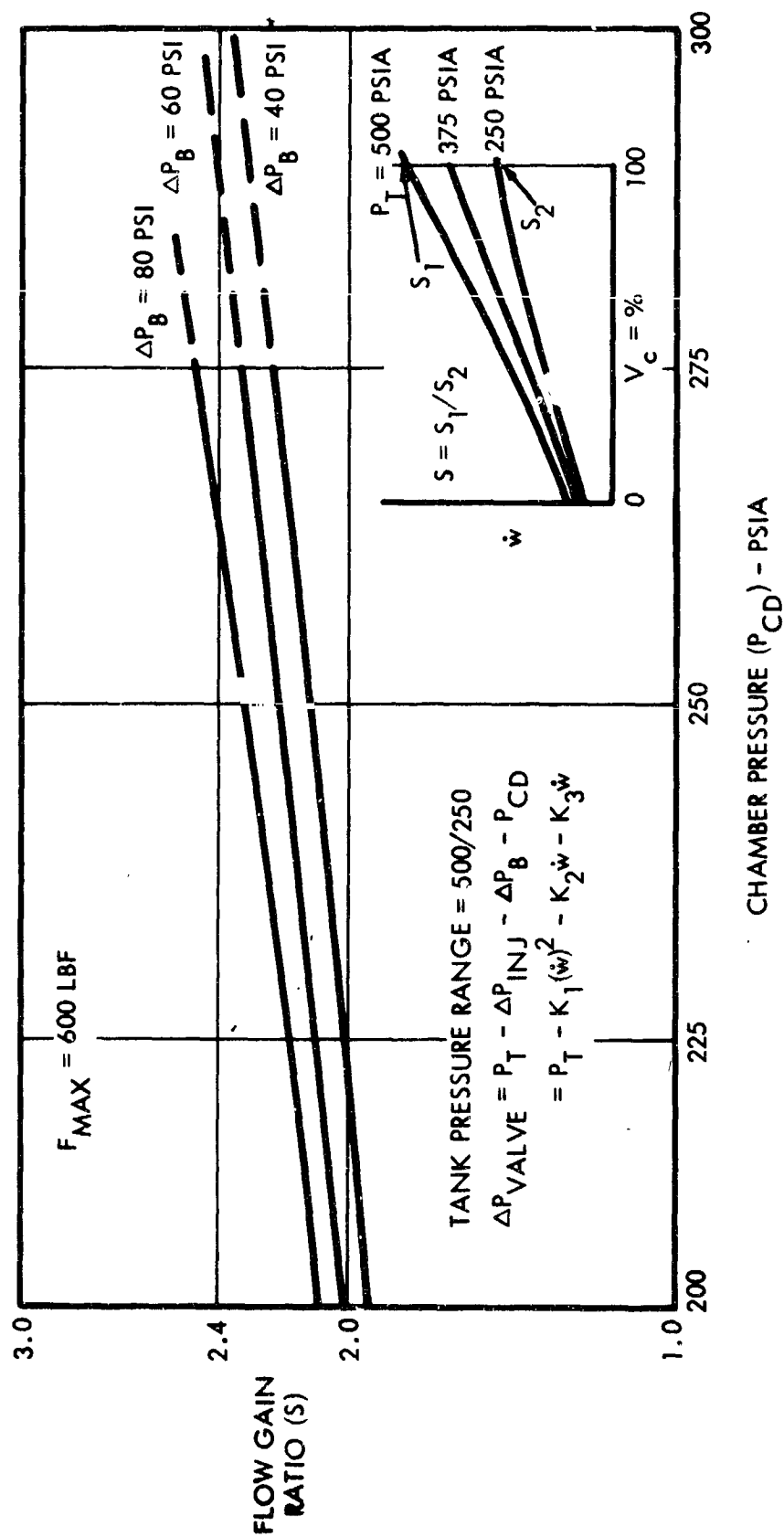


Figure 15. Flow Gain Ratio Versus Chamber Pressure

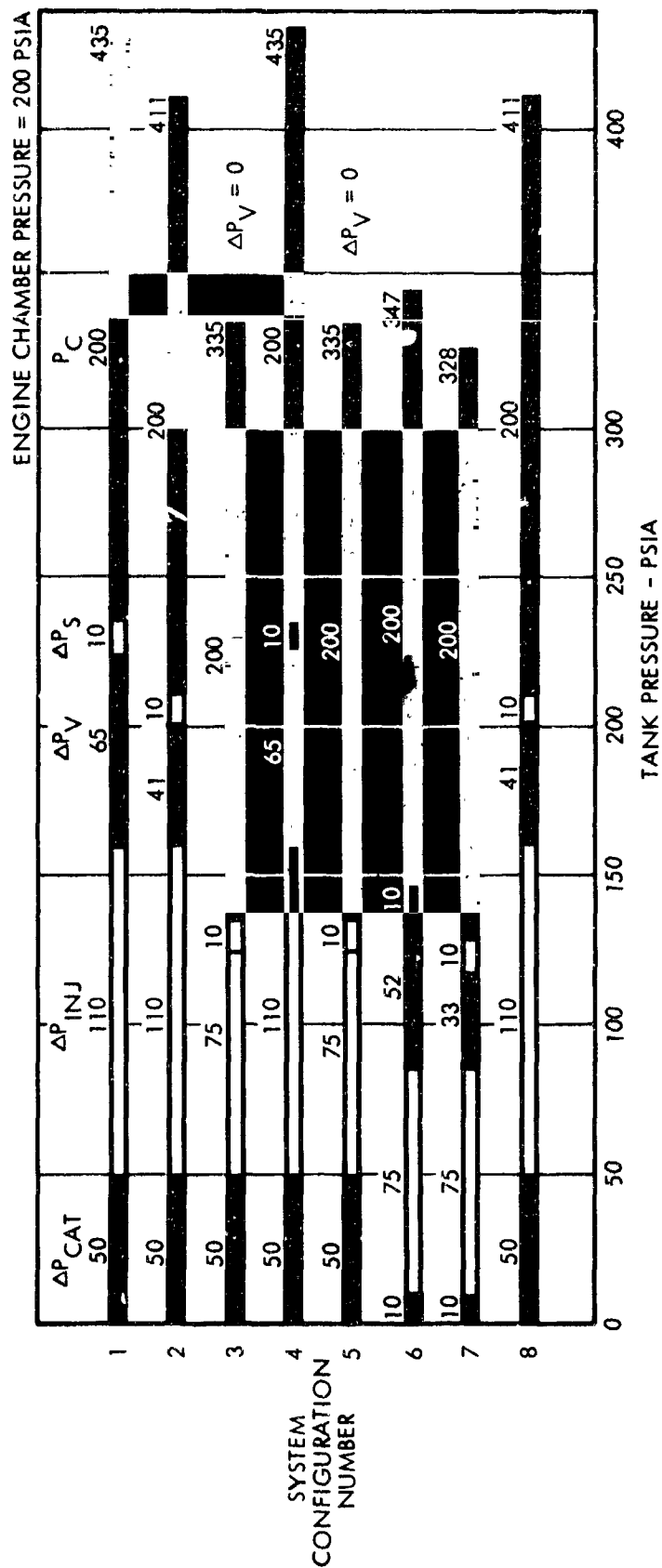


Figure 16. System Pressure Comparison

was required to verify the optimum chamber pressure, chamber diameter and expansion ratio. Thus, the detailed design was focused on a 600 lb<sub>f</sub> thrust catalytic unit and a more precise analysis of thruster parameters influencing system weight was undertaken. The system models were refined to include nozzle/chamber shapes and contours, catalyst bed weight and pressure drop as a function of geometry, performance estimates under various throttling conditions and ambient pressures, and propellant tank weight as related to system operating pressure budget. Thrust chamber, propellant, pressurant, and tank weights were then recalculated as a function of maximum chamber pressure, expansion ratio, and chamber diameter to arrive at optimum conditions.

#### Thrust Chamber Weight

The engine dimensions were computed by varying chamber pressure and diameter as parameters in the following equations. The engine weight was computed by summing the weights of the components:

$$W_E = W_{CH} + W_N + W_{CAT}$$

where  $W_{CH}$  = chamber weight

$W_N$  = nozzle weight

$W_F$  = fixed weight

$W_{CAT}$  = catalyst weight

The weight of catalyst influences the required chamber volume and was approximated from:

$$W_{CAT} = .0495 C \dot{M}^{.554} A_{CAT}^{.446} / P_C^{.306}$$

where  $C$  = empirical anti-flooding constant

$A_{CAT}$  = chamber cross sectional area, in<sup>2</sup>

$\dot{M}$  = maximum flow rate, lb<sub>m</sub>/sec

$P_C$  = maximum chamber pressure, psia

Since the chamber must be designed for the maximum upstream chamber pressure, it was first necessary to compute the catalyst bed pressure drop.

Grant's\* generally accepted packed bed drop equation relating catalyst bed porosity, specific surface area, mass flux, length, and operating pressure to pressure drop was used. The weight of the chamber was then computed from the sum of the shell weight and catalyst retainer weight.

$$W_{CH} = A_S T_S \sigma_S + A_R T_R \sigma_R$$

where  $A_S = \pi D_C^2$  (spherical chamber)

$T_S = P_{CU} D_C / 4$ , shell thickness

while  $A_R = f(V_{CAT}, D_C \text{ and head space})$  from chamber volume versus height subroutine

and  $T_R = (\Delta P_{CAT} D_R^2 / 3.2 \sigma_R)^{1/2}$ , retainer thickness

The nozzle weight was determined from a structural criteria curve input based on the thrust level and expansion ratio while the fixed weight is a constant derived for the particular engine configuration and includes such items as injector, screens, mount plate, thermal barrier, throttle valve and filter.

#### Propellant Consumption

The quantity of hydrazine used for the representative Mars landing mission was based on the thrust profile presented previously in Figure 2. This mission profile was evaluated for a range in thrust level (or total impulse) to identify the approximate payload capability. The thrust-time curve was integrated to obtain a total impulse which corresponds to the approximate lander weight of 1200 lbs for the 600 lb<sub>f</sub> engines. Since the specific impulse of the engine is a function of the throttle ratio, it was necessary to integrate the propellant consumption for each thrust increment by dividing the corresponding total impulse by the specific impulse as follows:

---

\* A. F. Grant, Jr., Basic Factors Involved in the Design and Operation of Catalytic Monopropellant Hydrazine Reaction Chambers, JPL Report No. 22-77, December 1954.

$$W_p = \sum \left[ \frac{F_1 t_1}{I_{s_1}} + \frac{F_2 t_2}{I_{s_2}} \dots + \frac{F_n t_n}{I_{s_n}} \right]$$

#### Propellant Tank Weight

The propellant tank was sized to allow sufficient ullage for employing a nitrogen blowdown pressurization system at a ratio of 2 to 1. A single spherical 6 Al-4V titanium with a safety factor of 2.2 was employed in this study. Assuming an isentropic blowdown with a 50 percent pressure decay, the resultant tank volume is approximately 2.7 times the volume of propellant. Figure 17 shows the effects of specific heat ratio on required tank volume for a range in pressure ratio.

The tank weight was derived from elementary stress relationships and an empirical curve fit of typical flight weight tanks. By combining the above factors, the tank weight can be expressed as:

$$W_T = K_T P_T D_T^{2.35}$$

$$\text{where } D_T = (6ZW_p / \pi p_p)^{1/3}$$

Figure 18 shows the spherical titanium tank weight data as a function of pressure and diameter.

#### Pressurant Weight

Propellant tank pressure was determined by summing the chamber pressure and system pressure losses at full thrust for each system. With the initial tank pressure and volume established, the pressurant weight was computed from the perfect gas law.

#### System Weight

The system weight was based on the simplified propulsion system concept shown in Figure 1 and does

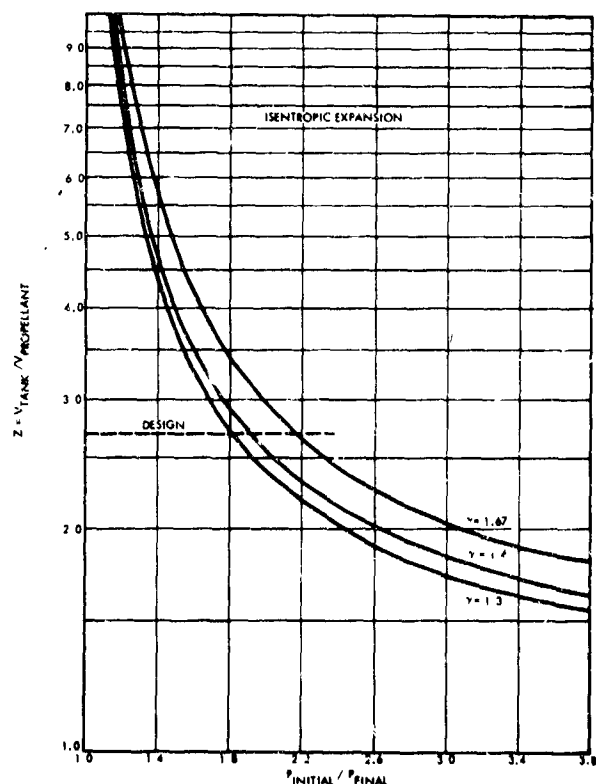


Figure 17. Propellant Tank Volume Ratio

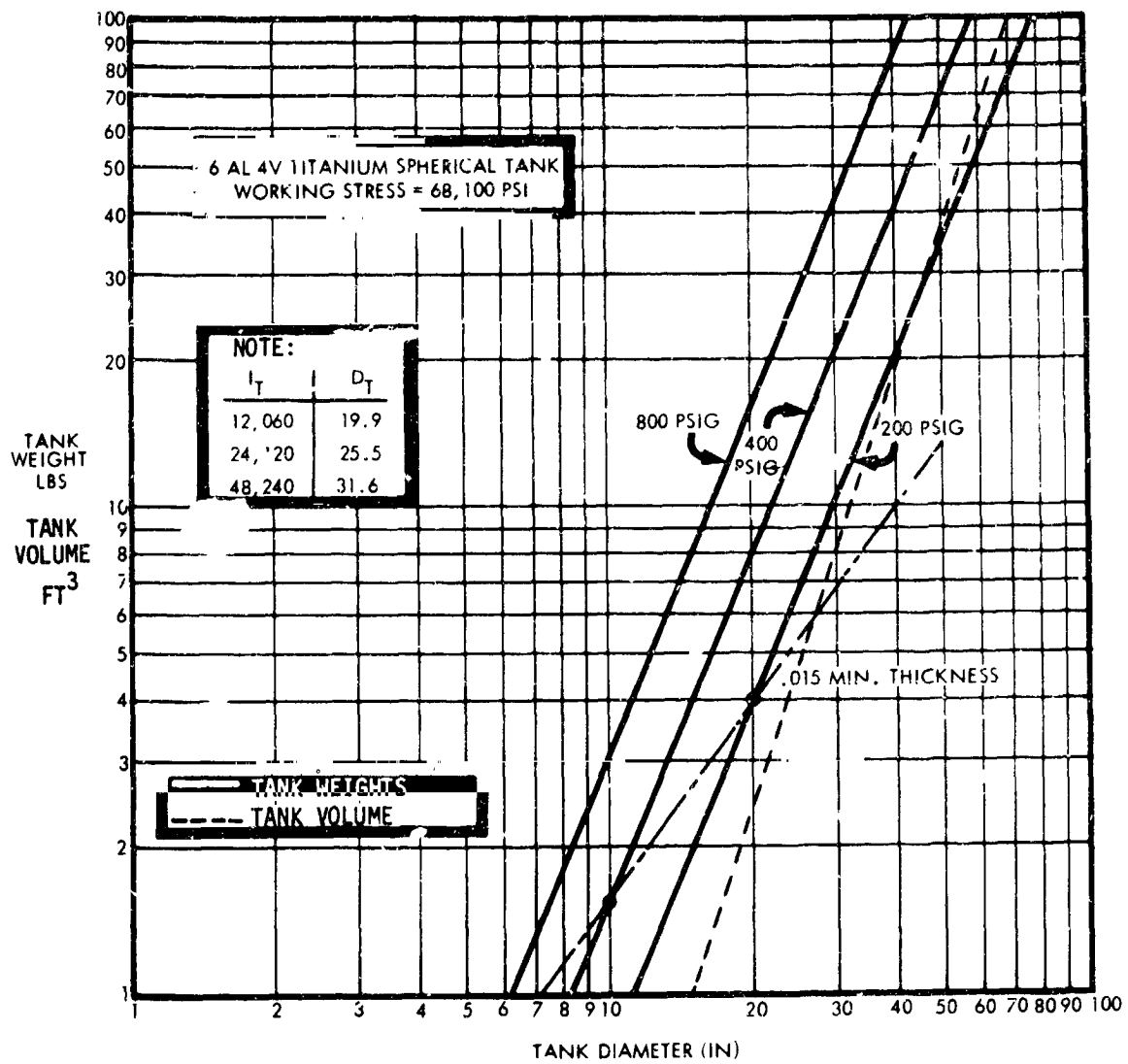


Figure 18. Spherical Propellant Tank Weight

not include payload, support structure or avionics. The expression for system weight can then be stated as:

$$W_s = 3W_E + W_p + W_T = W_{gas} + W_c$$

The component weight ( $W_c$ ) includes two squib actuated valves, a filter and associated service connections and plumbing and was fixed at 5 pounds for the 600 lb<sub>f</sub> thrust, 1200 lb<sub>m</sub> payload case.

### Results

The engine design optimization studies were performed not only for a range in engine chamber pressure, chamber diameter and expansion ratio, but also considered two chamber geometric shapes: spherical and  $\sqrt{2}$  major/minor axes ratio elliptical. A comparison of the two designs is shown in Figure 19 with some of the more significant facts tabulated. The increased dimensions and appreciable increase in volume with potential reduced response were the primary factors in the elimination of the spherical chamber despite its slightly lighter weight.

In determining the optimum chamber shape and more importantly the chamber pressure and diameter, a careful assessment of the catalyst bed pressure drop is required. An inspection of the appropriate equations indicates that if the chamber pressure is too high the propellant tank weight becomes excessive, while with low chamber pressures the system weight may also be increased due to lower engine specific impulse and high catalyst bed pressure drop. This situation is illustrated in Figure 20. The effects of chamber pressure and shape on system weight are shown in Figure 21. This figure is representative of a family of plots for chamber pressures of 150 to 400 psia.

The results of the engine design optimization study are shown in Figures 22 and 23. These are compilation plots of the optimum conditions for each chamber pressure for atmospheric pressures of 0.3 and 0.1 psia, respectively. Figure 22 shows that for the atmospheric pressure of 0.3 psia, the optimum chamber diameter was 6.0 in., the expansion ratio was 19.6 and the chamber pressure was 280 psia. The calculations were repeated for an atmospheric pressure of 0.1 psia, which is nearer the

THRUST = 600 LB<sub>F</sub>  
 CHAMBER PRESSURE = 200 PSIA  
 EXPANSION RATIO = 20:1  
 $P_A = 0.3$  PSIA

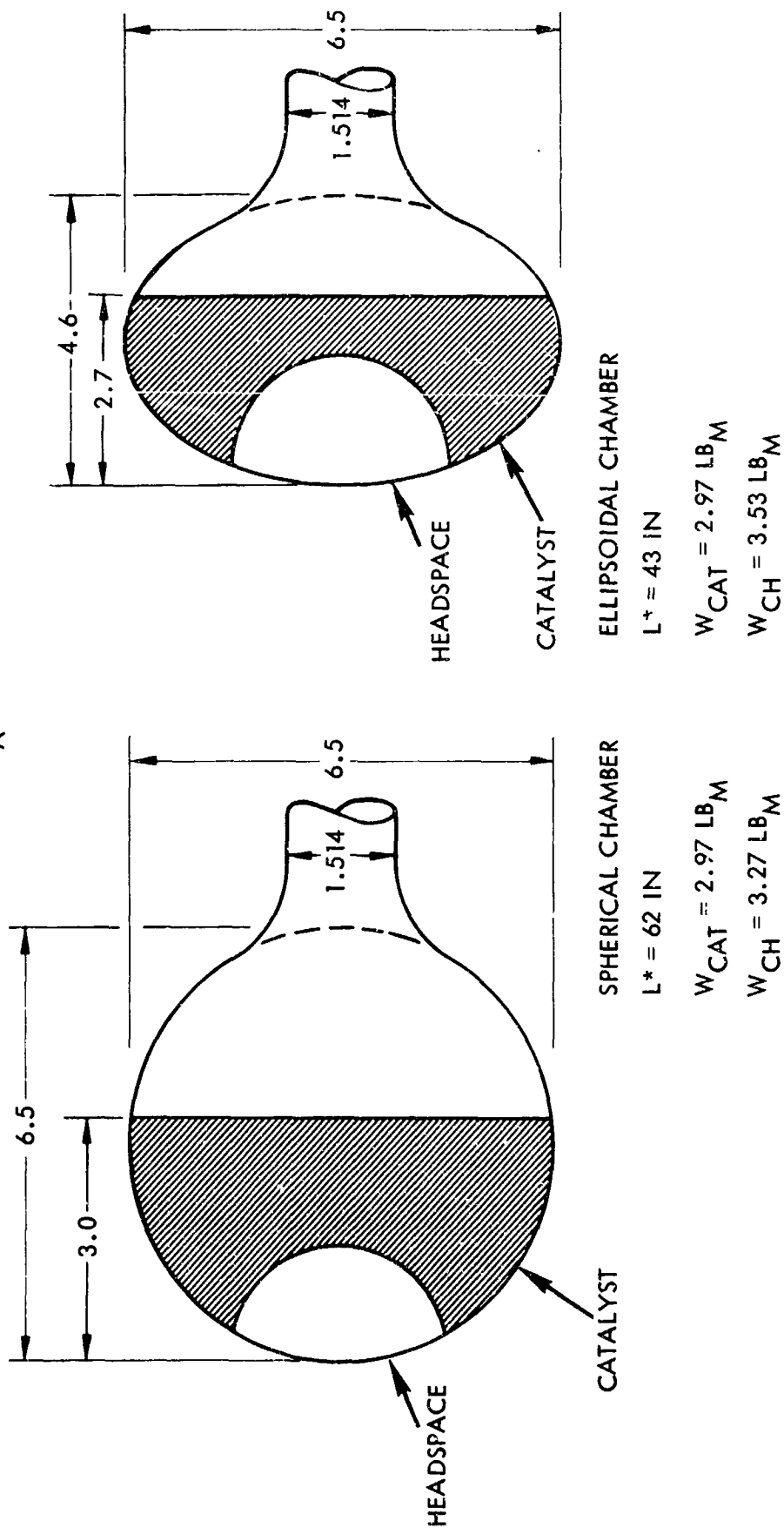


Figure 19. Spheroidal Chamber Comparison

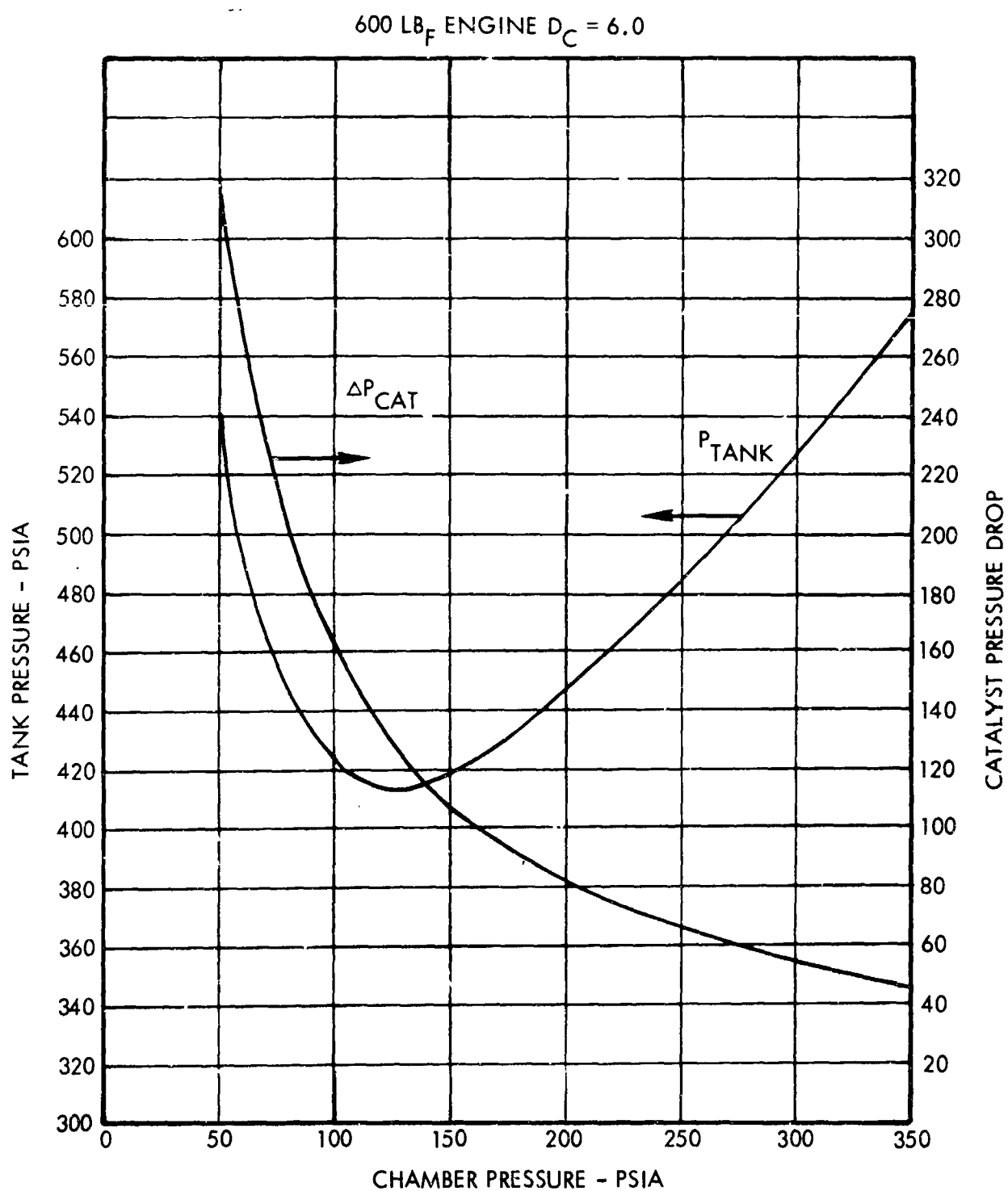


Figure 20. Effects of Maximum Chamber Pressure on Tank Pressure

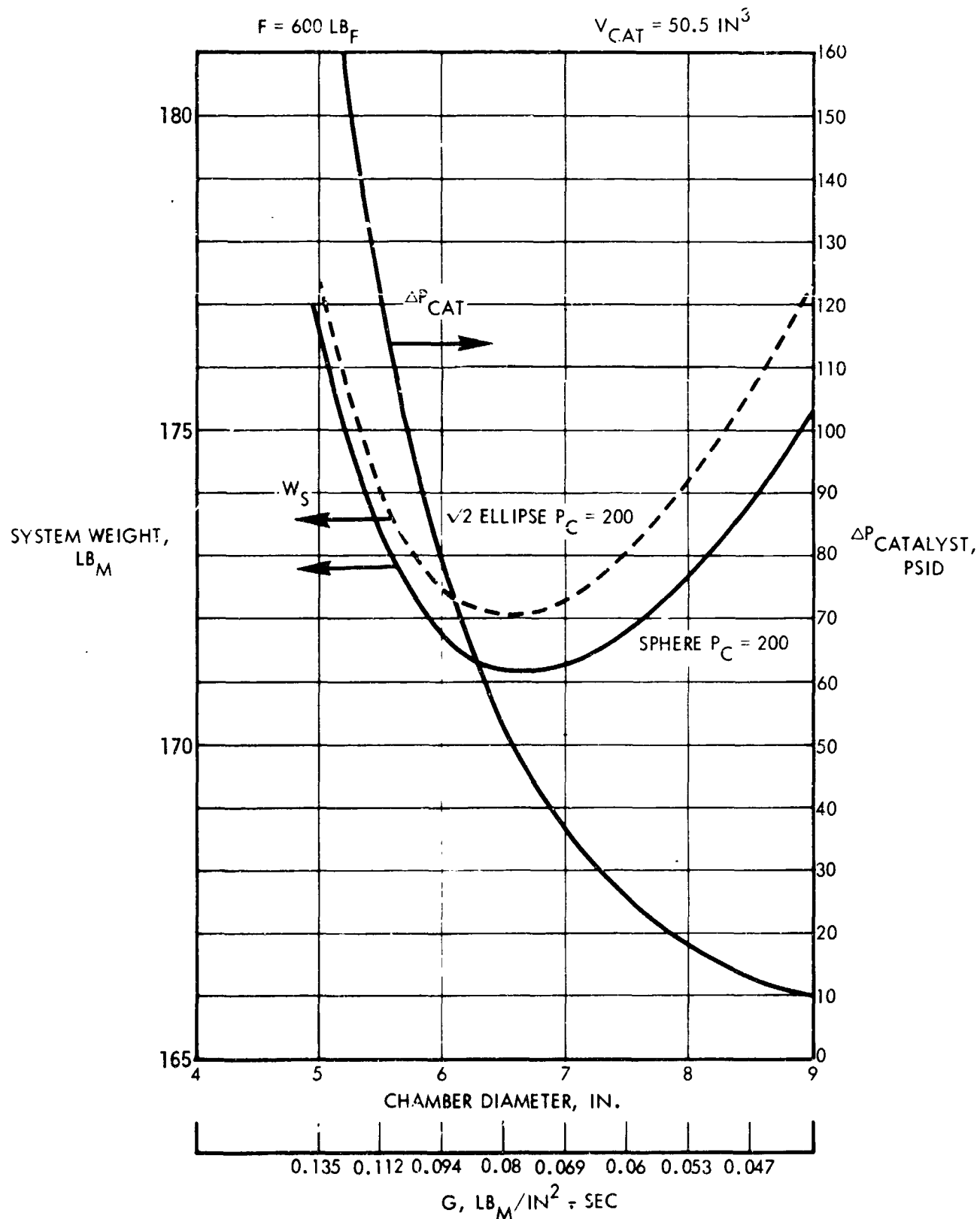


Figure 21. Engine Chamber Diameter Optimization

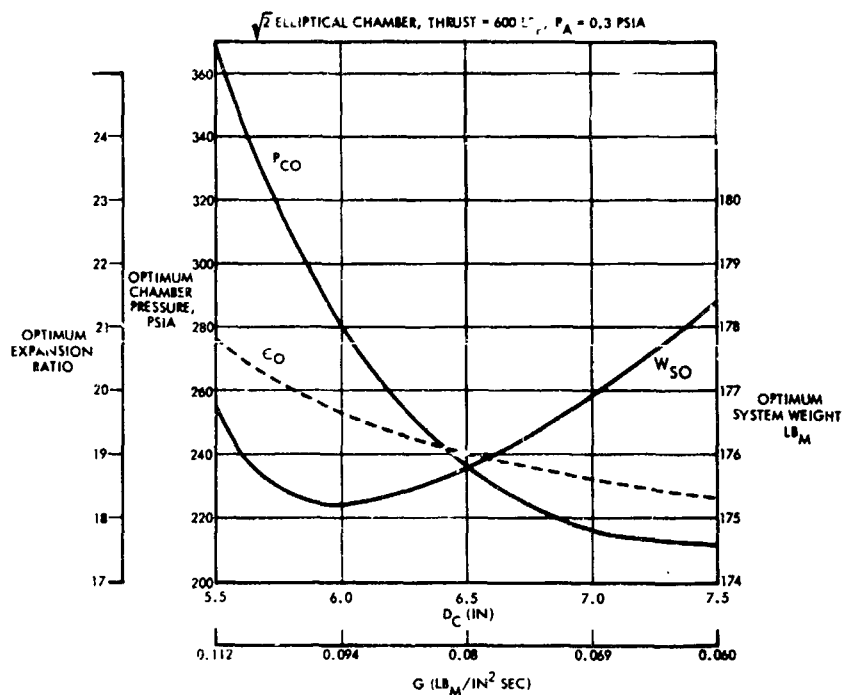


Figure 22. Optimum Chamber Diameter and Design Parameters,  $P_a = 0.3$  psia

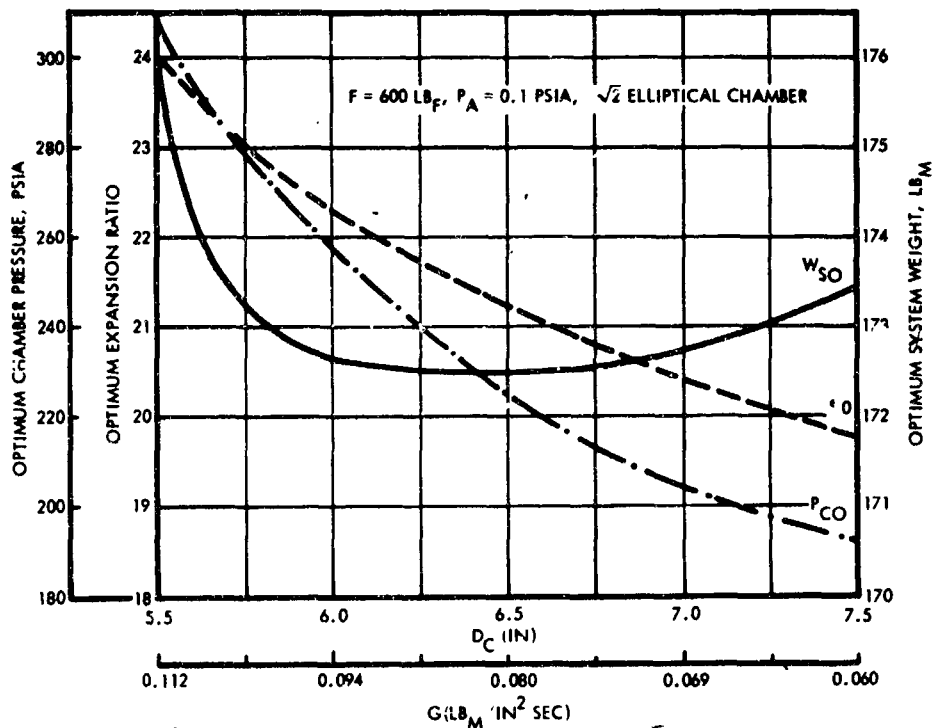


Figure 23. Optimum Chamber Diameter and Design Parameters,  $P_a = 0.1$  psia

expected value for the Mars surface pressure,\* and the results are shown in Figure 23. In this case the optima were:  $d_c = 6.5$  in.,  $p_c = 225$  psia and  $\epsilon = 21.2$ . Based on these results, the parameters selected for the TTS design were:  $d_c = 6.5$  in.,  $\epsilon = 20:1$ , and  $p_c = 200$  psia. The selection of a chamber pressure slightly below the nominal calculated is justified by the tendency toward a lower optimum point for increased  $\Delta V$  missions and the pressure budget margin afforded to improve valve linearity, thruster matching, and system design contingency. Note that the overall system weight penalty for this pressure margin is less than 1 pound in 172.

#### 2.2.2 System Design

The detailed mechanical design of the TTS was thus initiated based on the study results. The primary improvements to the design as conceived at the end of the Phase I were:

- Optimization of the chamber pressure at 200 psia and expansion ratio at 20:1
- Selection of a  $\sqrt{2}$  elliptical chamber rather than a spherical design to improve the volumetric efficiency
- Increasing the chamber diameter from 6.0 to 6.5 inches to reduce catalyst pressure drop and propellant mass velocity
- Changing the cylindrical thermal barrier to a conical design to alleviate chamber stress
- Incorporation of a TZM cantilever catalyst support plate
- Development of a six bolt mount plate with overcenter loading and thermal insulator to improve design efficiency
- Improvement in the throttle valve service ports to reduce overhang and optimize integration with the engine.

The resulting design is shown in Figure 24\*\* with the LTV electro-mechanical throttle valve. The design also provides for mounting of the Moog rotary valve and will accept an adapter plate between the thrust

---

\*Based on Mariner '69 data, the Martian atmospheric pressure is nearer 0.1 psia than the conservative 0.3 psia assumed originally.

\*\*This Figure represents the final design (see Section 2.3.3).

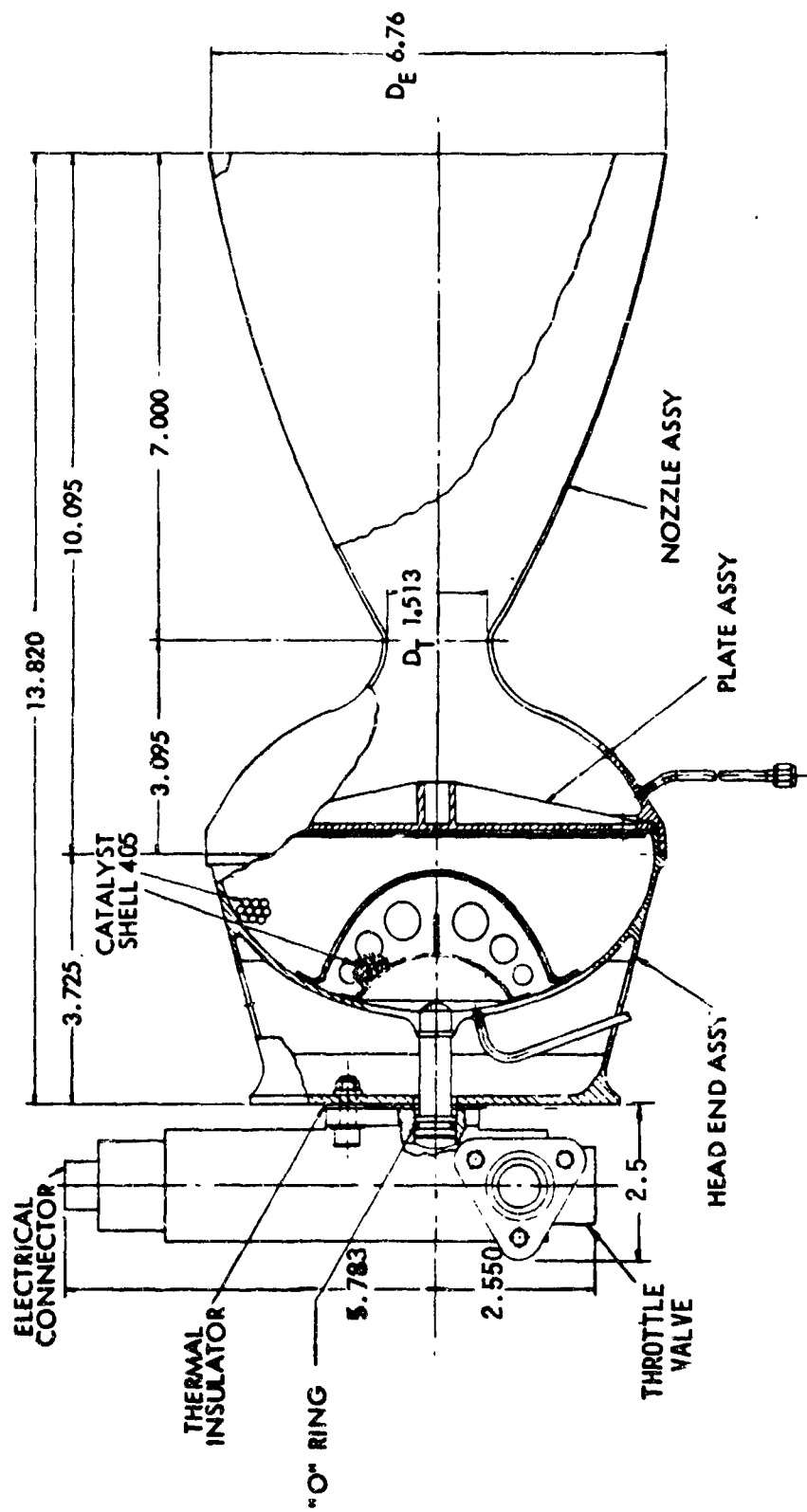


Figure 24. Throttleable Thrustor System Final Configuration

chamber and valve to provide measurement of pressure in the injector. Pertinent analyses and component designs are discussed below.

A propellant inlet filter (not shown) is also provided on the valve inlet. This filter has a 35 micron absolute rating and is capable of handling 0.25 grams of AC fine dust with a maximum drop of 10 psi at rated flow. The selected design incorporates a conical pleated screen element which has been qualified on a previous TRW program. Since the unit was built basically for ground testing, a flight weight design could possibly reduce the weight as much as 50%. The filter is made entirely of 300 series stainless steel, and is of an all welded construction.

#### Thermal Analysis

A primary consideration in the design of the TTS was the heat transfer from the reactor to the throttle valve. Temperature profiles were established for two baseline designs; one employing a cylindrical thermal barrier attached to a relatively cool section of the thrust chamber and one employing a conical thermal barrier attached to a relatively hot section of the chamber outside diameter. A schematic of the model is shown in Figure 26. The results of these studies indicated that relatively modest temperatures are expected at the throttle valve with either design. The most extreme temperature environment was determined to be for a 67 second 20% thrust test based on the 24,120 lb<sub>f</sub>-sec total impulse requirement. This data was used in determining the thermal stress in the thrust chamber and thermal barrier. Typical resultant temperature distributions are shown in Figures 26 and 27 for the selected conical thermal barrier. As Figure 27 shows, the EPR injector "O" ring seal remains below the 275°F sterilization temperature at all times; therefore heat soak following shutdown is not expected to present any problems. The heat balance at the valve chamber interface is shown in Figure 28. As indicated, the temperatures at this location are so low that very little heat is lost by radiation. Details showing the method of reducing the thermal stress in the head end assembly is shown in Figure 29. The access holes were provided to facilitate valve mounting and serve no purpose thermally.

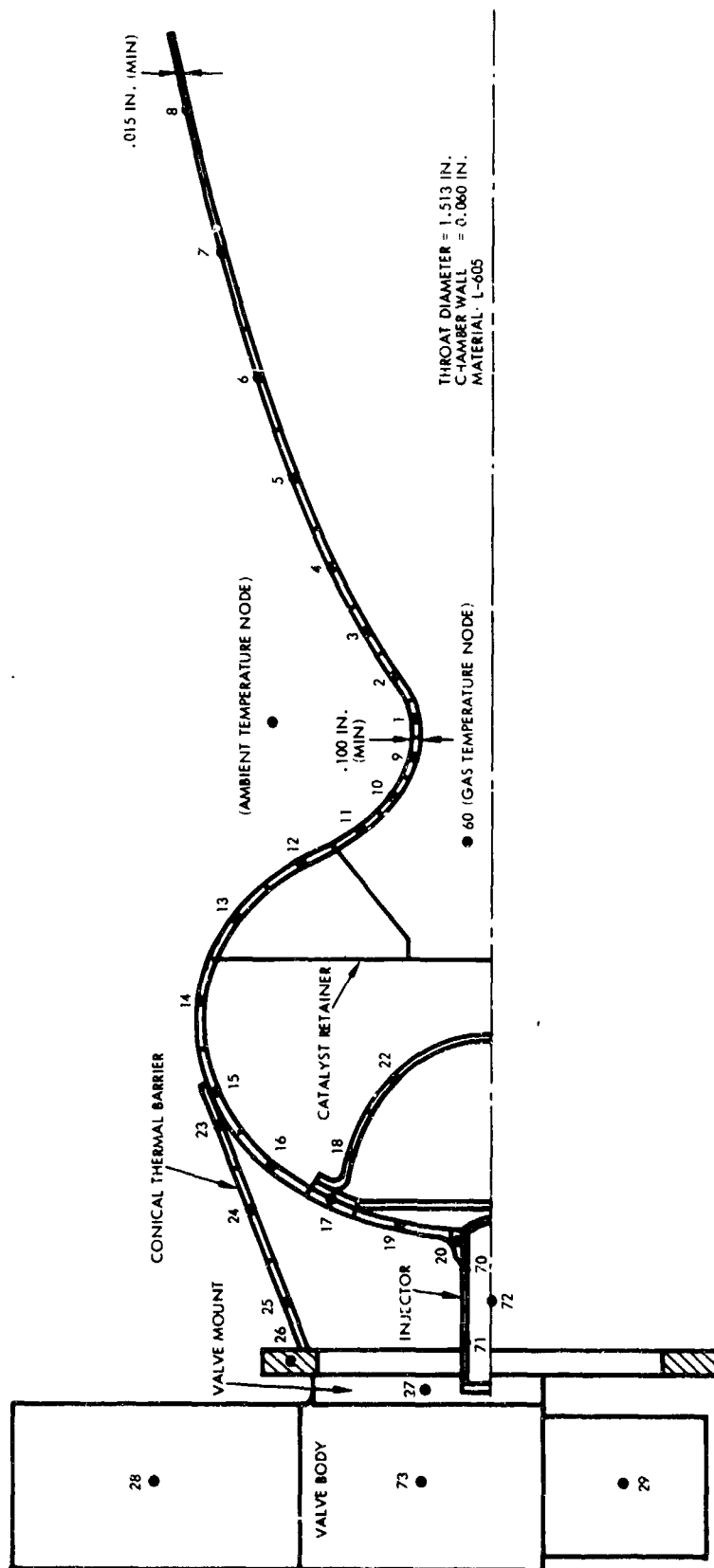


Figure 25. Torispherical Chamber with Conical Thermal Barrier

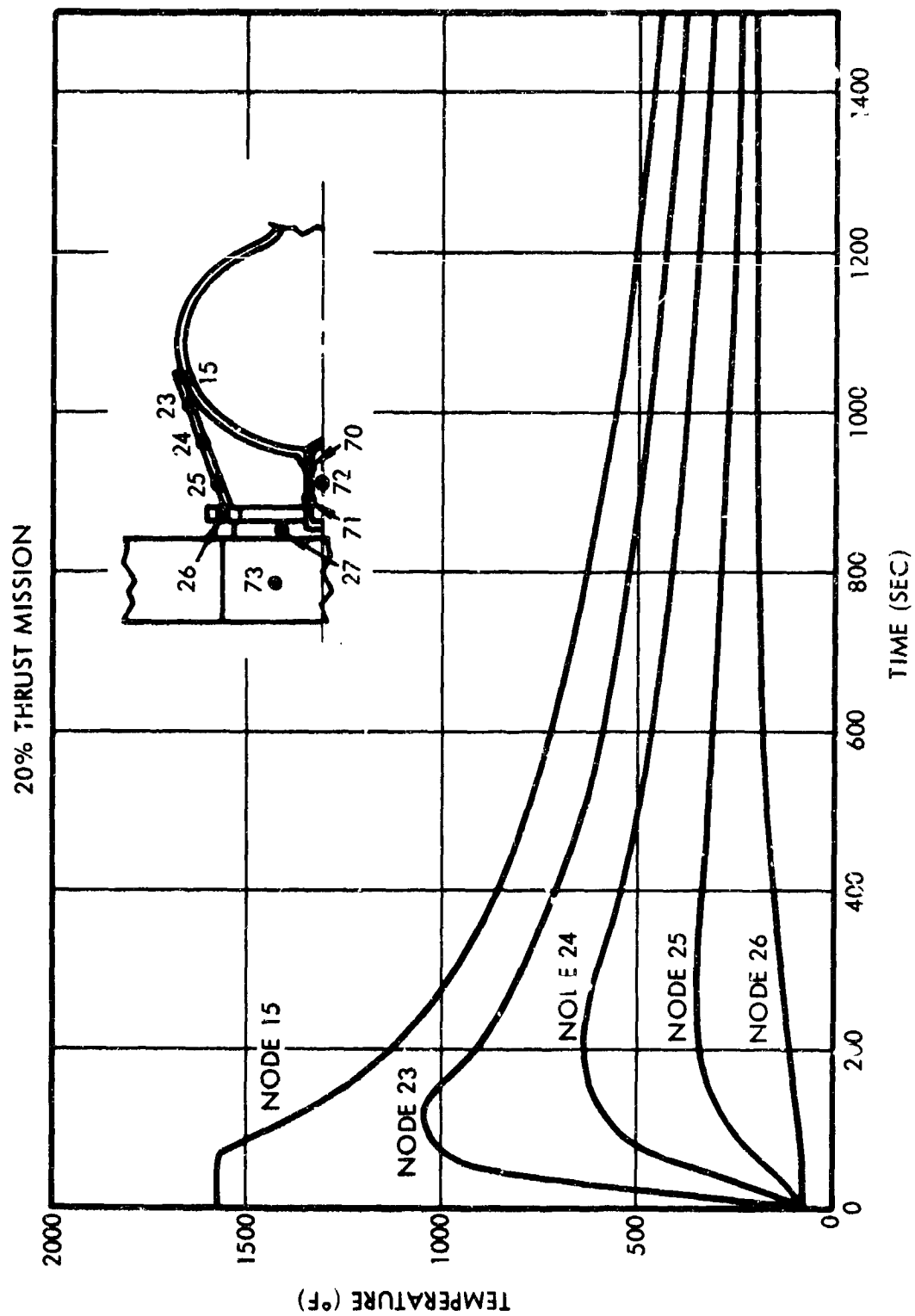


Figure 26. Temperature History of Ends of Conical Thermal Barrier

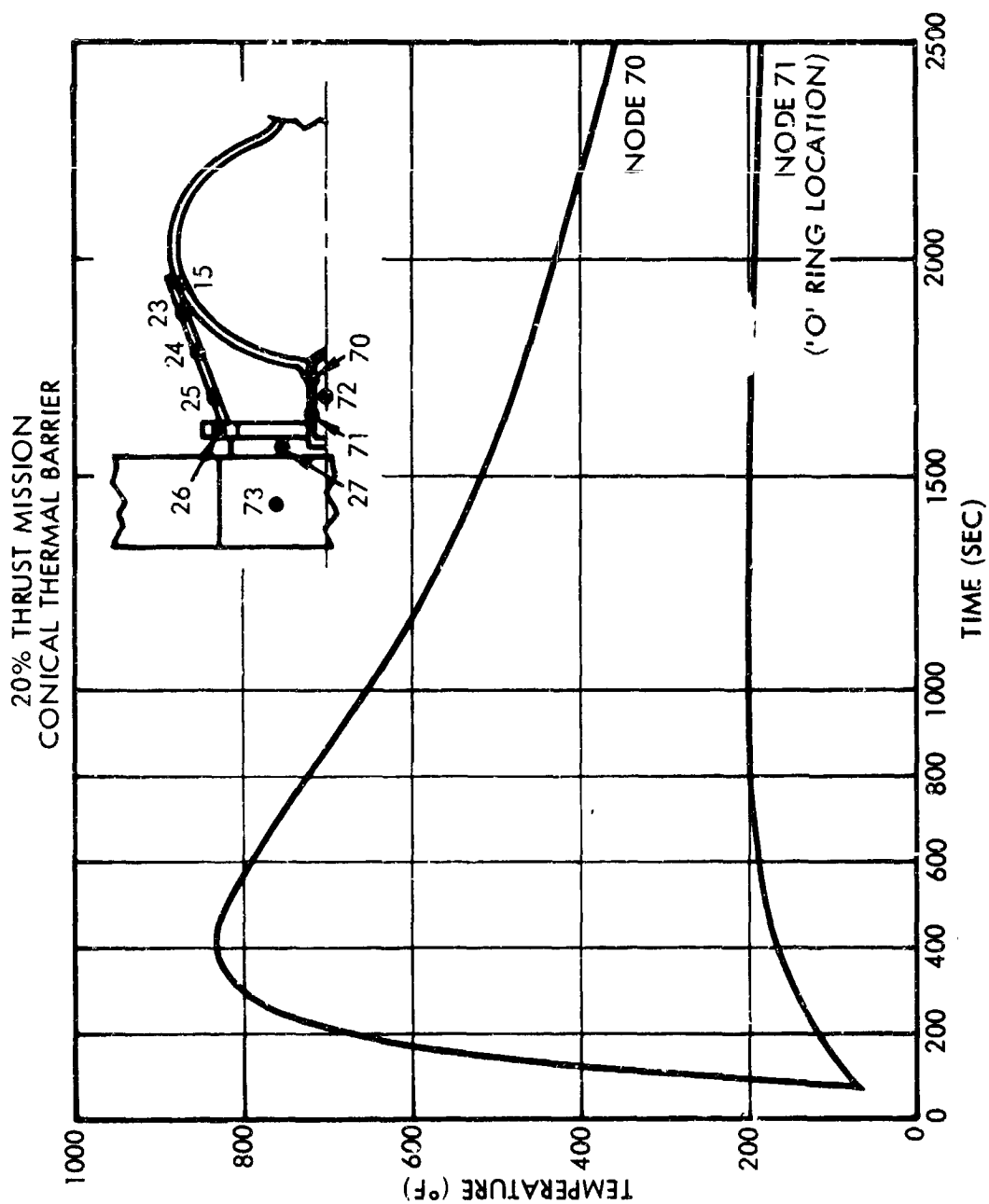


Figure 27. Temperature History of Ends of Injector Tube

**(NODE 27)**

20% THRUST MISSION

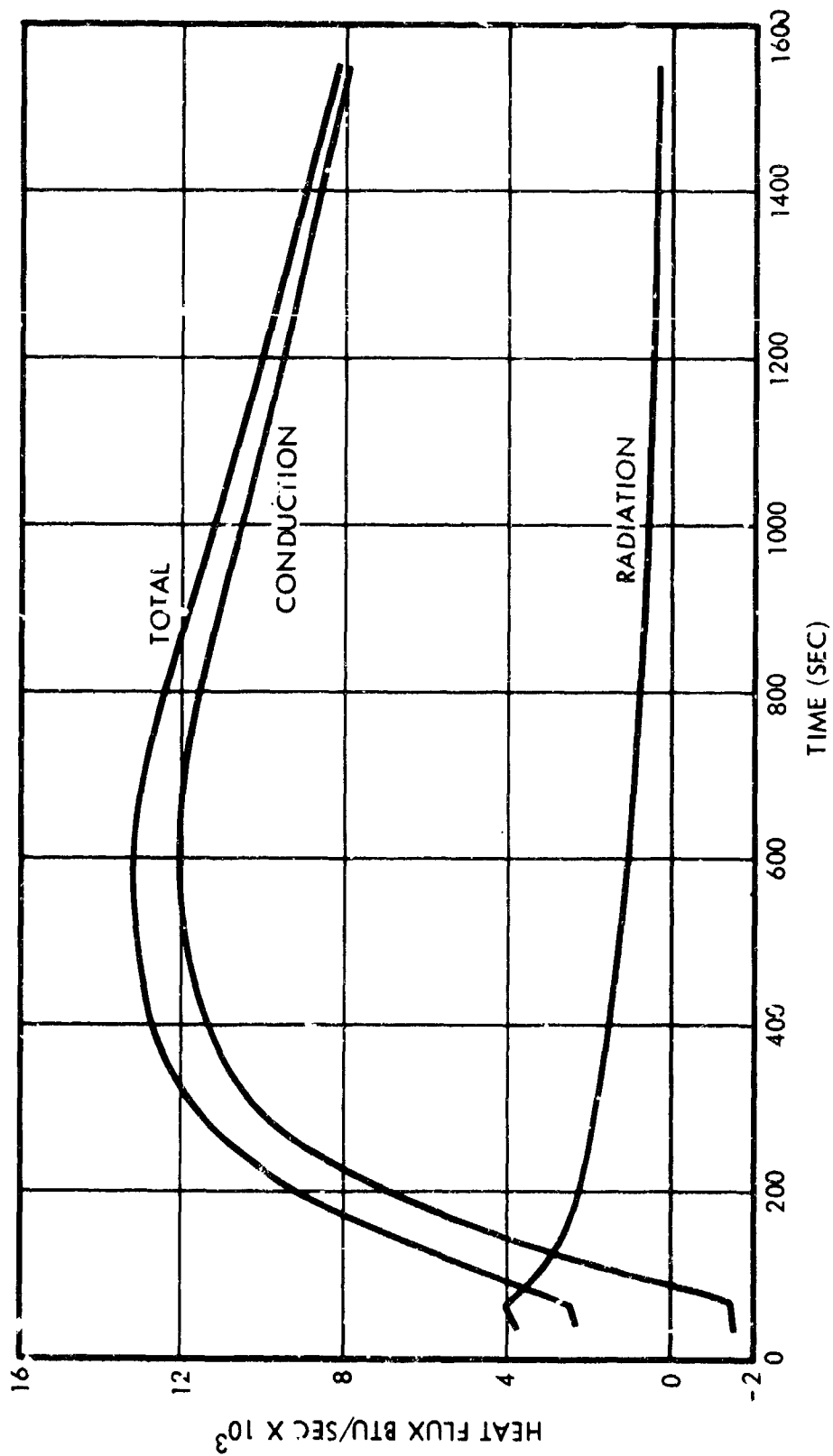


Figure 28. Heat Balance at Valve/Chamber Interface

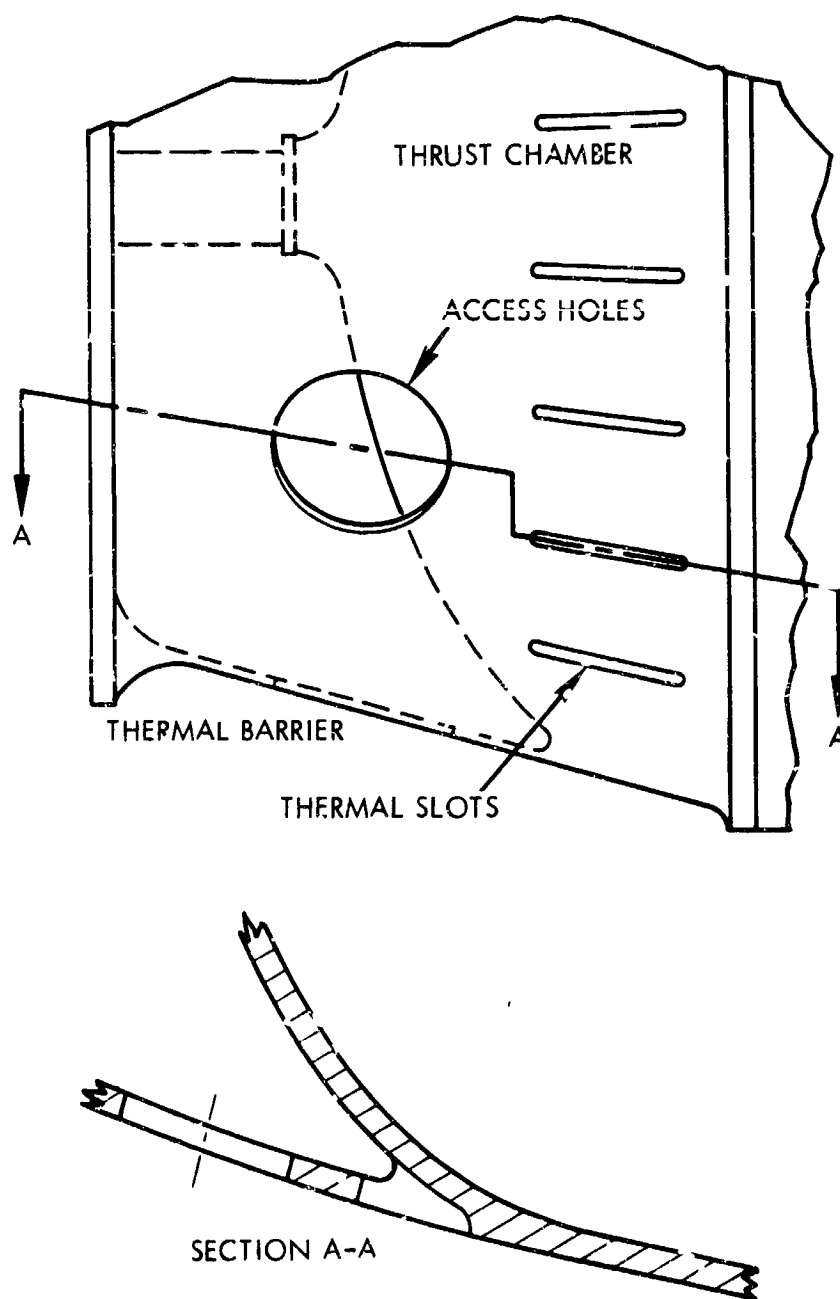


Figure 29. Thermal Stress Reduction Technique

### Stress Analysis

The stress analysis performed on the Throttleable Thrustor System considered both steady state and dynamic (vibration) loads in addition to thermal stress effects. The results of the steady state analysis are presented in Table 5. It may be noted that in all cases a positive margin exists in the assembly. As a result of this analysis the conical thermal barrier and overcenter mount plate were selected for maximum structural efficiency. In addition, an edge supported catalyst retainer plate was recommended to reduce thrust chamber stresses.

The dynamic analysis considered three modes of structural compliance: shear displacement of the nozzle cone, rotational displacement of the cone and rotational displacement of the throat. The mass and rotational inertia of two rigid body mass components were considered: 1) the chamber and catalyst, and 2) the nozzle downstream of the throat. Structural natural frequencies were found to be 657, 1406, and 2094 Hz. No gross design changes were required as a result of this analysis which was based on the vibration spectrum shown in Figure 30.

When stress analysis indicated that the pressure sense lines for  $p_{cu}$  and  $p_{cd}$  should be of minimum size to reduce discontinuity stresses, a study was initiated to investigate the effects of sense line diameter on transducer response. Since the expected chamber pressure oscillations are less than 200 Hz, the response and amplification of 1/8 x 3 inch lines were determined to be well within acceptable tolerances. In addition, a response test was performed on a TRW experimental engine with parallel transducers attached with 1/8 and 1/4 lines and only a negligible attenuation was observed.

#### 2.2.3 Throttle Valve Design

Specification EQ 2-229 (Appendix A) was prepared for the flow control assembly and a procurement was initiated based on this specification. The nominal flowrate versus command voltage schedule was specified at the mid tank pressure (360 psia) to minimize variations in system gain over the 2:1 blowdown range as previously discussed. A maximum allowable pressure loss of 50 psid at maximum flow (2.61 lbs/sec at maximum thrust) and maximum tank pressure results in the pressure schedule of Table 6.

Table 5. Stress Analysis Results Summary

SECTION	DESCRIPTION	MATERIAL	THICKNESS IN.	YIELD MARGIN OF SAFETY
1	CHAMBER	L-605	0.06	+ 0.09
2	CHAMBER INJECTOR INJECTOR AT CHAMBER	L-605 L-605	0.10 0.03	+ 0.84 + 0.56
3	CATALYST RETAINING PLATE EDGE SUPPORT	L-605	0.06 TOP SEC 0.10 LOWER SEC	+ 0.085 + 0.0
4	CATALYST RETAINING PLATE	TZM	—	+ 0.30
5	THROAT	L-605	0.06	+ 1.58
6	NOZZLE EXIT	L-605	0.012	HIGH
7	MOUNTING BOLTS	6A6-4V	4-1/4"	+ 0.16
8	MOUNT PLATE	L-605	1/8 X 1/2	+0.275
9	THERMAL BARRIER SLOTTING 0.06", 0.75" LONG	L-605	0.06	+ 0.09 + 0.00

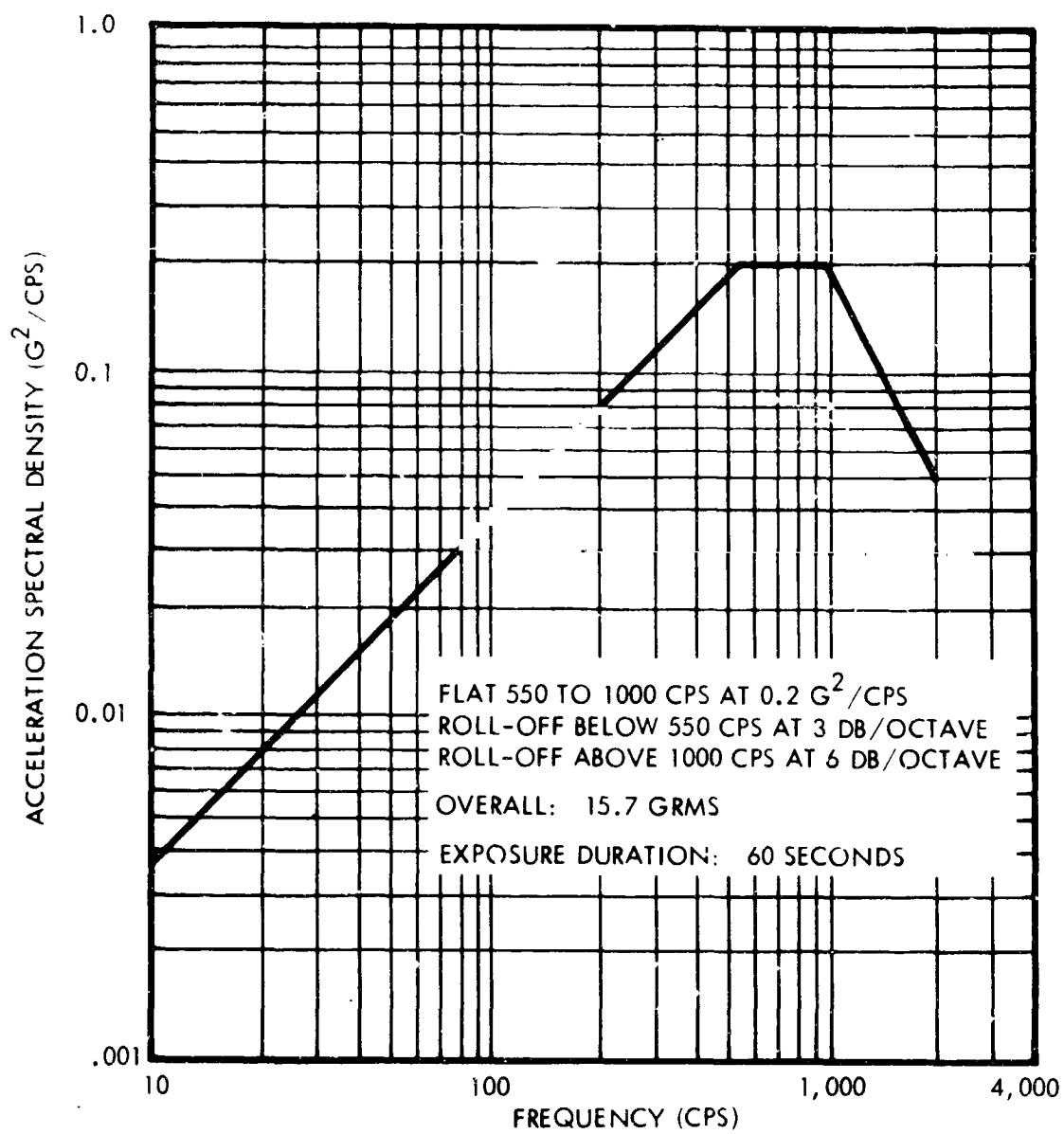


Figure 30. TTS Launch and Boost Vibration Spectrum

Table 6. Flowrate/Differential Pressure Schedule

Throttle Setting (%)	Flowrate (lbs/sec)	Differential Pressure (psid)
100	2.12	33
95	2.01	54
90	1.91	74
75	1.59	133
50	1.06	224
25	0.53	305
15	0.32	334
10	0.21	348

The vented leakage requirement was based on the premise that leakage across dynamic seals could be vented overboard; allowances were eventually made, however, for storing this leakage during the operating period. No requirement for an integrated shutoff capability was specified since for missions of the near future a single startup and shutdown is required and this is most reliably implemented upstream of the throttle valve through the use of normally open and normally closed ordnance valves. The assembly weight and power requirements were based on state-of-the-art throttle valves and design studies of expected advancements within the anticipated development time. The step response, frequency response and linearity requirements were based on the results of JPL and industry studies of typical terminal landing vehicle stability conditions. Since the guidance and control system corrects the lander velocity/altitude profile by incrementally changing the engine(s) thrust level, it is especially important that the control linearity vary as little as possible. Step and frequency response requirements are based on the differential throttling concept by which the three lander engines are used to maintain pitch and yaw control and to perform the initial pitch up maneuver necessary to achieve the correct flight path. The heat sterilization requirement primarily affected materials selection although actuator operation and lubrication were additional factors.

Selection of the throttle valves for this program was made after a survey of potential vendors. LTV Electrosystems, Inc. and Moog West were eventually chosen because of the near term availability of hardware resulting from previous work by both companies.

#### Design Description

The general design features of the LTV liner displacement throttle valve are shown in Figure 31. The LTV valve is of stainless steel and aluminum construction to allow hermetic sealing of the actuator cavity as well as minimum assembly weight. This was achieved through the use of a low pressure bellows which would isolate the actuator from vacuum to preclude loss of actuator lubricant during coast and from hydrazine during operation. Further load reduction was obtained by the use of a pressure balance plug which minimizes the effects of varying propellant supply pressure. Elastomeric (EPR) seals were used on both the balance plug and metering pintle shaft.

The valve inlet and outlet ports were located so that the valve overhang with respect to the engine was minimized; this was accomplished by locating the inlet near the end of the valve and the outlet close to the center.

The electromechanical actuator used to position the valve included a D.C. torque motor and ballscrew assembly which translates rotary motion into linear displacement. Direct measurement of valve position is provided by AC in - AC out linear variable differential transformer (LVDT) with a separate modulator/demodulator unit included in the electronics package. The electronic circuit, shown in Figure 32, indicates the basic position feedback control loop and key components. The actuator assembly is identical to the one used on the Minuteman III LITVC system and, therefore, represents a minimum development risk subassembly. Materials and lubrication studies indicated that the Micronic 631 grease (Bray Oil Co.) and actuator components provide high reliability even if the low pressure bellows should fail.

The Moog rotary plug design, shown in Figure 33, possesses several potential advantages over a linear valve, but with some associated development risk. Potential advantages include improved response, reduced

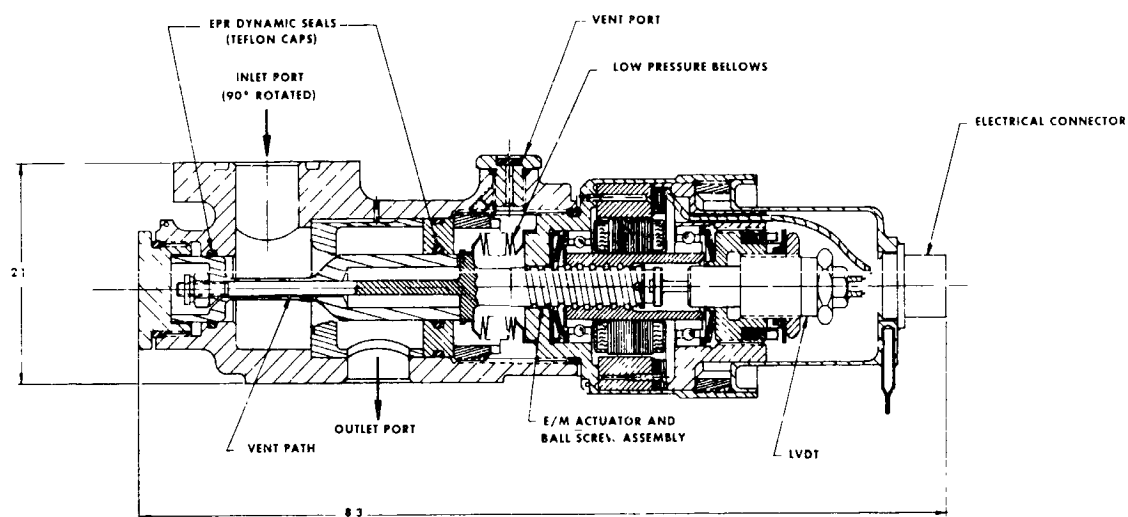


Figure 31. LTV Throttle Valve

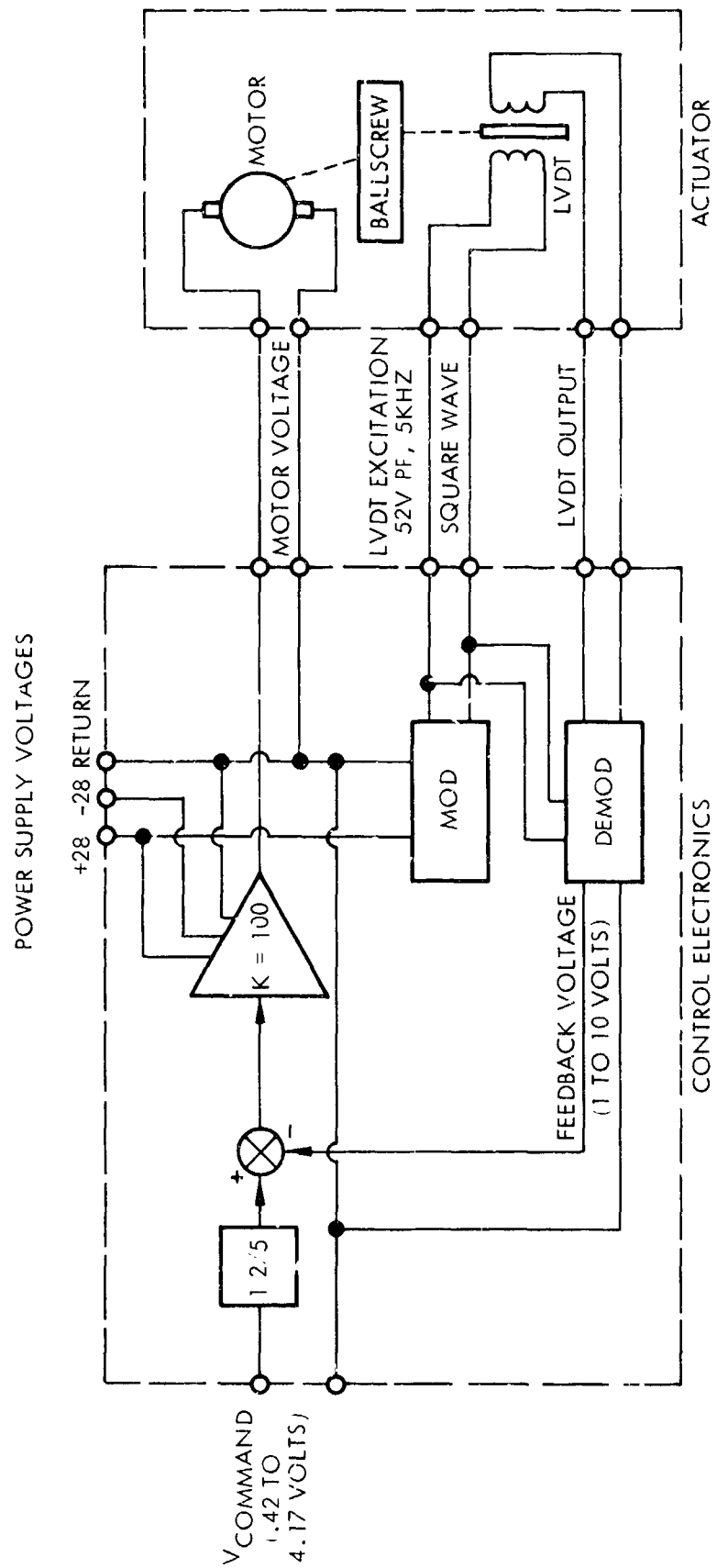


Figure 32. Valve Electrical Schematic

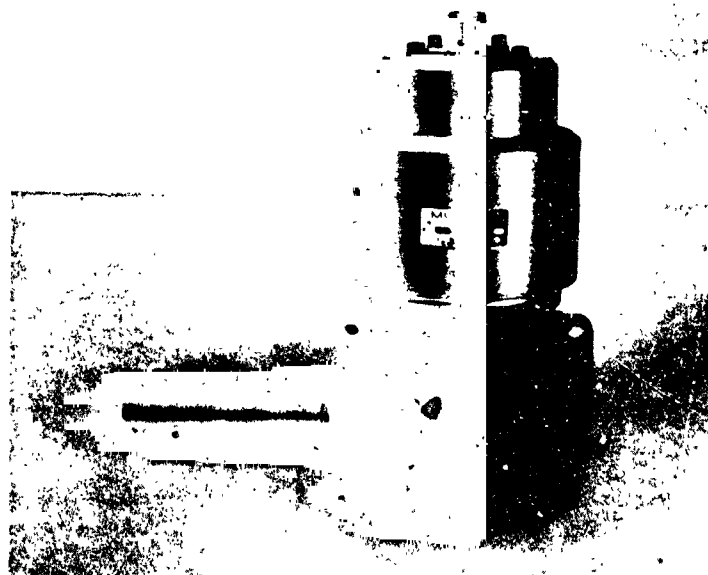
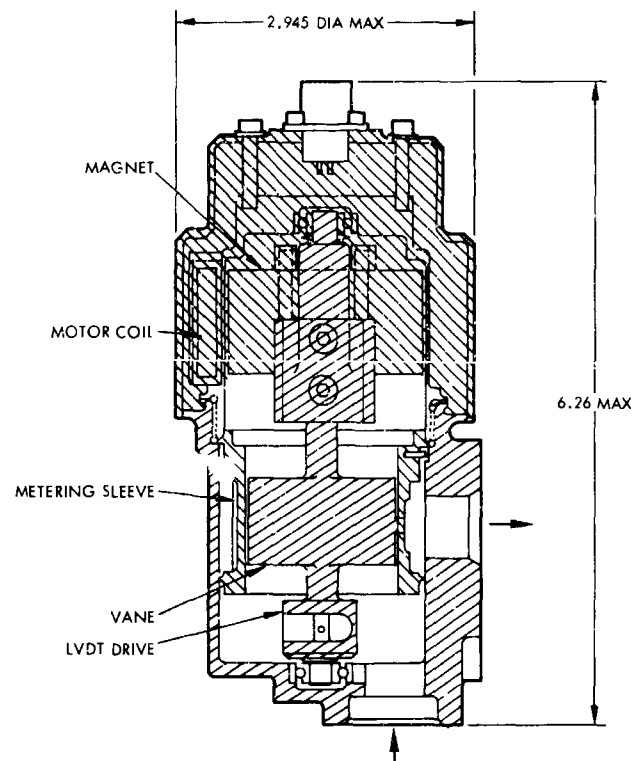


Figure 33. Moog Throttle Valve

pressure losses and elimination of all dynamic seals. The latter is achieved by eliminating the linear displacement and submerging the LVDT and rotary torque motor in hydrazine. Flow is metered by a vane which operates directly off of the motor shaft and regulates the flow area of shaped slots in a sleeve. Since the motor only has to rotate approximately 40 degrees, the valve response time can be reduced to about 30 - 40 milliseconds.

The rotary valve assembly is made of series 300 stainless steel and weighs 2.7 lb<sub>m</sub>. The design allows total hermetic sealing. The propellant inlet is at one end of the assembly with the outlet near the geometric center to provide minimum overhang. The LVDT used for position measurement is driven off a metal band drive and extends perpendicular to the motor axis, thus, giving the assembly an "L" type geometry. The use of a rotary variable differential transformer (RVDT) would be desirable in minimizing the valve envelope and weight and represents an area of additional design and development. Principal areas for further evaluation include minimum allowable tolerances, load balancing and relative accuracy of the LVDT position feedback linkage.

#### 2.2.4 Thrust Chamber Design

The structural and thermal aspects of the thrust chamber design have already been discussed, and this section deals primarily with the injector and catalyst bed design. The catalyst bed is made up of all Shell 405 catalyst - 14-18 mesh contained in the hemispherical area below the injector and 1/8 x 1/8 inch pellets filling the remainder of the bed.\* The catalyst bed was designed for a maximum pressure drop of 80 psi and the injector, 90 psi. The pressure distribution and anticipated gas temperature over the flow range are shown in Figure 34.

The single element injector is of the basic TRW "headspace" design (see Figure 24). Ninety-one orifices of 0.031 inch diameter are electrical

---

\*Note that the thrust chamber as it was originally assembled contained a 3.2 inch diameter cylindrical bed of 14-18 mesh catalyst extending from the headscreen to the catalyst retainer plate. This bed design produced excessive chamber pressure roughness,  $\sim \pm 25\%$ , and was modified to the configuration shown in Figure 24.

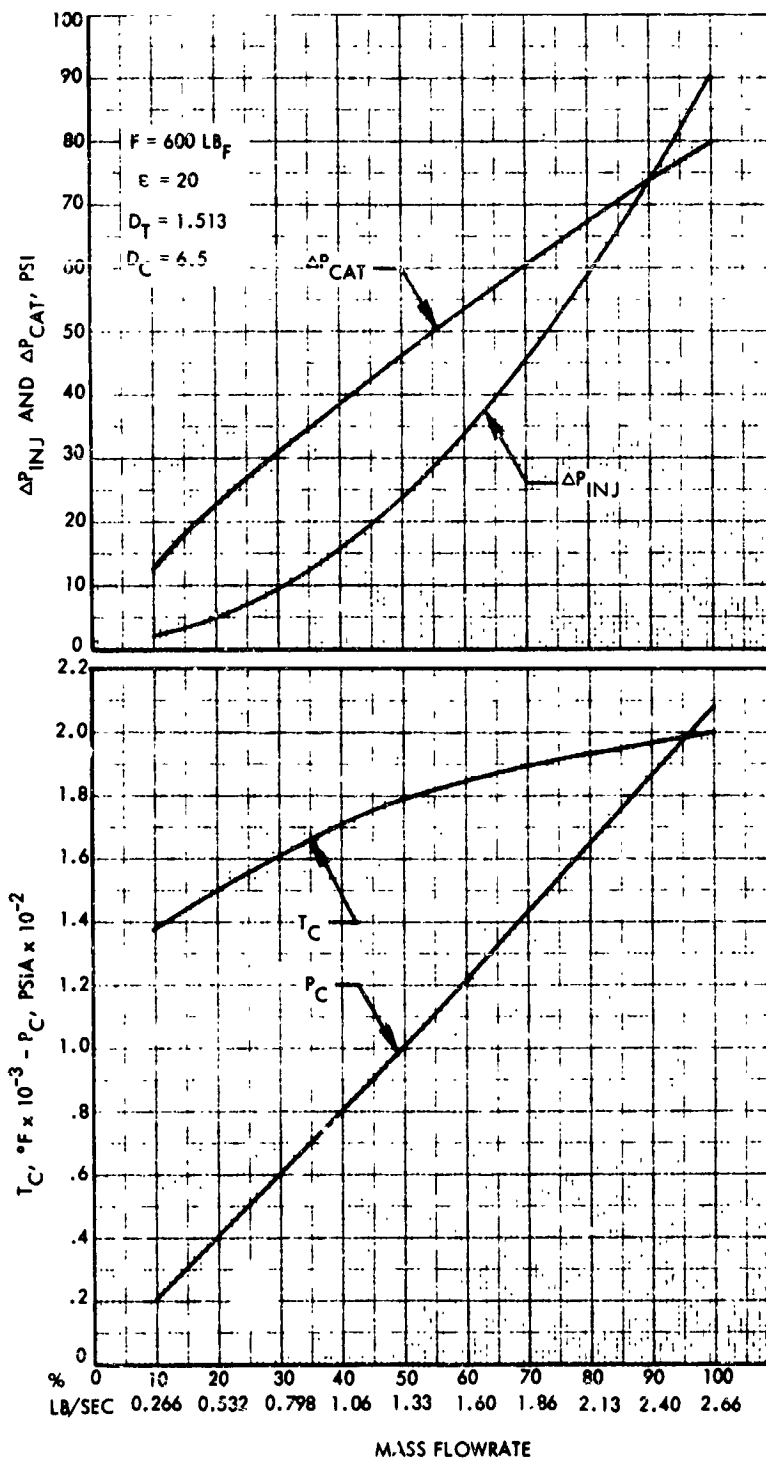


Figure 34. TTS Predicted Performance

discharge machined over 90 degrees of its hemispherical tip. The injector flows into a 3 cubic inch open volume. This open volume serves as an internal manifold and to enhance propellant distribution and vaporization.

The nozzle is based on the Rao contour for an expansion ratio of 20:1. The entire thrust chamber and nozzle are machined from L-605.

### 2.3 Phase III - Fabrication and Test

Fabrication of the TTS was initiated upon JPL approval of the Phase II design and culminated with the production of the unit pictured in Figure 35. The weight breakdown for this unit, as pictured, is presented in Table 7 for the "original" and modified configurations. Both configurations were identical externally except that the modified unit was 0.060 inch shorter. The internal modifications are discussed in Sections 2.2.4 and 2.3.3 of this report. Note that the thrust chamber was cut open at the girth weld to make necessary modifications to the catalyst bed and was then re-welded without difficulty.

The test program, as originally planned, included a component and system level test sequence with a total hot firing time of 500 seconds. Simulated altitude, ignition transient, and thermal environmental tests as well as sea level performance and sterilization were contained in this series as shown in Figure 36. This test sequence was completed through sea level performance tests using the LTV valve,\* but was terminated at that point because of fund limitations. Chamber pressure roughness was encountered with the "original" unit, and it was reworked as noted in Section 2.3.3. The modified unit was subjected to three sea level tests and demonstrated very good compliance with the design goals.

The remainder of this section is devoted to pertinent details of the fabrication and testing of the TTS and its components.

---

\*The Moog rotary valve was ordered later than the LTV valve and was not delivered in time for inclusion in this test program.

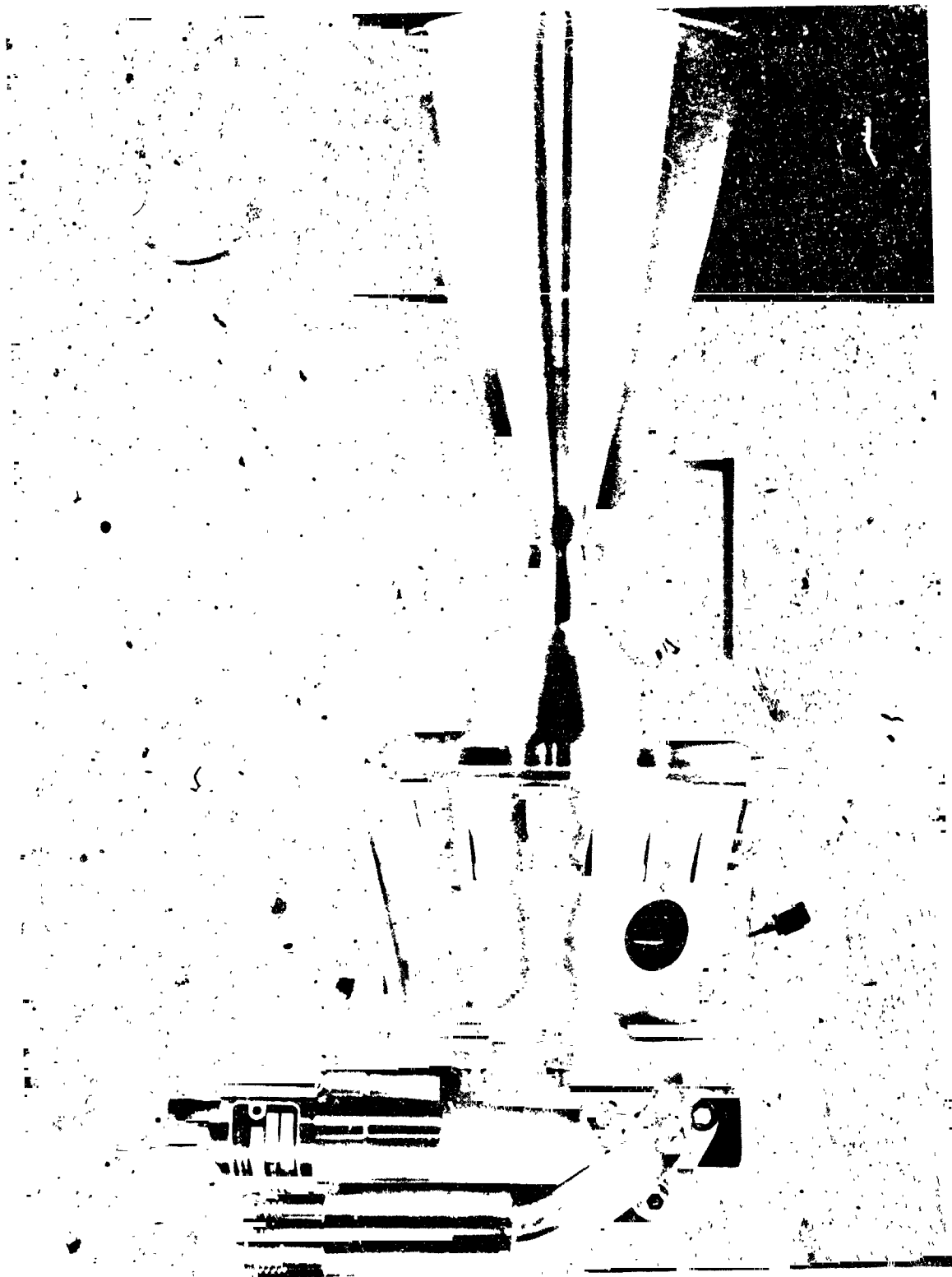


Figure 35. Throttleable Thruster System

Table 7. TTS Weight Comparison

	Material	Predicted Weight, lb	Actual Weight, lb	
			Original	Modified
Chamber and Nozzle	L-605	4.50	5.44	5.28
Thermal Barrier	L-605	0.45	0.42	0.42
Injector	L-605	0.10	0.04	0.04
Screens	Inconel	0.30	0.20	0.17
Mount Plate	L-605	1.20	1.88	1.88
14-18 Mesh Catalyst	Shell 405	0.98	1.02	0.43
1/8" Catalyst	Shell 405	1.91	1.85	2.40
Catalyst Support Plate	TZM	1.00	1.01	1.14
Throttle Valve	7075-T73	2.50	2.30	2.30
Filter	304 L	0.30	0.68	0.68
Miscellaneous (insulator, bolts, etc.)		-	0.06	0.06
TOTALS		13.24	14.90	14.80

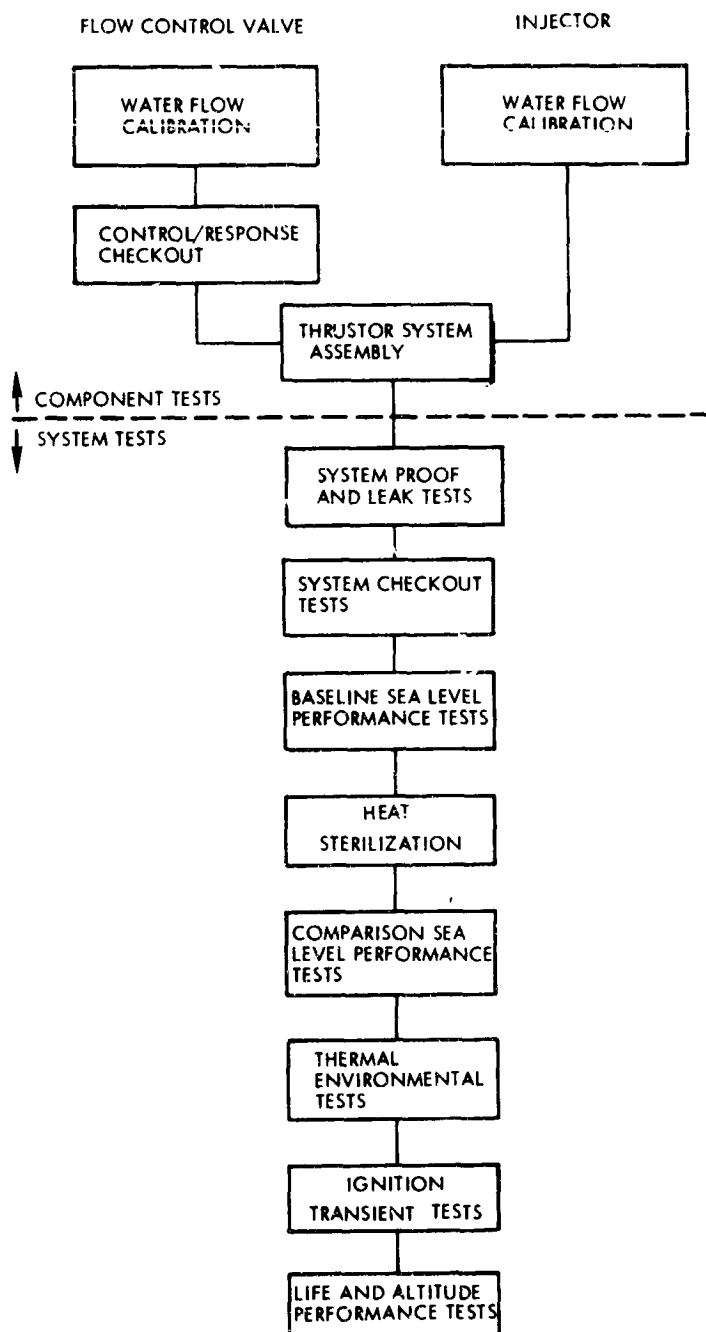


Figure 36. Throttleable Thrustor Test Sequence

### 2.3.1 Thrust Chamber Fabrication

An outline of the assembly sequence and detail parts is presented in Figure 37. The head end hardware was assembled and the fine catalyst loaded. Prior to electron beam (EB) welding of the chamber to the nozzle, the TZM plate was disilicide coated and installed after loading the coarse catalyst. The TZM was disilicide coated to prevent oxidation at an elevated temperature due to back flow after shutdown. The more significant details of the manufacturing process and pertinent observations are contained in the following paragraphs.

#### Chamber/Nozzle

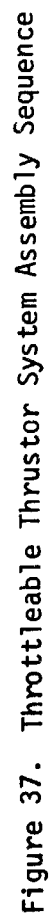
Due to time and schedule constraints the engine chamber and nozzle were machined from solid billets. All machining was performed in a tracer lathe with the internal surfaces completed first. The shell was then filled with a rigid plastic to allow contour machining of the outside diameter to a minimum wall thickness at the nozzle exit of .015 inches. In a future production it is expected that these parts would be machined from forgings to reduce costs.

#### Injector

Since the injector is made of a very tough material (L-605) and a large number of accurate holes are needed in the showerhead configuration, the EDM process was selected for this detail. This fabrication technique produces a very accurate and quite repeatable orifice enabling a minimum of calibration testing. The sizing was initially specified for a small hole which was hydro-honed to produce the desired flow characteristics by an improvement in the discharge coefficient.

#### Head Screens

The head screens were formed using soft tooling. The head screen assembly was spot welded together and installed in the chamber. All joints were coated with a chrome/nickel braze alloy. A furnace braze technique was then used to fuse all screens together and to attach the assembly to the thrust chamber in one operation.



### TZM Plate

The TZM plate was produced by precision milling techniques although the EDM process might be considered in a production situation. The primary difficulty in fabricating parts of this material is the undesirable brittleness which causes chipping of the edges.

### Welding

The present head end design employs two TIG welds to attach the thermal barrier to the mount plate and engine chamber. During this welding operation sufficient heat is developed to cause an undesirable amount of chamber distortion. In future units a redesign is planned which would require only one EB weld. The final chamber/nozzle weld was performed by this method with complete success. After all welding was completed the mount plate was final machined to produce engine alignment surfaces.

#### 2.3.2 Acceptance Tests

Acceptance testing of the TTS rocket engine assembly included certain in-process as well as other non-destructive and performance tests. The throttle valve, filter, injector and engine assembly were tested on a component basis and are discussed in the following paragraphs. Successful completion of these tests was a prerequisite to any hot firing demonstration tests.

### Throttle Valve Calibration - LTV Unit

Acceptance tests of the valve were conducted at LTV with flow and response characterization tests subsequently conducted at TRW. These tests have demonstrated the ability of the valve to meet, generally, the performance requirements of the TRW specification (Appendix A). The results of the water flow calibration tests are shown in Figure 38 and a comparison of requirements and performance is presented in Table 8.

The principal problem encountered during development was meeting the  $\pm 3\%$  flow accuracy between the 90 and 100% throttle settings. The major tradeoff required was between minimum stroke for response and a larger stroke for flow accuracy. In order to meet the accuracy requirement, it

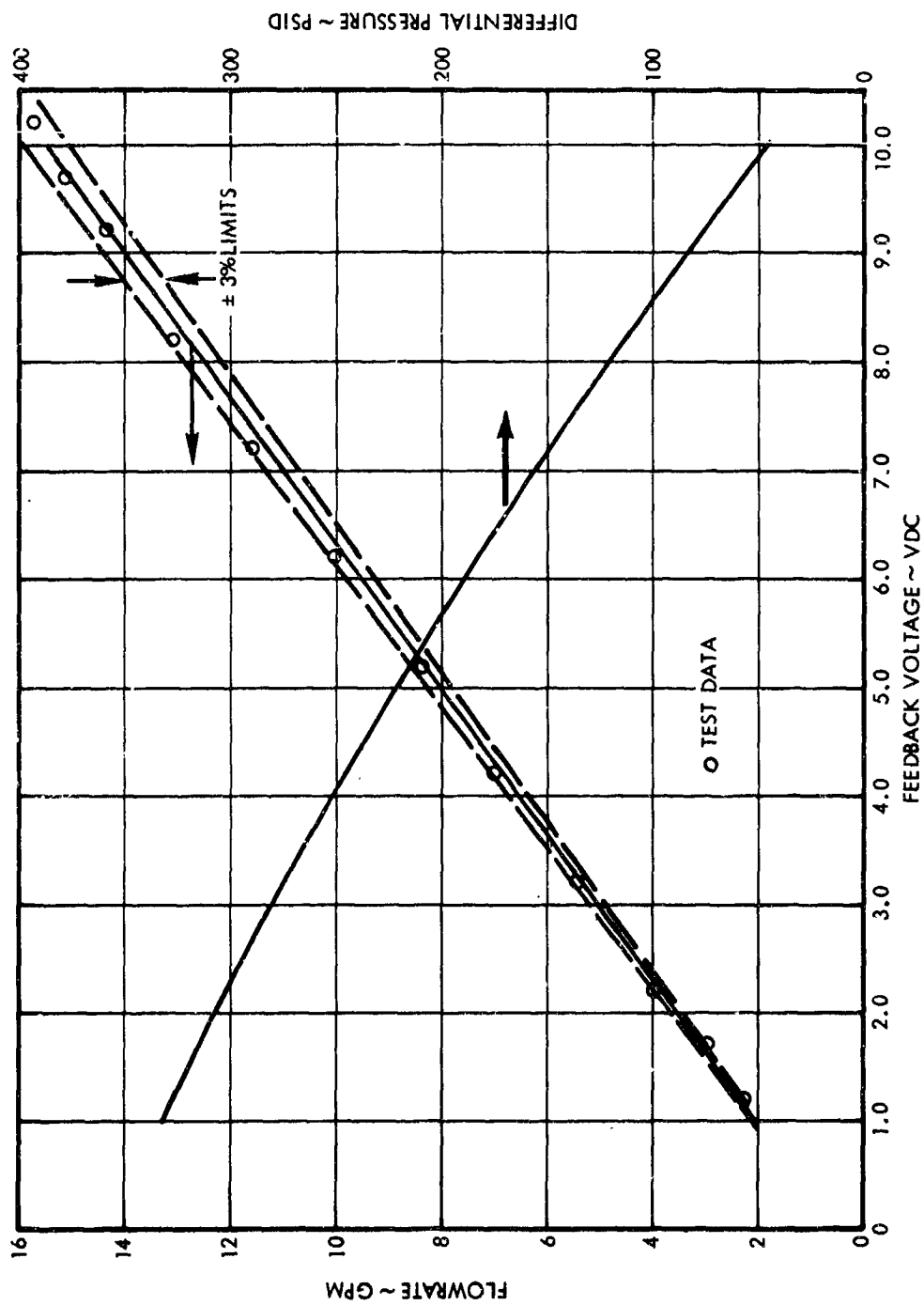


Figure 38. LTV Valve Water Flow Calibration

Table 8. LTV Throttle Valve Performance Summary

PARAMETER	REQUIREMENT	ACTUAL
Proof Pressure	1000 psia	1000 psia
Vented Leakage	0.004 in <sup>3</sup> /sec N <sub>2</sub> H <sub>4</sub> at 480 psia	None Measureable at 500 psia for 15 minutes
Weight	2.5 lbs	2.2 lbs
Position Hysteresis	1% of Stroke	1.1% Maximum
Power Consumption (Stall)	70 watts at 28 vdc	63 watts at 28 vdc
Step Response	60 ms to 90% of any step	Dry: 55 ms for 100% Step (Stroke) Wet: 62 ms for 100% Step (Stroke)
Overshoot	15% command step	0%
Frequency Response	Amplitude Ratio $\geq 0.95$ and Phase Angle $\geq -15^\circ$ at 5 Hz and 60 $\pm$ 10% command	Amplitude Ratio = 0.98 Phase Angle = - 16°
Maximum Flowrate $\Delta P$	$\Delta P \leq 70$ psid at 2.61 lbs/sec	68 psid
Linearity	$\pm 10\%$ of Nominal	+35% Max @ 10% Throttle -13% Min.@ 95% Throttle
Accuracy	$\pm 3\%$ of Nominal	$\pm 3\%$ of nominal

was necessary to revise the flow/differential pressure schedule of Table 6 and allow a 70 psi pressure loss at maximum throttle instead of the desired 50 psi. This was acceptable from a system standpoint since the thruster chamber pressure had been selected at the lowest reasonable level to allow margin for such a situation (see Section 2.2).

Further design tradeoffs involving valve seat diameter, stroke and ballscrew lead (gain) would be required to reduce the required pressure loss; the latter would be the most likely approach although it would mean the modification of a qualified component. While the slope (linearity) of the flow schedule exceeded the desired  $\pm 10\%$  level at some points, this is an area in which an iterative design/test procedure is normal to achieve a final plug contour.

Response testing of this valve showed that all requirements could be met. The step (dry) and frequency response data is summarized in Figures 39 and 40, respectively. The effect of the pressure balance plug on minimizing the variation between up throttle and down throttle response times can be seen in Figure 41; it was concluded that additional development would further reduce the variation.

It should be noted that the flow control assembly was 0.3 lbs lighter (2.2 lb) than required and has the potential for further weight reduction while a maximum motor stall power of 63 watts was achieved as opposed to the 70 watt requirement. Analytical studies conducted during the program also indicated that this motor power level could be reduced to 56 watts without affecting the response or accuracy requirements. After completion of these calibration tests, the valve was integrated with the thruster assembly for environmental and hot firing tests.

#### Throttle Valve Calibration - Moog Unit

The Moog rotary valve was not delivered in time to include it on an engine firing or make a direct comparison with the LTV unit. However, it can be concluded that the original evaluation of these throttle valves was essentially valid.

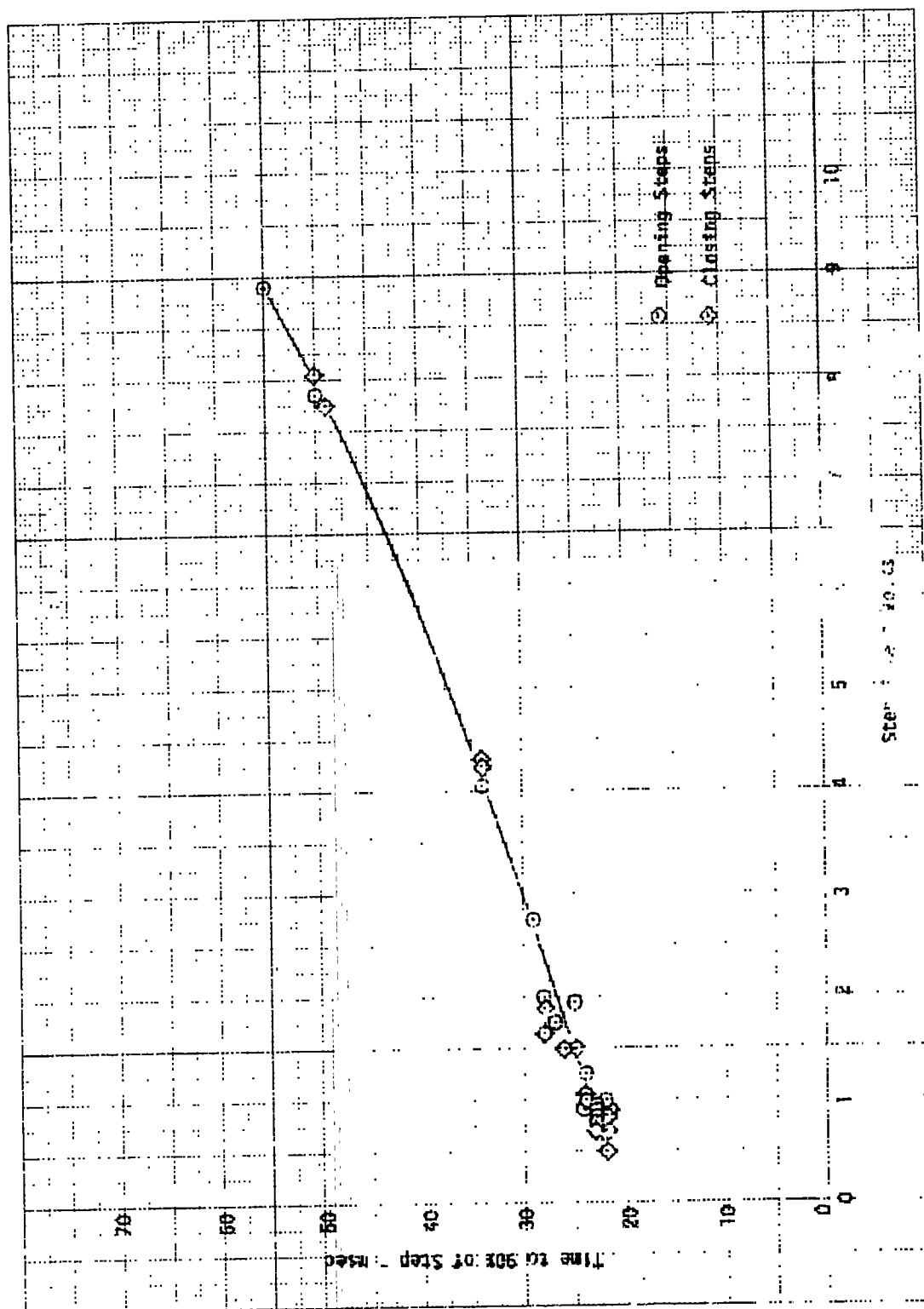


Figure 41. LTV Valve Step Response Without Flow

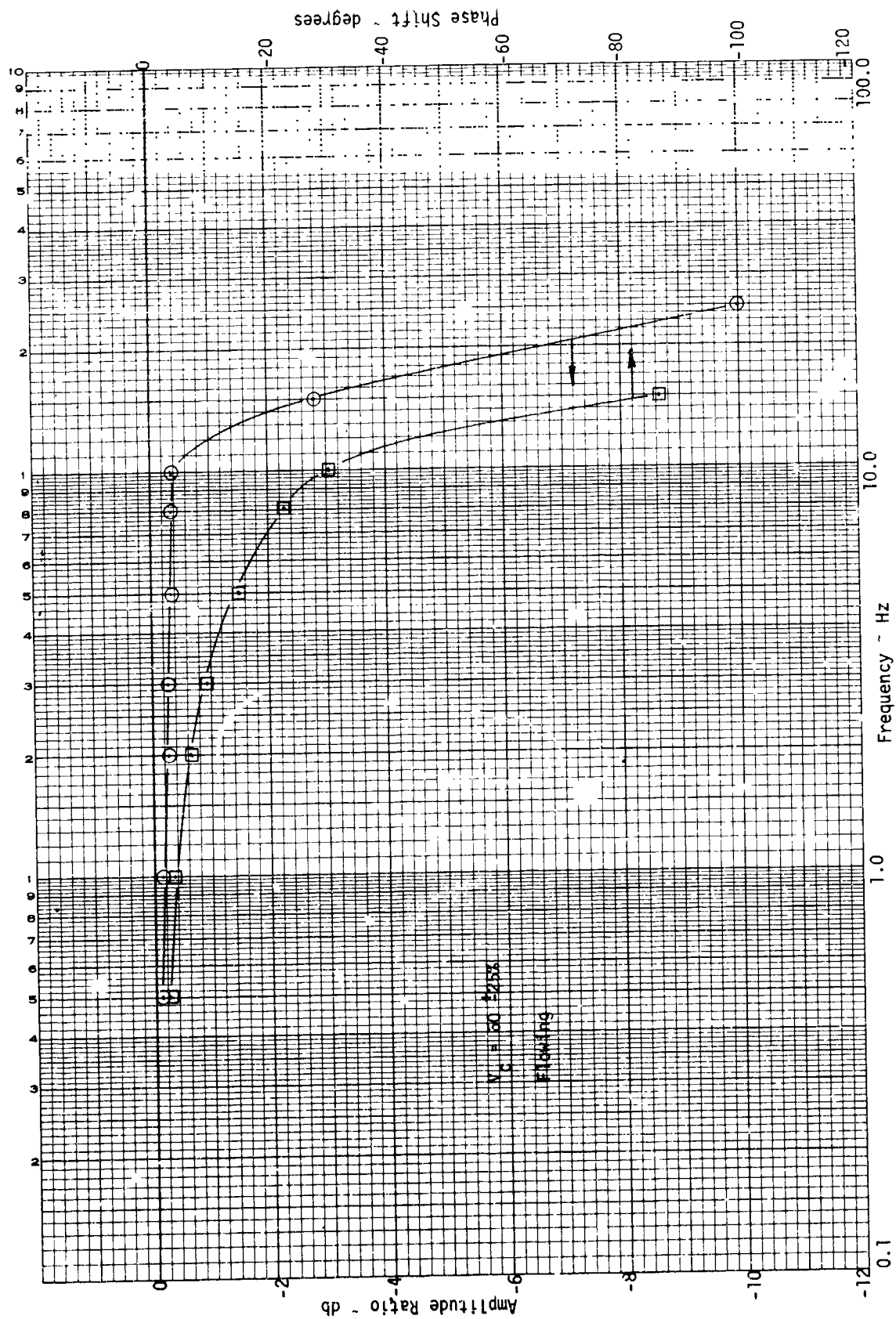


Figure 42. Valve Position Frequency Response

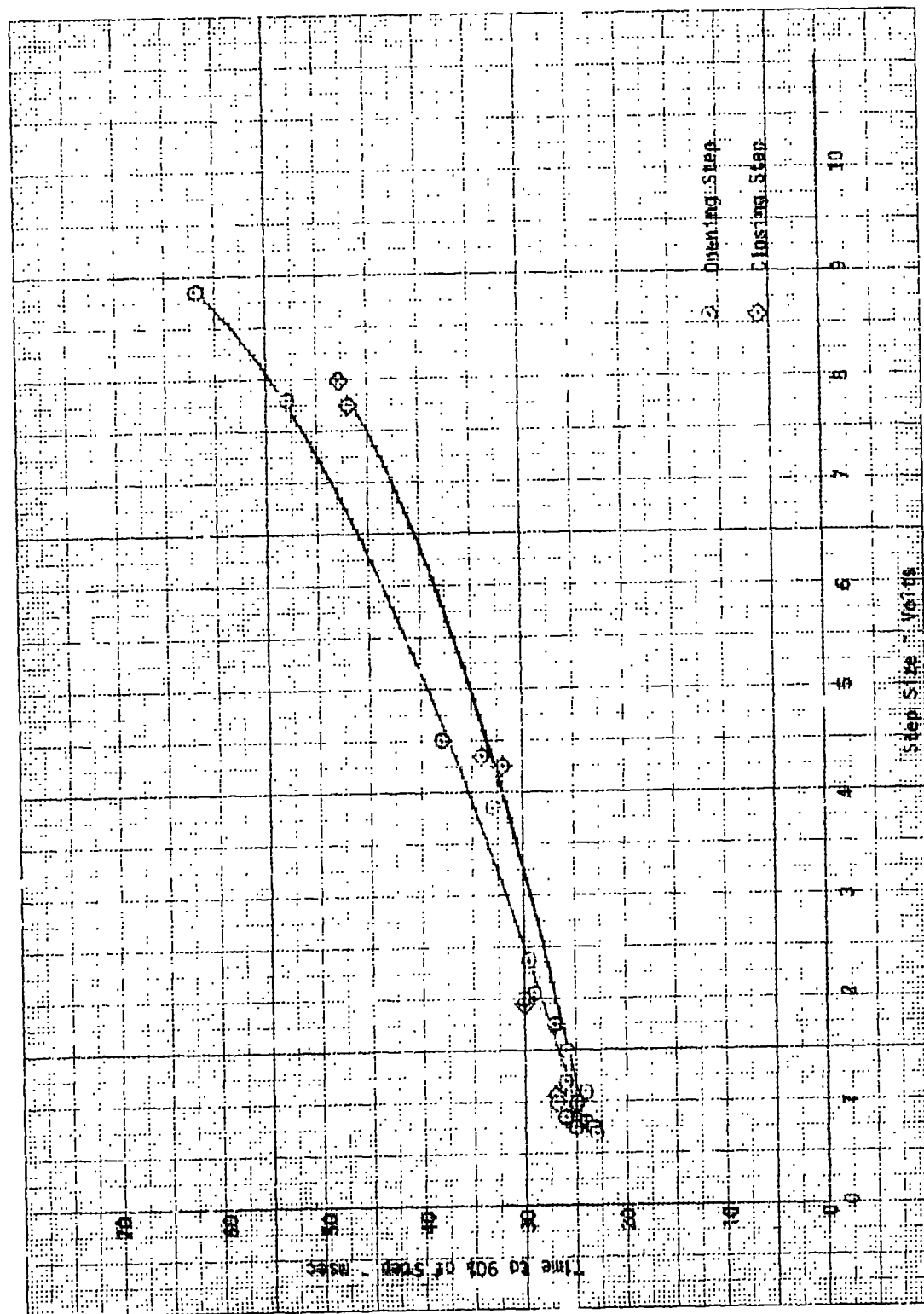


Figure 43. LTV Step Response With Flow

The testing performed on the Moog rotary valve to date has yielded the following results:

- Step response is on the order of 35 milliseconds. Further improvement may be possible with changes in the control loop compensation networks.
- Initial flow tests with a TRW built servo amplifier indicated that the valve had a nonlinear flow characteristic. It was determined by Moog that this resulted from a nonlinear demodulator output from the Moog electronics which gave a false position signal during the orifice shaping. Moog subsequently shaped a new orifice to achieve the desired flow schedules.
- An increase in friction level was noted during the testing due to rough spots on the bearings. This was corrected by replacing the bearings and assuming concentricity.

#### General Observations

The LTV valve represents the product closest to a qualified status and therefore would be the minimum development risk unit. The principal disadvantage of this unit was the need for a 70 psid pressure drop at maximum throttle as compared with the desired value of 50 psid. It should be noted, however, that the reduction in chamber pressure to 200 psia permits a higher valve pressure differential while still keeping the tank pressure less than 480 psia. Further design and reliability tradeoffs would be required to evaluate the relative merits of ballscrew gain (pitch), seat diameter and stroke changes to meet the latter value. The Moog rotary valve while experiencing certain design problems has the inherent capability for faster response as well as increased reliability due to the elimination of all dynamic seals. These potential advantages warrant the further development of this valve for use in future applications.

#### Filter Calibration

Acceptance test of the filter was performed at the Wintec Division of Cemar Corporation and consisted of flow capacity, proof pressure, external leakage and cleanliness. The results of the flow capacity test with water are shown in Figure 42. As can be seen, the maximum pressure drop for the assembly is approximately 9.0 psi at rated flow (~19 GPM).

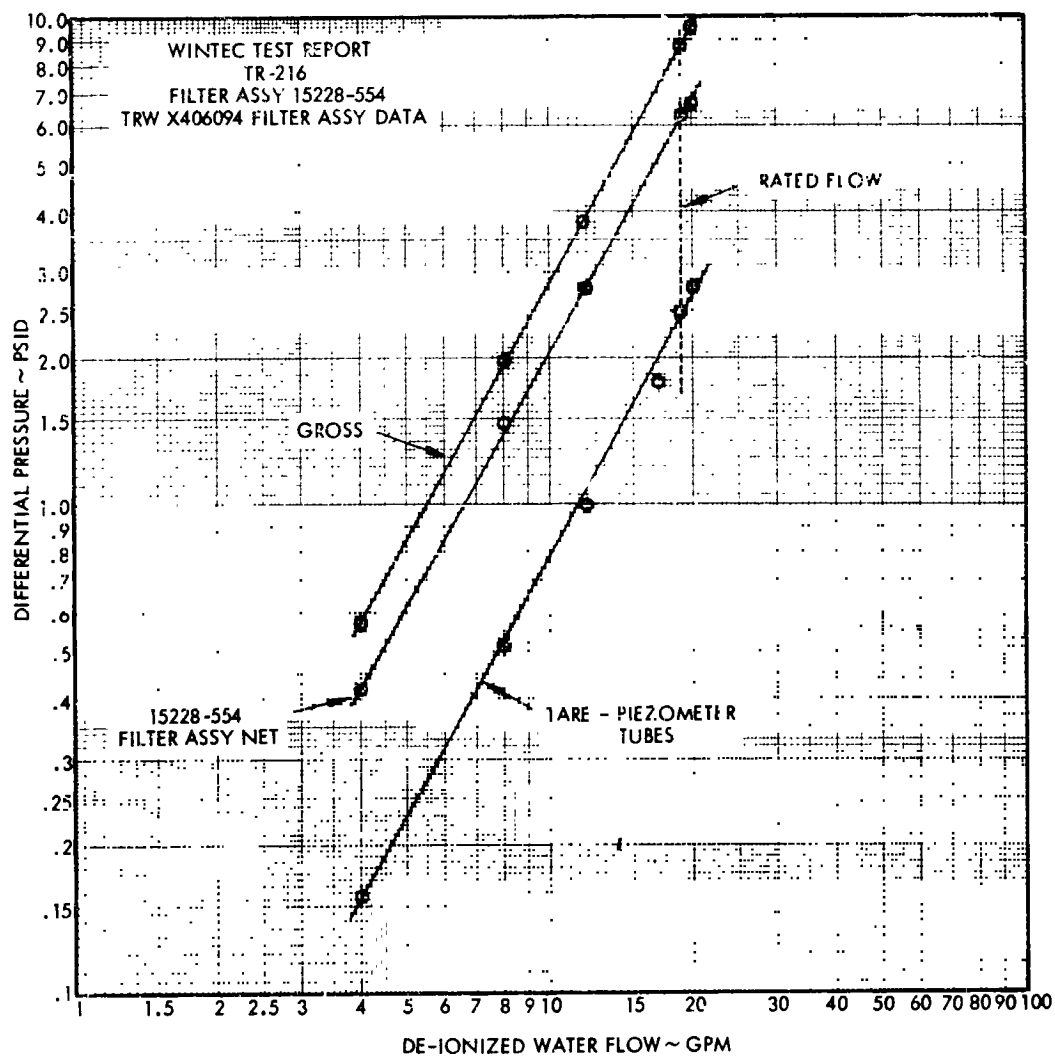


Figure 42. Filter Performance

### Engine Leak Test

The engine leak check was performed immediately after EB welding the chamber to verify the absence of weld porosity. This test was accomplished by pressurizing the assembly to 100 psig with helium and using the Mass Spectrometer method. The throat is sealed by the use of a special throat plug held in place by appropriate tooling. Leakage less than  $1 \times 10^{-7}$  scc/sec constitutes acceptance. In addition to the leakage test, a dye penetrant inspection was also performed to detect any serious flaws. The use of X-ray inspection has been found to be inadequate to achieve the desired confidence in the welding operation. Consequently, the primary structural integrity test is the proof pressure verification.

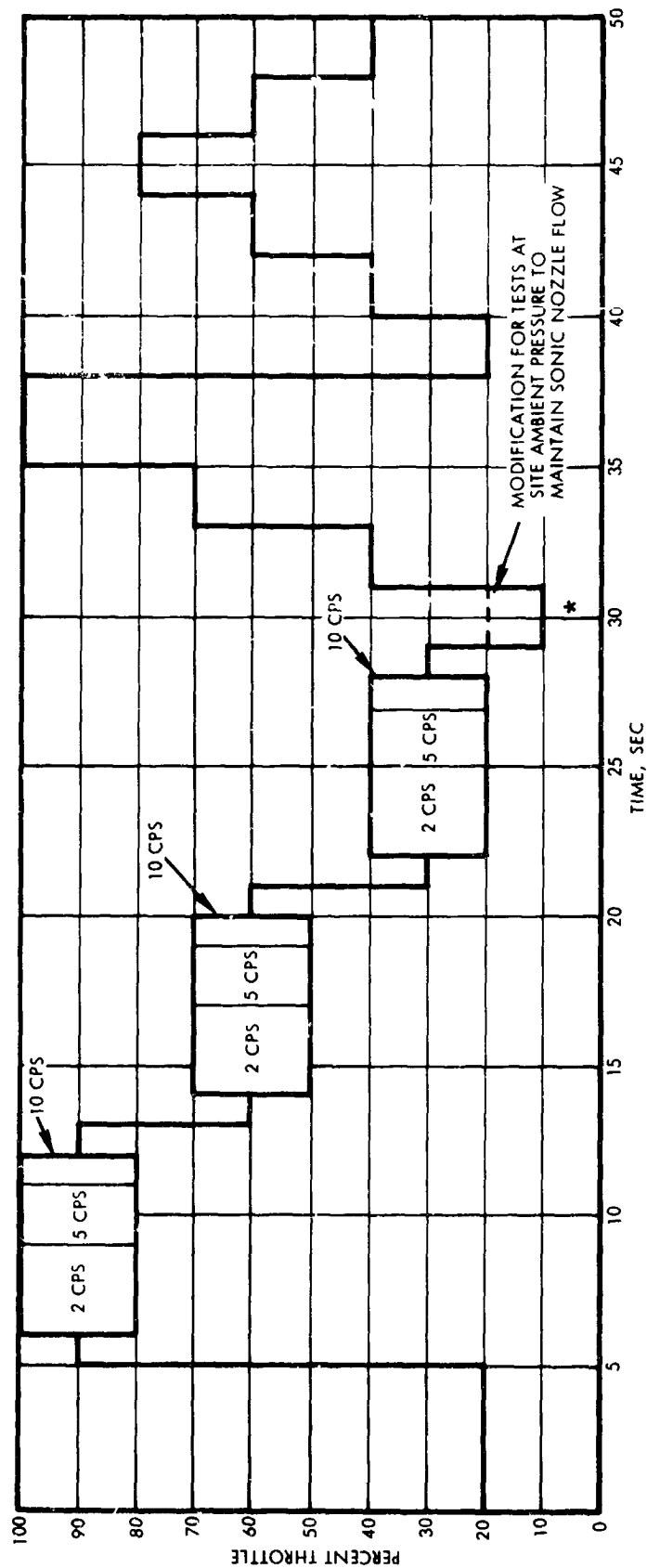
### Engine Proof Test

The proof pressure test of the chamber was accomplished by sealing the throat with an aluminum plug held in place by Cerro-Bend (a low melting point metal). This permits a more realistic test since the stresses are imparted directly to the chamber shell without the use of a holding fixture which could absorb part of the tensile load. The test was performed at room temperature with 1000 psig nitrogen. This high pressure simulates stress conditions at 1.5 times the maximum upstream pressure while the engine is operating, since a factor must be applied to compensate for the reduction in properties of L-605 at an elevated temperature. When the proof test was completed, the throat plug was removed by melting the Cerro-Bend.

#### 2.3.3 Operational and Environmental Testing System Checkout and Baseline Sea Level Performance

The first test firing of the TTS was a 10 second checkout divided into 3 1/3 second intervals at 40%, 100%, and 70% thrust. Thruster operation was generally satisfactory except chamber pressure roughness of up to  $\pm 34.4\%$  was observed. The chamber pressure oscillations were not truly sinusoidal, but were pronounced at 13-15 cps.

It was concluded that despite the rough operation the testing would be continued in an attempt to obtain performance data. The duty cycle shown in Figure 43 was run, producing the following results:



\* Test broken and restarted at this point because of insulation fire.

Figure 43. Duty Cycle for Baseline Performance Test

- Characteristic exhaust velocity of 4370-4400
- Maximum catalyst bed pressure drop of 100 psi decreasing to 34 psi at 20% thrust
- Chamber pressure roughness increasing with thrust level from  $\pm 9\%$  at 120 lbf thrust to  $\pm 26\%$  at 600 lbf thrust.

Response data was clouded by data reading difficulties caused by the rough operation, but appeared to comply generally with the system requirements.

It was concluded that data of sufficient accuracy and validity was being obtained to permit assessment of sterilization effects. Thus, the sterilization series was undertaken as planned.

#### System Sterilization

The sterilization requirement for the TTS program was developed from previous studies of the allowable Mars contamination levels. Consequently, an inert gas heat sterilization method was identified which involves 6 cycles of 64 hours per cycle at 275°F. Due to schedule constraints this task was reduced to 3 cycles of 35 hours per cycle at 275°F. The sterilization was performed after the initial series of engine checkout and sea level baseline performance tests. Final verification of the heat compatibility of the rocket engine assembly was determined by an absence of performance degradation during a repeat of the initial test series. The total duty cycle for the sterilization tests are shown in Figure 44.

The rocket engine assembly was installed in the sterilization chamber with the nozzle down and all ports closed to the gaseous nitrogen atmosphere at 14.7 psia. The sterilization atmosphere during the test was:

Gaseous Nitrogen	97%
Oxygen	2.5% maximum
Other Gases	0.5% maximum
Water Vapor	Less than 0.1% by weight

#### Comparison Sea Level Performance Tests

Upon completion of the sterilization cycle, the TTS was fired to determine any effects from the heat cycling. A 10 second test like that

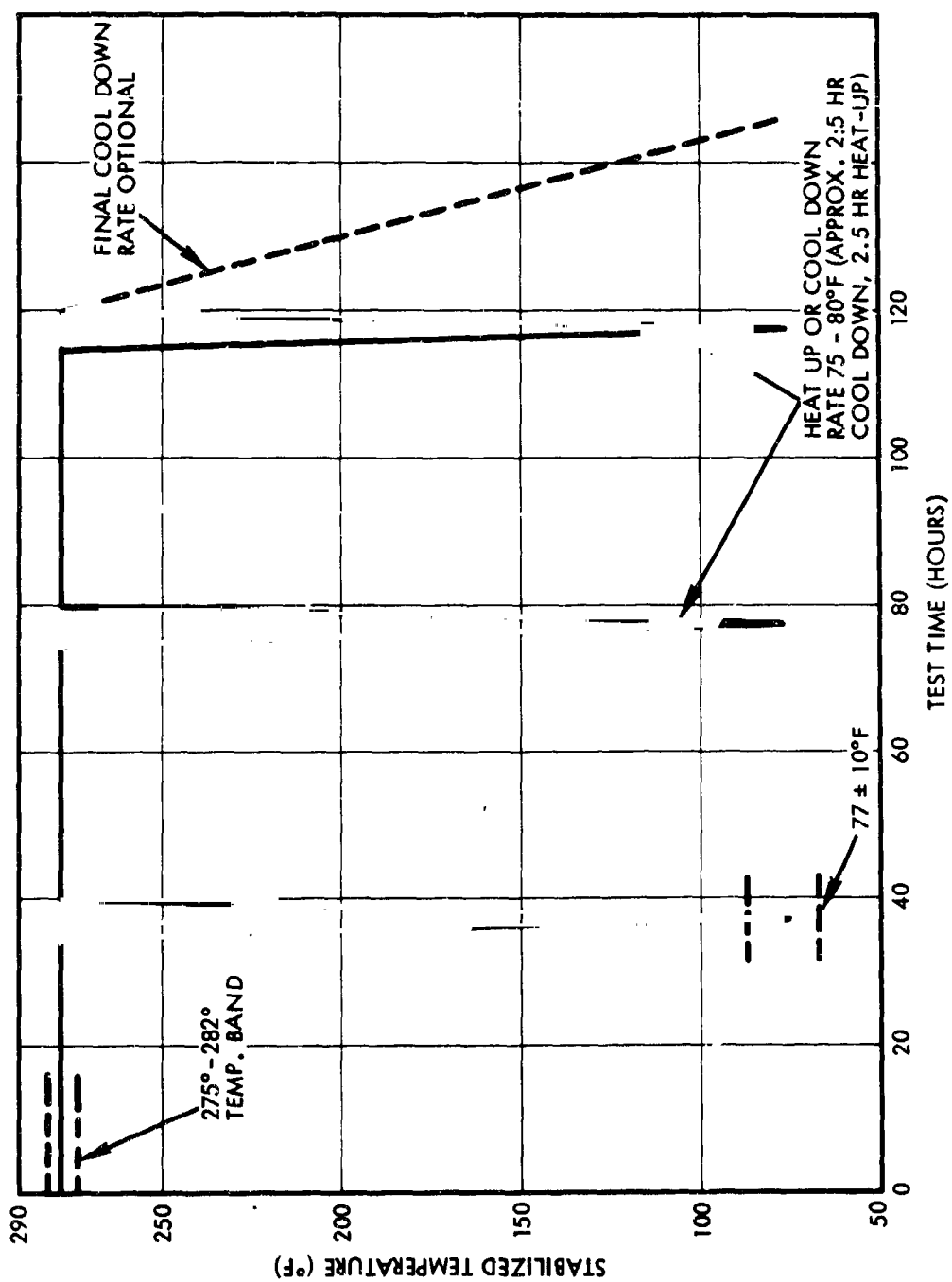


Figure 44. Heat Compatibility Test Time - Temperature Profile

used for checkout was planned. The first firing was terminated after 3 seconds because of a propellant leak in the facility. The second firing completed the planned cycle, and the run extended to 12.9 seconds because of a facility propellant valve failure.

Performance was within measurement accuracy of that obtained from the earlier firings, and it was concluded that the sterilization cycle had not influenced the operation of either the valve or thruster.

Chamber pressure roughness was somewhat less than previously observed, but this was attributed primarily to facility modifications intended to reduce coupling. This operating characteristic was considered to be unsatisfactory, and it was decided to modify the catalyst bed to correct the roughness.

#### Thrust Chamber Modification

The rough operation was ultimately attributed to poor propellant distribution through the catalyst bed because of the high resistance of the 14-18 mesh catalyst located directly below the injector and extending the length of the bed (see Section 2.2.3). The catalyst bed was redesigned to reduce the depth of 14-18 catalyst to a maximum of 1.2 inches contained in a hemispherical area below the headscreen, as shown in Figure 24.

The thrust chamber was cut open at the girth weld. The catalyst bed and screens were removed and replaced. Catalyst used in repacking the bed was the same as that used in the original engine except for 0.55 pound of 1/8 x 1/8 inch catalyst necessary to fill the volume left by the removed portion of the 14-18 mesh. This make up catalyst was taken from a similar thruster with comparable firing duration. It had not, however, undergone the sterilization cycle.

Prior to repacking the catalyst bed the girth weld region was machined true and thoroughly cleaned, and the reworked headscreen assembly was brazed into the upper portion of the shell.

The thrust chamber was electron beam welded together for the second time without difficulty. Dye penetrant and leakage checks were quite satisfactory. The thruster was thus in its original external configuration except for the 0.060 inch reduction in length resulting from the machine cut at the girth.

### Modified TTS Performance Tests

A series of three sea level tests was conducted on the modified TTS using the same LTV throttle valve. The duty cycles for these tests are shown in Figure 45. These tests were all successful and generally demonstrated the performance goals. Table 16 compares these goals with the performance demonstrated in this test series. The only goal not met was step response of the valve and engine. However, the demonstrated valves satisfy the current requirements for the Viking Mars Lander. The sterilization time and testing time were reduced as schedule and budget expedients. There was no indication from the testing done that the goals would not be met. The throttling range was limited to 5:1 because of unchoked nozzle flow at lower chamber pressures and sea level ambient pressure.

Measured characteristic exhaust velocity,  $C^*$ , (Figure 46) remained essentially constant at 4400 ft/sec over the throttle range tested. All the data points are within  $\pm 1\%$ , and the 26% thrust point probably represents data scatter rather than an upward trend in performance.

Table 16. Performance Demonstration Test Results Summary

Function	Goal	Demonstrated
Thrust	600 lbf	Not measured
Throttle Ratio	10:1	5:1
Over Expansion	No separation @ 0.3 psia	Not measured
Vacuum Specific Impulse	210	220 to 230 lbf-sec/lbm <sup>*</sup>
Durability	500 sec	>174 sec (testing incomplete)
Sterilization	6 cycles of 64 hrs @ 275°F	3 cycles of 35 hrs @ 275°F
Vibration	15.7 grms random for one minute	Not tested
90% Step Response (engine)	75 msec	85 msec (80% step)
Step Response (valve)	60 msec	67 msec (80% step)
Amplitude Ratio (engine)	0.70 @ 60 $\pm$ 10% F	@ 60 $\pm$ 10% F
Phase Lag (engine)	<45°	29° @ 5 cps
Overshoot (engine)	<25%	<10%

\*Based on  $C^*$  results at sea level

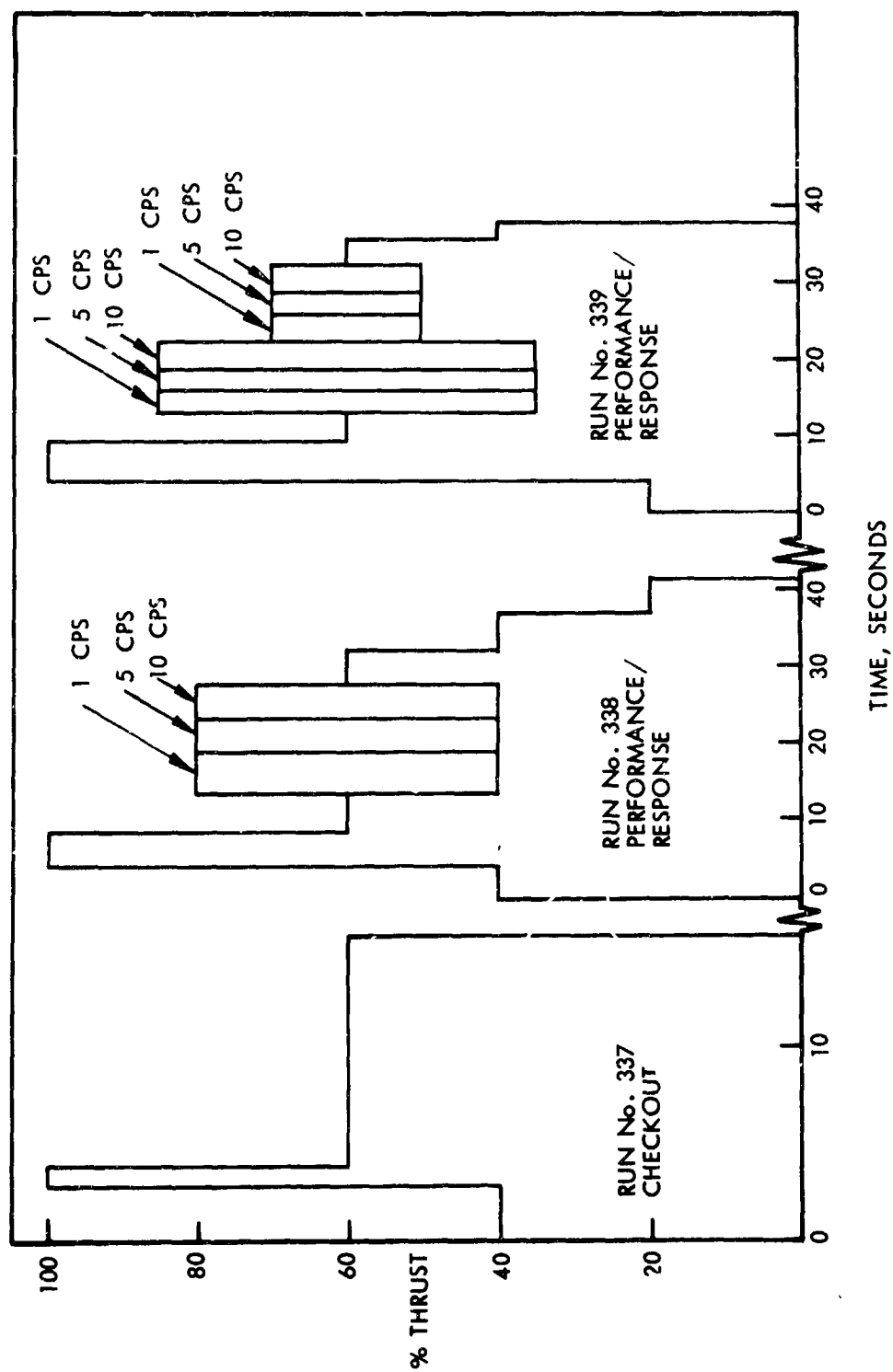


Figure 45. Modified TTS Test Sequence

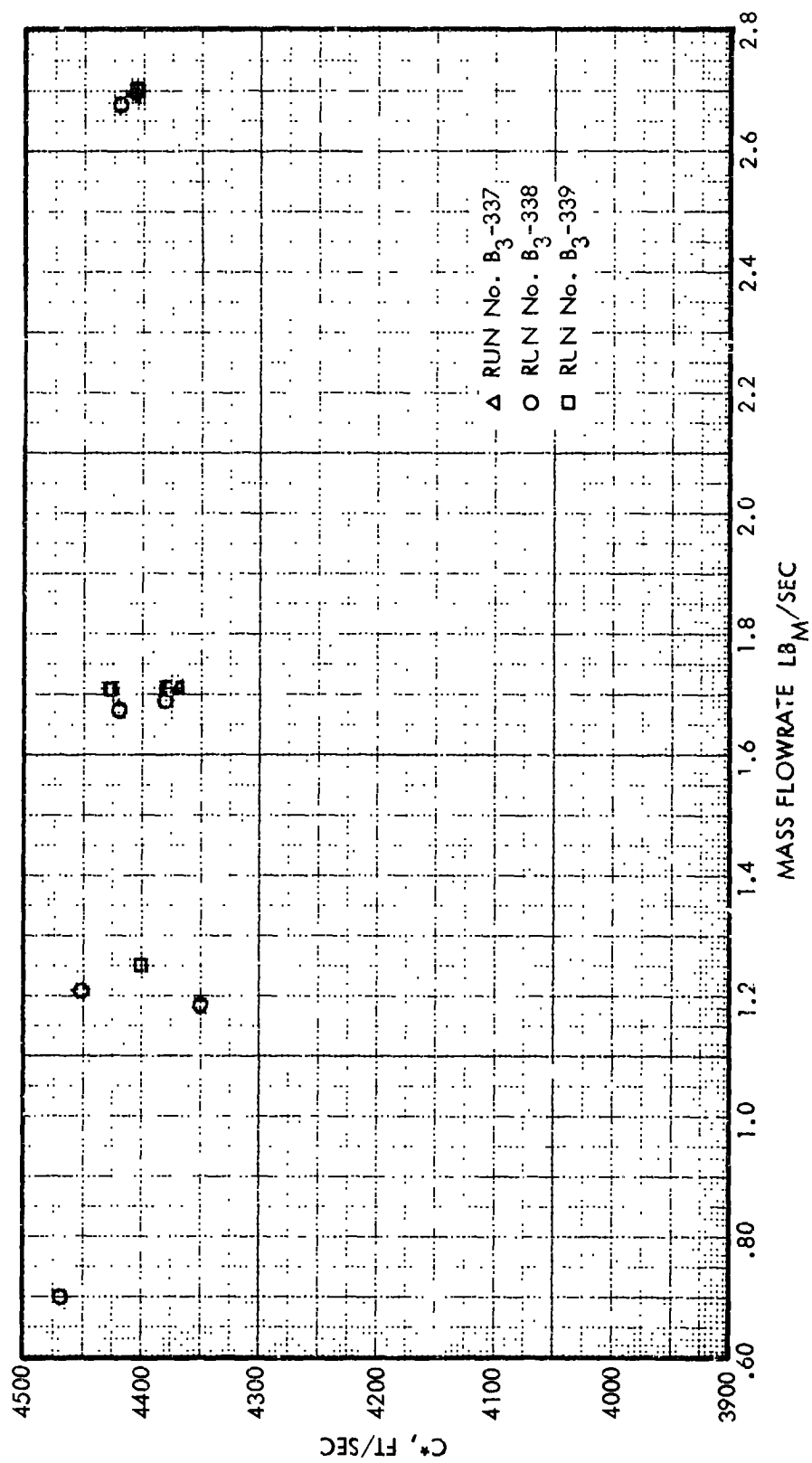


Figure 46. Modified TTS Engine C\*  
As A Function of Mass Flowrate

Chamber pressure, as a function of mass flow rate, reflects the flat C\* performance, as shown in Figure 47. Note the run-to-run reproducibility of the data points which indicates that performance is not shifting with thruster life.

Figure 48 presents the engine chamber pressure roughness as a function of mass flowrate. The roughness data shown represents the maximum pressure oscillation which occurred during each steady state step. The data shows that three points were slightly above the  $\pm 10\%^*$  level:  $\pm 10.2\%$  at full thrust, and  $\pm 11\%$  and  $\pm 11.5\%$  at the 40% level. If one were to consider an average roughness level, these points would be well within the desired limits.

Figures 49 and 50 present the throttle valve  $\Delta P$  and injector  $\Delta P$ , respectively, as a function of mass flowrate. These functions are in close agreement with previous test data.

The catalyst bed  $\Delta P$ , as a function of mass flowrate, is shown in Figure 51. The bed  $\Delta P$  of 100 psid at a mass flowrate of 2.68 lb<sub>m</sub>/sec is higher than expected, but did not affect the overall system operation.

Figures 52 and 53 present temperature measurements as a function of time for Runs B<sub>3</sub> - 338 and 339, respectively. Three temperatures are given: gas temperature, chamber weld temperature, and valve mount temperature. This lower gas temperature measurement is probably caused by a thermal short of the thermocouple to the chamber shell. The weld temperature is recorded with an open-end thermocouple tacked to the outside of the chamber where it cannot locally dissociate ammonia, and therefore, could record higher temperature than the gas measurement.

The frequency response data from Run B<sub>3</sub> - 339 was analyzed and the results from steps four through nine are summarized in Table 17 and shown in Figures 54 and 55. The engine step response and the valve opening and closing time are summarized in Table 18. This data is not available from the checkout test (B<sub>3</sub> - 337) because of transient switching problems.

---

\* There was no specific TTS requirement for roughness, and  $\pm 10\%$  was assumed as an arbitrary goal.

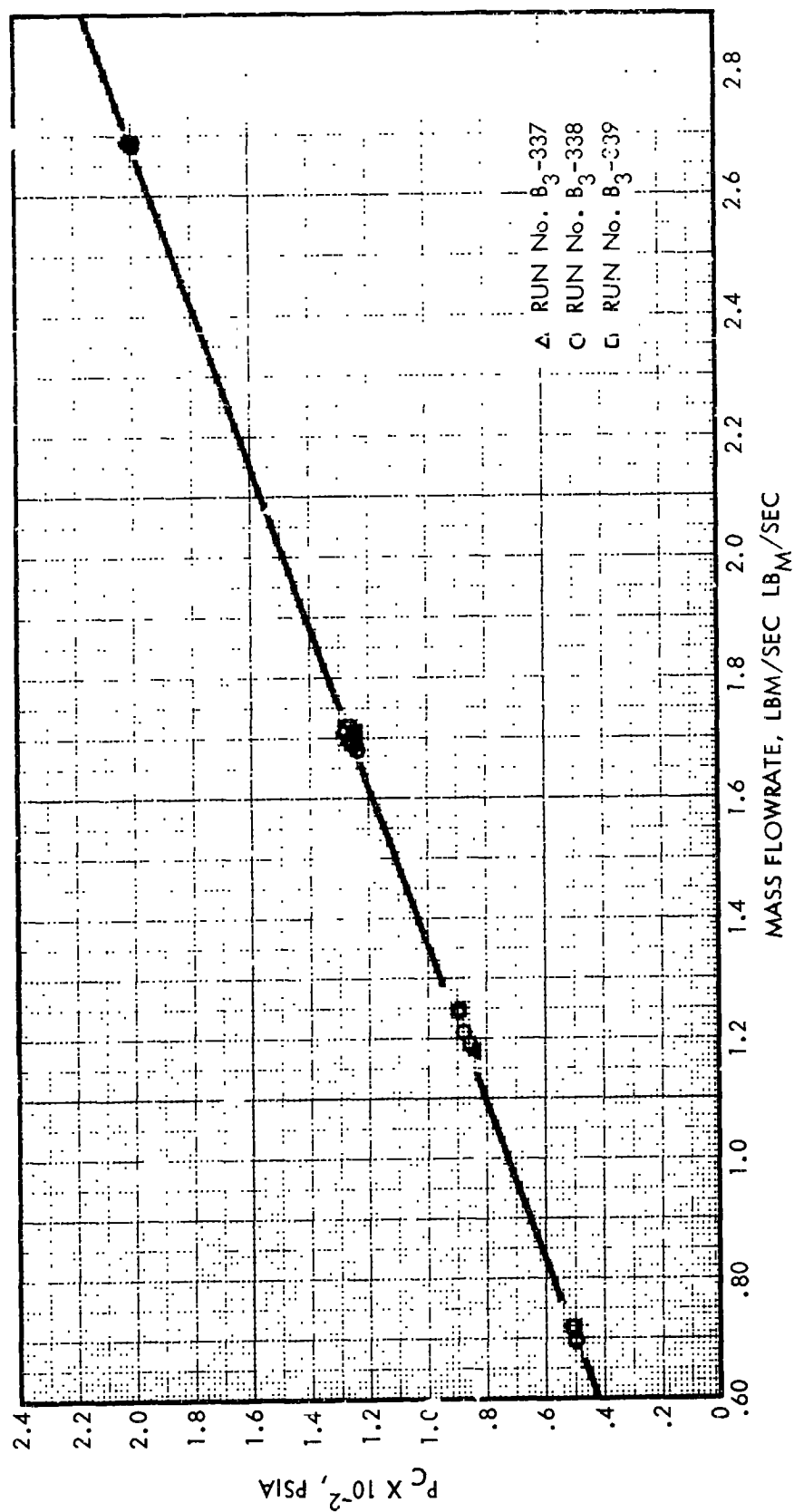
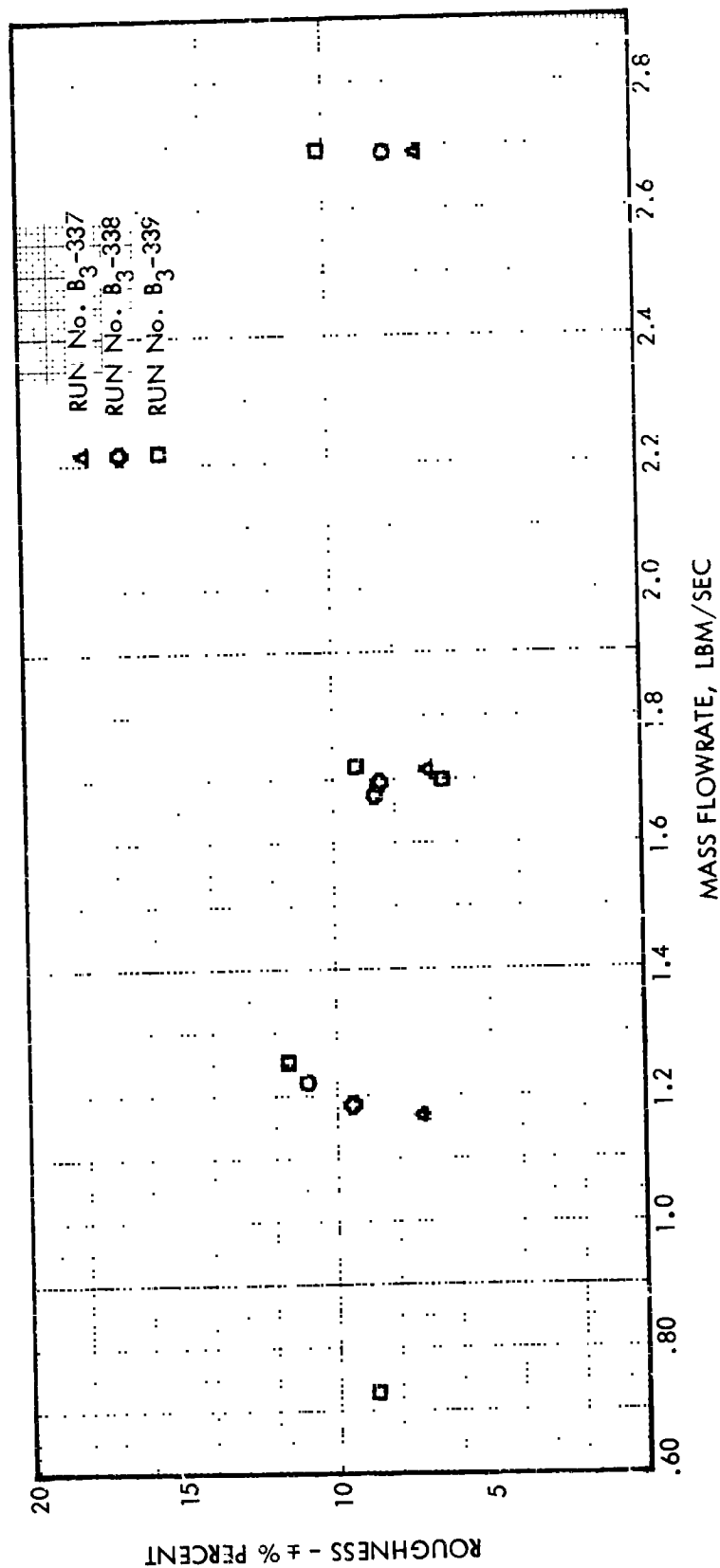


Figure 47. Modified ITS Engine Chamber Pressure  
As A Function of Mass Flowrate



\*THIS REPRESENTS THE MAXIMUM CHAMBER PRESSURE FLUCTUATION RECORDED IN EACH STEP

Figure 48. Modified TTS Engine Roughness\*  
As A Function of Mass Flowrate

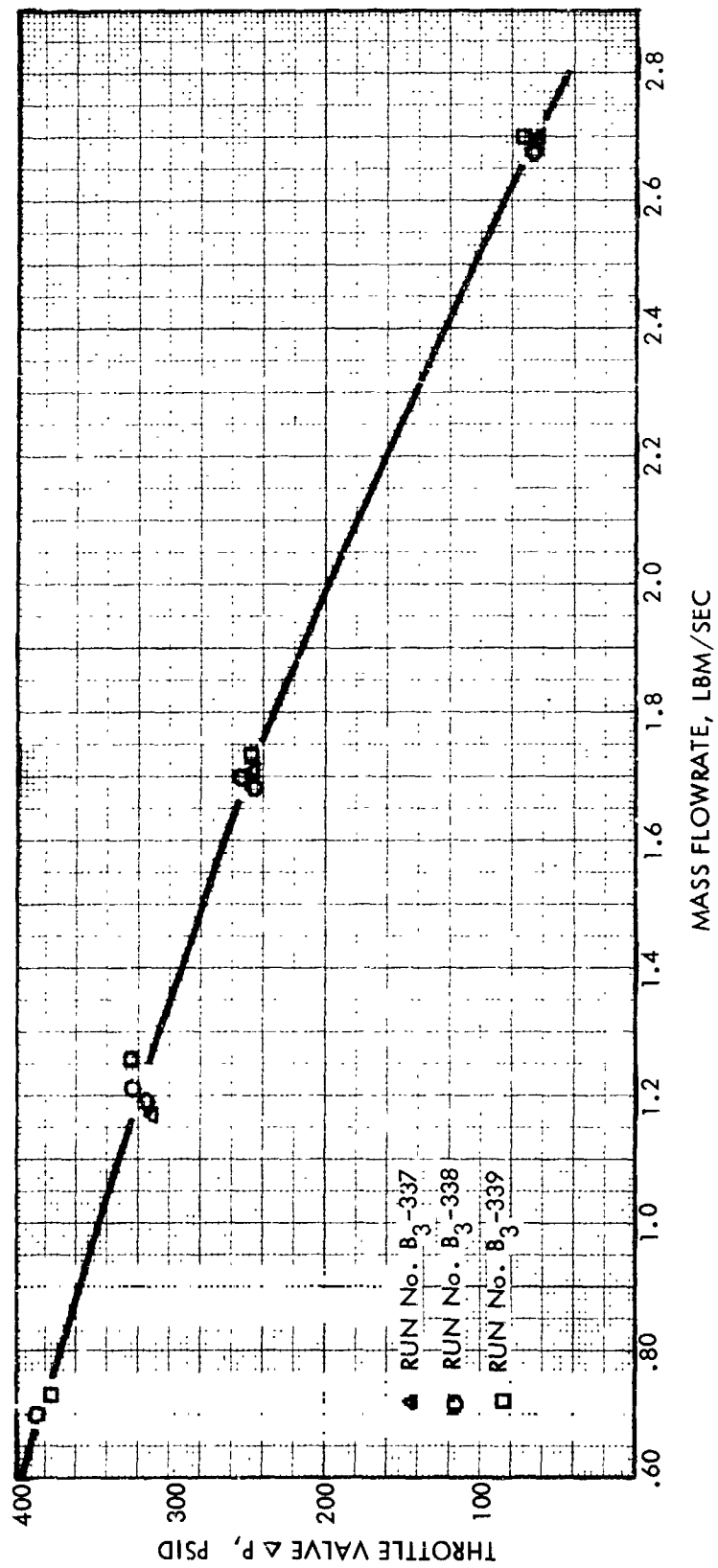


Figure 49. Modified TTS Engine Throttle Valve  $\Delta P$   
As A Function of Mass Flowrate

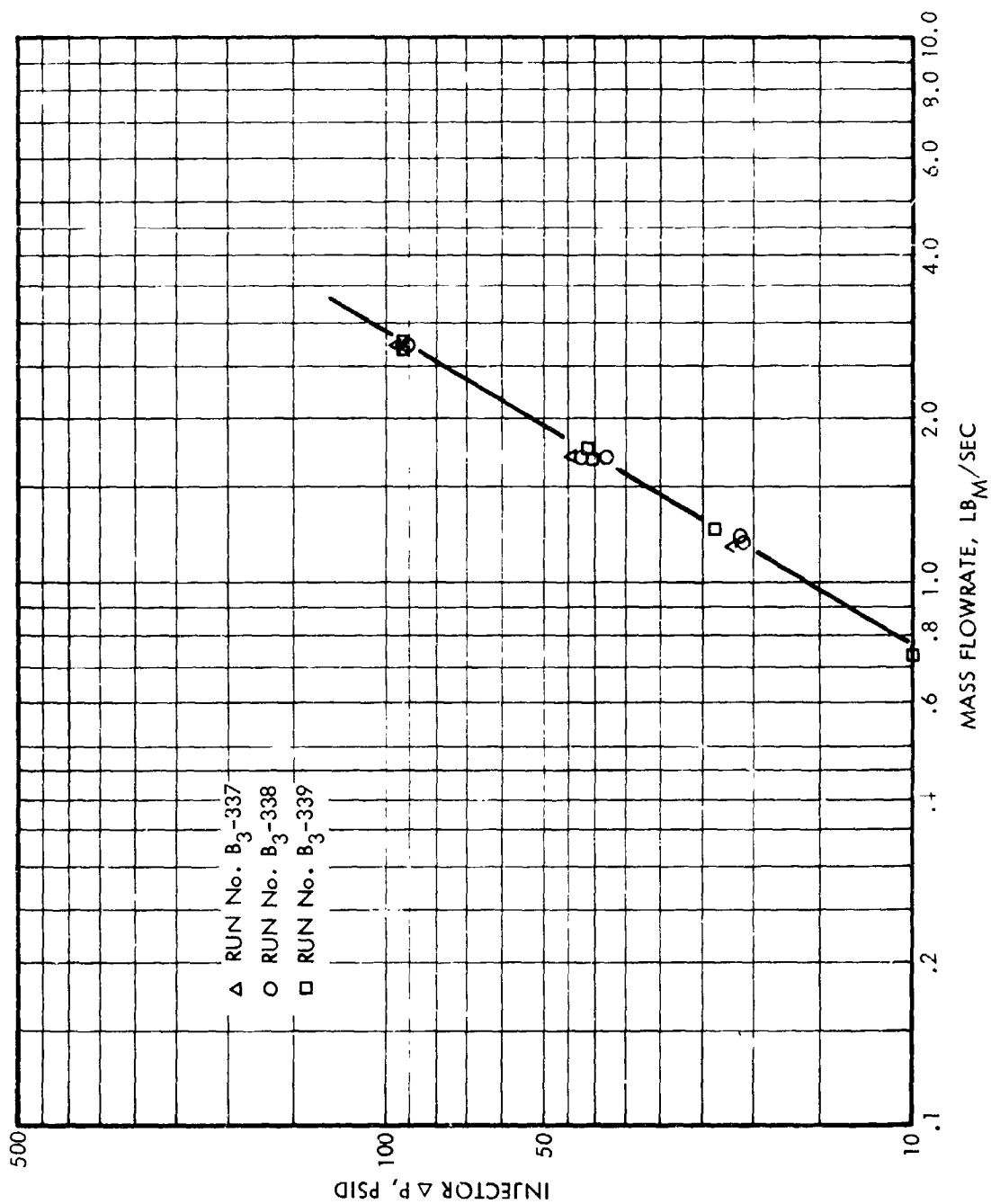


Figure 50. Modified TTS Engine Injector  $\Delta P$   
As A Function of Mass Flowrate

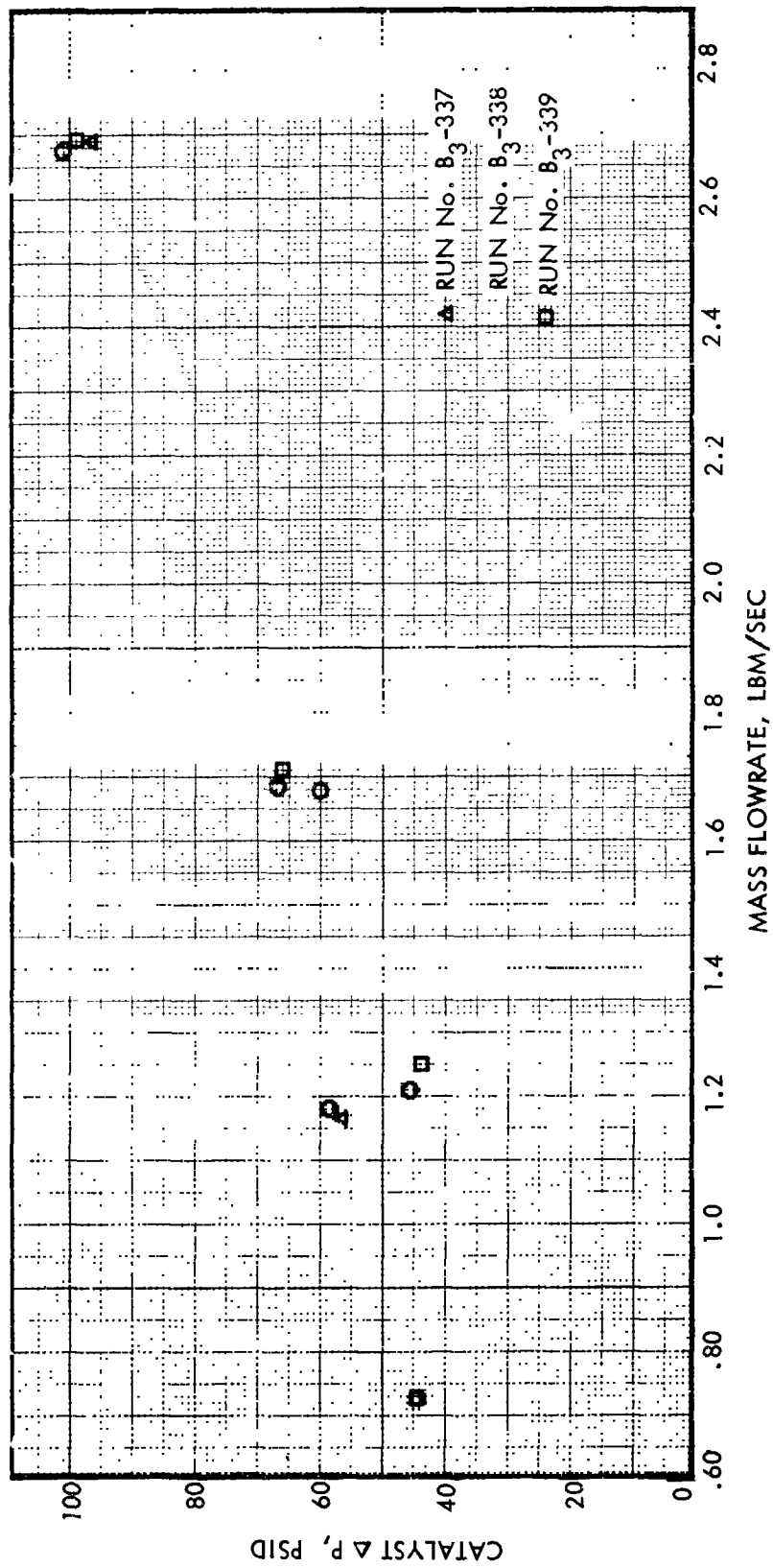


Figure 52. Modified TTS Engine Catalyst  $\Delta P$   
As A Function of Mass Flowrate

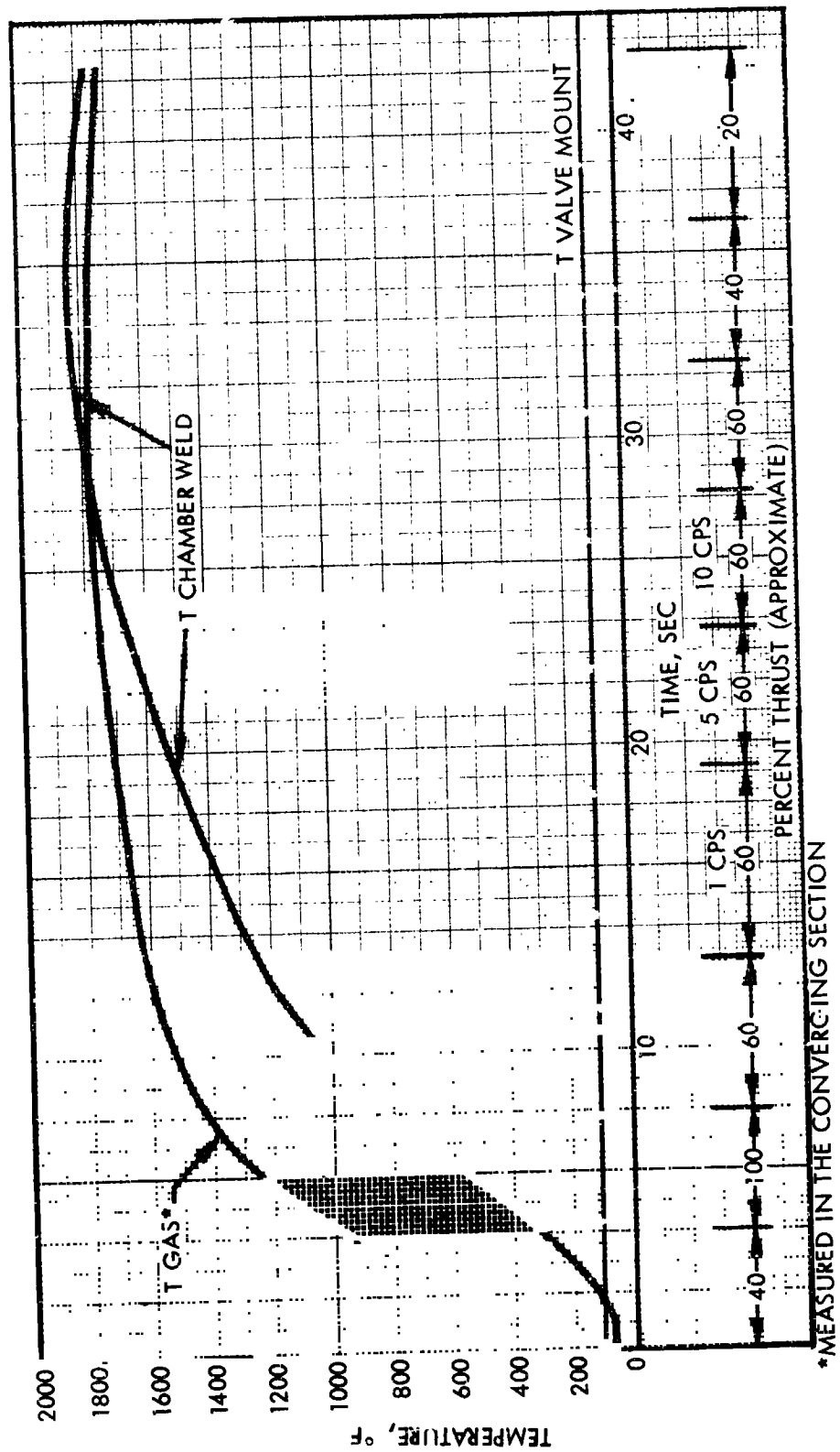


Figure 52. Modified TTS Engine Temperatures  
As A Function of Time for Run B<sub>3</sub> - 338

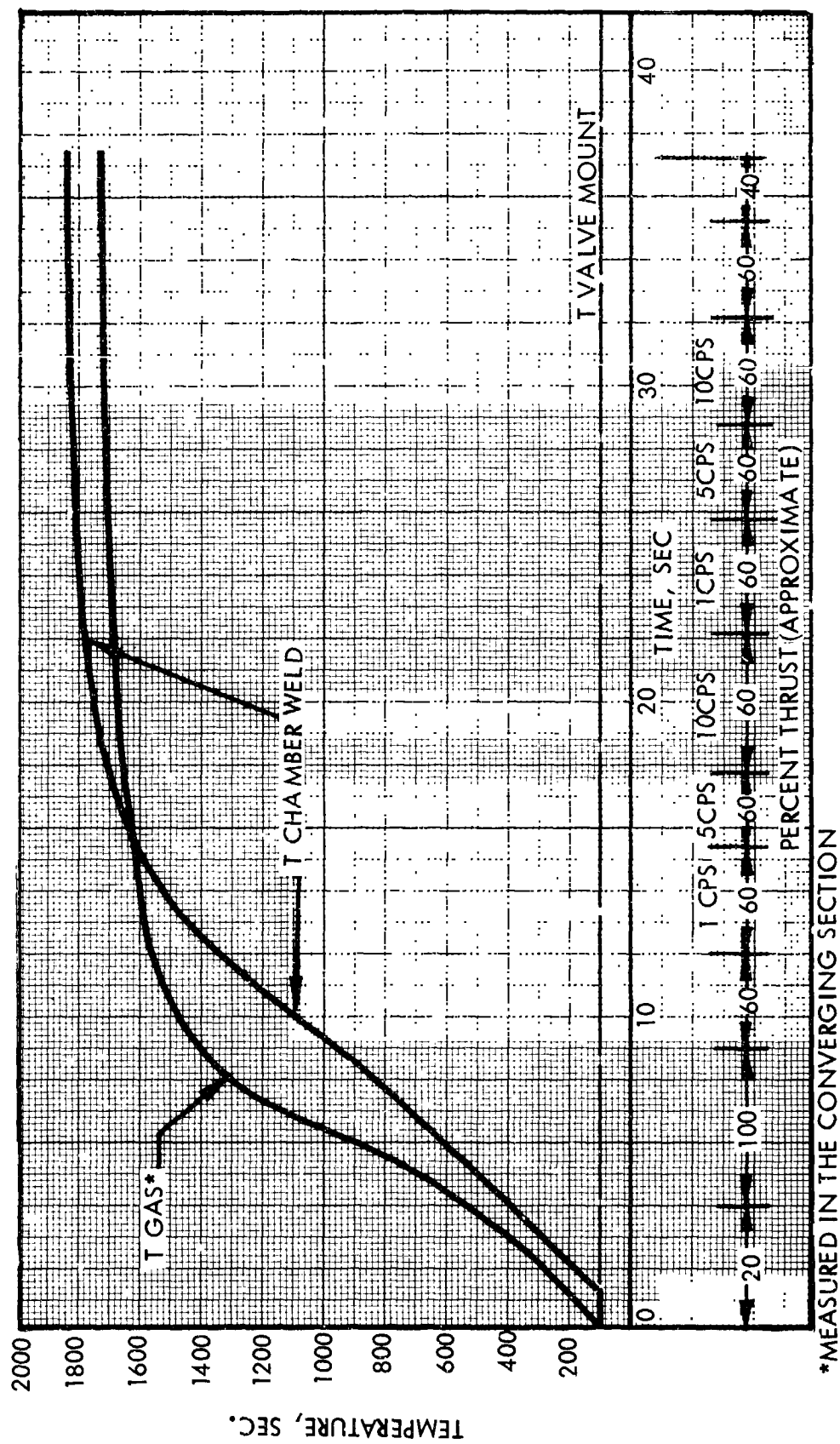


Figure 53. Modified TTS Engine Temperatures  
As A Function of Time for Run B<sub>3</sub> - 339

TEST B3-339  
 COMMANDED AMPLITUDE =  $60 \pm 25\%$

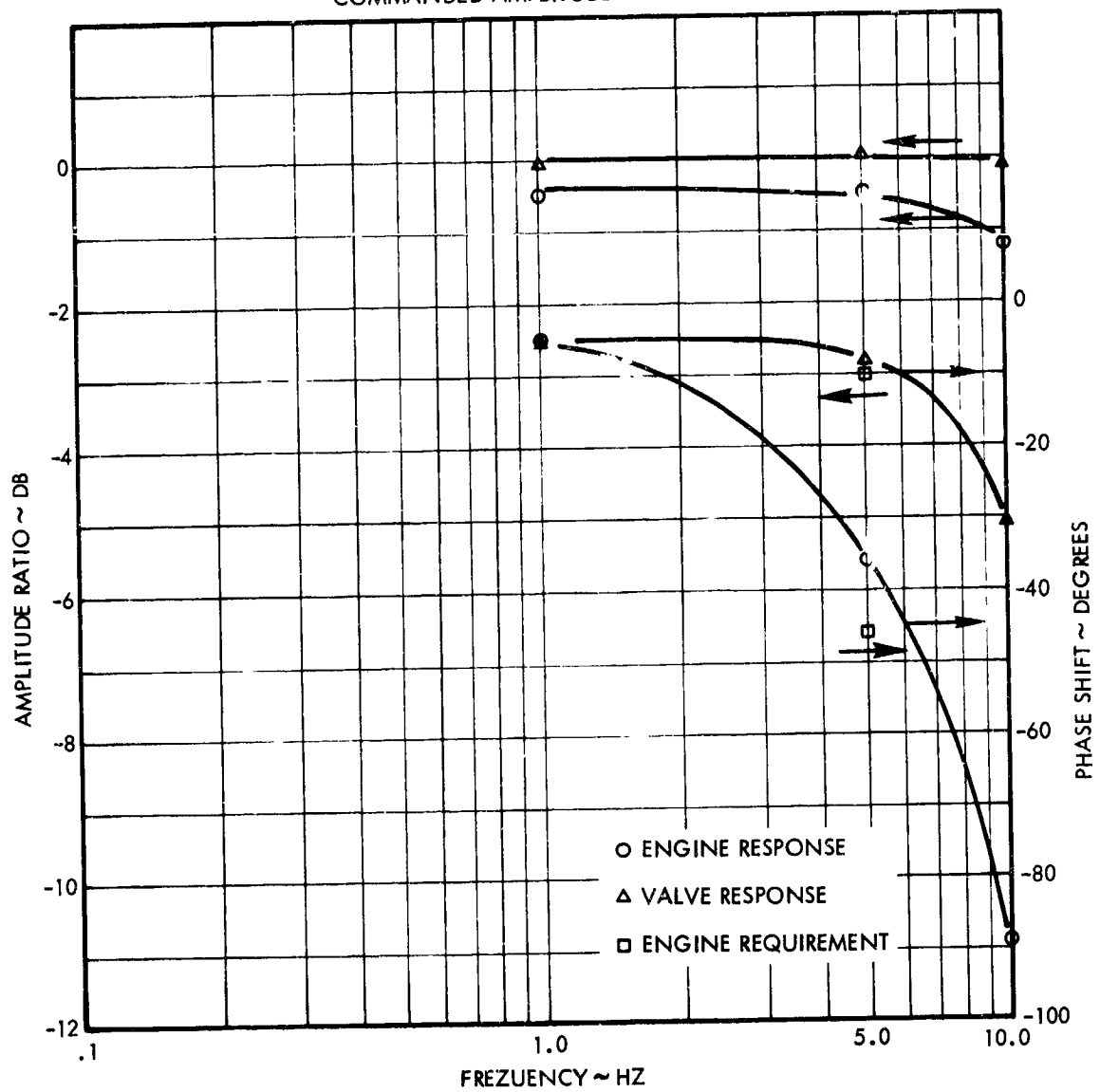


Figure 54. TTS Frequency Response Data

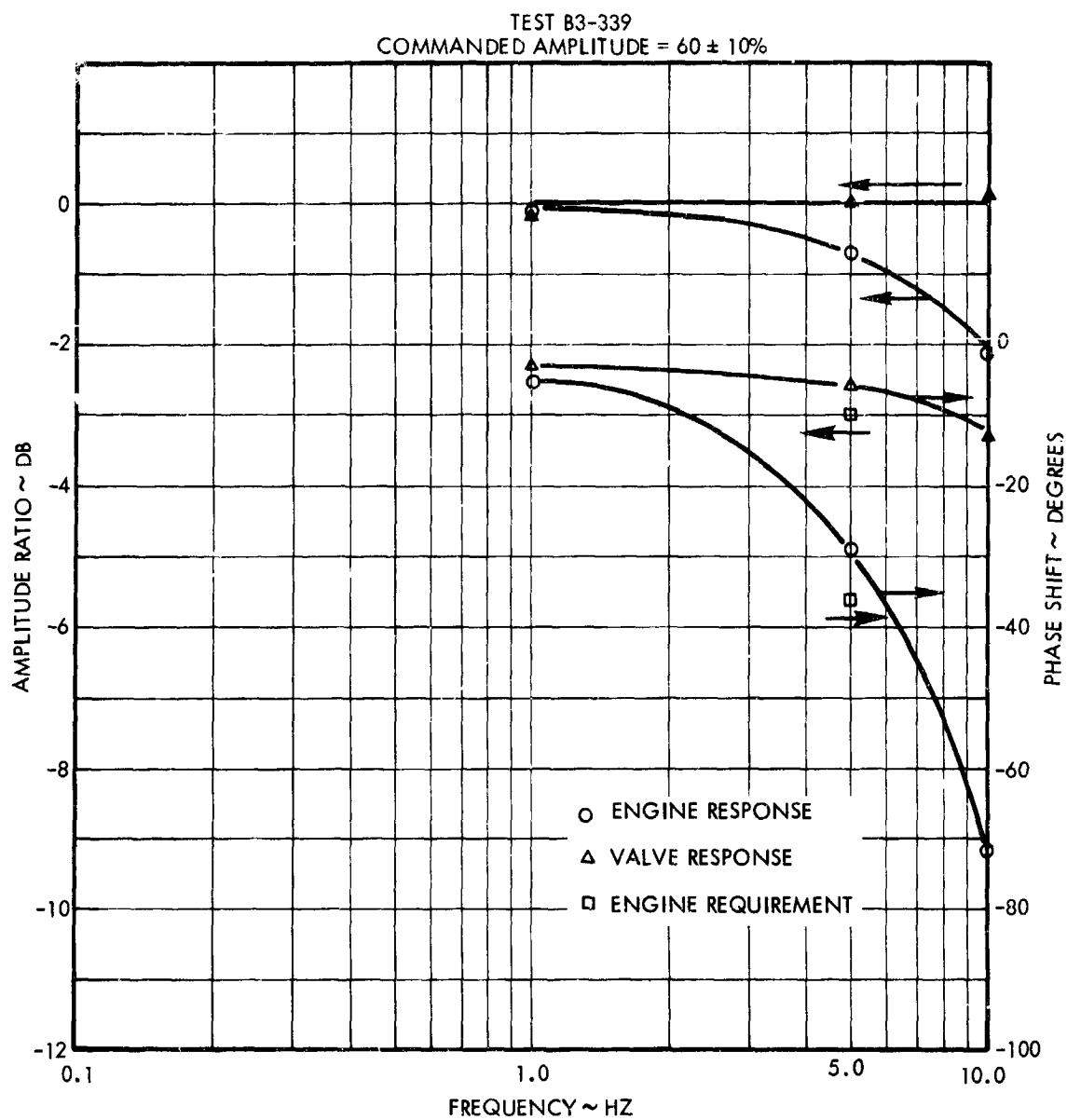


Figure 55. TTS Frequency Response Data

Table 17. TTS 60  $\pm$  25% Frequency Response Summary

Frequency (Hz)	Valve Response		P <sub>c</sub> Response	
	AMP Ratio (db)	Phase Shift (degrees)	AMP Ratio (db)	Phase Shift (degrees)
1.0	- .09	- 5	- .53	- 5
5.0	- .09	- 8	- .44	- 36
10.0	- .09	- 31	- 1.2	- 89

Table 18. Modified TTS Engine and LTV Throttle Valve Step Response Summary

Run	Step	Valve Response		Engine Response		Change in Thrust Level %
		Time to 90% Open, M.S.	Time to 90% Closed, M.S.	Time to 90% of Step-up, M.S.	Time to 90% of Step-down, M.S.	
B <sub>3</sub> - 338	2	37		76		40-100
	3		50		50	100-60
	8		28		40	60-40
	9		28		68	40-20
B <sub>3</sub> - 339	2	67		85		20-100
	3		38		50	100-60
	11		26		44	60-40

### 3. CONCLUSIONS AND RECOMMENDATIONS

The 600 lb<sub>f</sub> maximum thrust throttling thruster system, including a flight weight thrust chamber and electromechanical throttle valve, has generally demonstrated the requirements currently defined for a planetary landing vehicle. Based on a study of various thruster-throttling concepts, this catalytic unit is near optimum for the defined mission. This study indicated that relatively low (200 psia) chamber pressure and expansion ratio are optimum, and that a catalytic thruster is lighter than a thermal decomposition unit of the same thrust at or below 1200 lb<sub>f</sub>, the maximum size studied.

The testing program was limited to one throttle valve (the Moog rotary was not available for the engine test program) and to sea level testing. Thus, demonstrated throttling range was limited and nozzle performance was not measured. Completion of life (>500 seconds) and throttle range (10:1) testing together with accumulating more comprehensive dynamic data is recommended. The marked difference in stability observed as a result of the catalyst bed modification should also be investigated in detail.

## BIBLIOGRAPHY

A. D. Harper, "Hi-Thrust Throttleable Monopropellant Engine System," AIAA Paper No. 69-420, presented at the 5th Propulsion Specialist Conference, U.S. Air Force Academy, Colorado, June 9-13, 1969.

TRW Systems, "First Quarterly Progress Report Throttleable Thrustor System," JPL Contract No. 952344, Report No. 69.4726.3-63, August 18, 1969.

TRW Systems, "Second Quarterly Progress Report Throttleable Thrustor System," JPL Contract No. 952344, Report No. 69.4726.3-86, October 20, 1969.

TRW Systems, "Third Quarterly Progress Report Throttleable Thrustor System," JPL Contract No. 952344, Report No. 70.4726.3-13, January 22, 1970.

Rocket Research Corporation, "Development of Design and Scaling Criteria for Monopropellant Hydrazine Reactors." Final Report RRC-66-R-76, Volume II, NASA Contract NAS7-372, January 18, 1967.

Elliot Ring, "Rocket Propulsion and Pressurization Systems," Prentice-Hall Inc., 1964.

Arthur S. Kesten, "Analytical Study of Catalytic Reactors for Hydrazine Decomposition," NASA Contract NAS 7-458, May 1969.

G. S. Bell, "Hydrazine Reactor Design Handbook," TRW Systems, June 1966.

A. F. Grant, Jr., "Basic Factors Involved in the Design and Operation of Catalytic Monopropellant Hydrazine Reaction Chambers," JPL Report No. 22-77, December 1954.

Appendix A  
SPECIFICATION - FLOW CONTROL ASSEMBLY

## PRELIMINARY SPECIFICATION - FLOW CONTROL ASSEMBLY

## 1.0 SCOPE

This specification establishes the preliminary requirements for performance, design and test for a flow control assembly consisting of a non-cavitating venturi throttle valve, electromechanical actuator and position feedback transducer; hereafter referred to as the assembly.

## 2.0 APPLICABLE DOCUMENTS

## 3.0 REQUIREMENTS

3.1 General Design

The design of the assembly shall utilize flightweight components wherever possible.

3.2 Mechanical Design

3.2.1 Configuration - The assembly shall consist of a non-cavitating venturi flow control valve, with removable pintle, a single torque motor, a ball nut, which is rotated by the torque motor, a ball screw shaft which extends or retracts the flow control valve pintle and a position feedback transducer. The position pickup of the feedback transducer shall be connected to the ball screw or the flow control valve pintle. External connections shall be provided for telemetering valve position data.

3.2.2 Seals - A soft bellows or diaphragm device shall be used to hermetically seal the torque motor cavity and prevent leakage of hydrazine or hydrazine vapor into the cavity.

3.2.3 Pressure

3.2.3.1 Operating Pressure - The assembly shall meet the requirements of this specification with the static pressure at the inlet to the valve between 240 and 480 psia.

3.2.3.2 Proof Pressure - The assembly shall be capable of withstanding a proof pressure of 1,000 psia for a period of three minutes. The assembly shall meet all requirements of this specification after removal of the proof pressure.

3.2.3.3 Burst Pressure - The assembly shall be capable of withstanding a burst pressure of 1,500 psia without bursting or leaking externally.

3.2.3.4 Pressure Transients - The assembly shall withstand pressure spikes of up to 3,000 psia for durations of 10 ms.

3.2.4 Operating Fluids

3.2.4.1 Propellant - The propellant shall be hydrazine per MIL-P-26536B.

3.2.4.2 Calibrating Fluid - Flow tests shall be run using distilled water.

3.2.5 Leakage

3.2.5.1 External - Overboard leakage shall be minimized. A total leakage rate of  $0.004 \text{ in}^3/\text{sec}$  of hydrazine with an operating pressure of 480 psia shall be used as a design goal.

3.2.5.2 Internal - The valve is not required to seal across the throttle seat.

3.2.6 Mechanical Stops - Mechanical non-jamming stops shall be provided to limit the throttle valve pintle overtravel. The stops shall limit the pintle stroke at -15% and +115% of full command stroke range.

3.2.7 Weight - An assembly weight of 2.5 lbm shall be used as a design goal.

3.2.8 Operating Mode - The assembly shall operate in a non-cavitating throttling mode over the total throttle setting and pressure ranges.

3.2.9 Hysteresis - A hysteresis of 1% of full stroke shall be used as a design goal.

3.3 Electrical Design Requirements

3.3.1 Response - The assembly shall meet all the requirements of Paragraphs 3.4.1 and 3.4.3 with a voltage of  $28 \pm 4 \text{ vdc}$  and a power limit of 70 watts.

3.3.2 Operation - The assembly shall operate with a motor voltage of  $28 \pm 4 \text{ vdc}$ .

3.3.3 Power - Maximum (stall) power consumption at 28 vdc shall be 70 watts.

3.4 Performance

3.4.1 Step Response - The assembly position step response as indicated by the position transducer, shall be such that 90 percent of any step change in commanded position shall be attained in 60 ms or less.

3.4.2 Frequency Response - In response to a 5 HZ sinusoidal command signal input of  $60 \pm 10\%$ , the position shall have a phase lag no greater than  $15^\circ$  and an amplitude ratio of .95. The amplitude ratio shall be 1.25 over the frequency range from 0 to 10 HZ.

3.4.3 Overshoot - The position overshoot due to any step command change shall not exceed 15 percent of the commanded position change.

3.4.4 Flowrate - The flowrate versus command voltage shall be as specified in Table 1 for an inlet pressure of 360 psia and propellant temperature of  $70 \pm 5^\circ\text{F}$ . The flowrate shall be within  $\pm 3\%$  of any commanded flowrate in the range of 2.12 to 0.21 lb/sec.

3.4.5 Pressure Drop - The allowable pressure drop across the assembly shall be as specified in Table 1. The supplier shall determine the pressure drop for a propellant flowrate of 2.61 lb/sec. at an inlet pressure of 480 psia, for the 100% throttle setting.

3.4.6 Linearity - The plot of flowrate versus command voltage shall be smooth and continuous and the slope at any point shall not deviate more than  $\pm 10\%$  from the nominal flowrate versus command voltage curve taken from the points in Table 1.

### 3.5 Environment

#### 3.5.1 Non-Operating

3.5.1.1 Vibration - While mounted by normal mounting provisions, the assembly shall withstand random vibration. The overall random vibration level is 15.7 grms with a power spectral density of  $0.2 \text{ g}^2/\text{HZ}$  between 550 and 1,000 HZ with a 3 db/octave rolloff below 550 HZ and a 6 db/octave rolloff above 1,000 HZ (to 2,000 HZ) for 60 seconds duration per axis.

#### 3.5.1.2 Temperature

- a. Transportation and Storage - Surrounding air temperature shall be between  $-20^\circ\text{F}$  and  $160^\circ\text{F}$ .
- b. Heat Sterilization Cycle - The assembly shall be capable of withstanding a heat sterilization cycle consisting of 64 hours at  $275^\circ\text{F}$  for a total of six cycles.

#### 3.5.2 Operating

3.5.2.1 Vibration - The operating vibration shall be the same as specified in Paragraph 3.5.1.1.

3.5.2.2 Temperature - The assembly shall be exposed to propellant between  $+40^\circ$  and  $+90^\circ\text{F}$  and to system hardware temperatures between  $+40^\circ$  and  $120^\circ\text{F}$ .

3.5.2.3 Pressure - The assembly shall be exposed to propellant pressures between 0 and 480 psia and environmental pressures between .44 and 32 in.Hg.

## 4.0 QUALITY ASSURANCE PROVISIONS

#### 4.1 Responsibility for Testing

Unless otherwise specified in the contract or purchase order, the supplier is responsible for all testing specified herein. The supplier may use his own facilities or any commercial laboratory acceptable to the customer.

4.1.1 Witnessing of Tests - TRW shall have the right to witness all tests, and shall be notified when tests are to be conducted so that a representative may be designated for this purpose.

#### 4.2 Acceptance Testing

4.2.1 Functional - The following component testing will be performed by the supplier:

- a. No-flow step response (Paragraph 3.4.1)
- b. No-flow frequency response (Paragraph 3.4.2)
- c. Max stroke (Paragraph 3.2.6)
- d. Hysteresis (Paragraph 3.2.9)
- e. Proof pressure (Paragraph 3.2.3.2)
- f. External leakage (Paragraph 3.2.5.1)
- g. Power consumption (Paragraph 3.3.3)
- h. Stroke versus command voltage
- i. Operating mode (Paragraph 3.2.8)

4.2.2 Characterization - The following component testing will be performed by the supplier:

- a. Water flow calibration of the throttling device to ascertain the pressure drop versus flowrate characteristics as a function of throttle valve position per Paragraphs 3.4.4, 3.4.5 and 3.4.6.
- b. Water flow testing of the throttling device to ascertain the dynamic response characteristics of the assembly per Paragraphs 3.4.1, 3.4.2 3.4.3.

#### 4.3 Test Plan

The supplier shall submit to TRW a proposed test plan. TRW shall evaluate said plan and notify the supplier of acceptability within one week of receipt.

TABLE I  
FLOW SCHEDULE

<u>THROTTLE SETTING</u>	<u><math>\dot{W}</math></u>	<u><math>\Delta P_V</math></u>
100%	2.12 lbs/sec	33 psid
95	2.01	54
90	1.91	74
75	1.59	133
50	1.06	224
25	.53	305
15	.32	334
10	.21	348

Appendix B  
NEW TECHNOLOGY REPORTS

In keeping with the new technology reporting provisions of the contract, the following items were reported:

<u>Title</u>	<u>Innovator(s)</u>	<u>Reference</u>	<u>Date</u>
Thermal Decomposition Engine	A. D. Harper	Second Quarterly Progress Report, Report No. 69.4726.3-86, pp. IV-1 - IV-3	20 October 1969
Radial Flow Reactor	R. J. Kenny	Second Quarterly Progress Report, Report No. 69.4726.3-86, pp. IV-2 - IV-6	20 October 1969
High Efficiency Monopropellant Reactor	C. R. Hunter R. J. Kenny	Second Quarterly Progress Report, Report No. 69.4726.3-86, pp. IV-6 - IV-9	20 October 1969
Throttleable Monopropellant Rocket Engine	P. B. Mitchell	Second Quarterly Progress Report, Report No. 69.4726.3-86, pp. IV-9 - IV-11	20 October 1969

All of these items evolved in the course of studying various concepts applicable to planetary landers. They represent "new" combinations and applications of old ideas. None of these are considered to offer any significant gain for the specific missions investigated.